

## INFORMATION TO USERS

This manuscript has been reproduced from the microfilm master. UMI films the text directly from the original or copy submitted. Thus, some thesis and dissertation copies are in typewriter face, while others may be from any type of computer printer.

**The quality of this reproduction is dependent upon the quality of the copy submitted.** Broken or indistinct print, colored or poor quality illustrations and photographs, print bleedthrough, substandard margins, and improper alignment can adversely affect reproduction.

In the unlikely event that the author did not send UMI a complete manuscript and there are missing pages, these will be noted. Also, if unauthorized copyright material had to be removed, a note will indicate the deletion.

Oversize materials (e.g., maps, drawings, charts) are reproduced by sectioning the original, beginning at the upper left-hand corner and continuing from left to right in equal sections with small overlaps.

Photographs included in the original manuscript have been reproduced xerographically in this copy. Higher quality 6" x 9" black and white photographic prints are available for any photographs or illustrations appearing in this copy for an additional charge. Contact UMI directly to order.

ProQuest Information and Learning  
300 North Zeeb Road, Ann Arbor, MI 48106-1346 USA  
800-521-0600

UMI<sup>®</sup>



University of Alberta

Structure Function Study of L-CAM:  
Insight into the Role of the First Extracellular  
Domain in the *trans* Cell-Cell Interaction

By

Margaret Renaud-Young



A thesis submitted to the Faculty of Graduate Studies and research in  
partial fulfillment of the requirements of the degree of  
Master of Science

Department of Biological Sciences

Edmonton, Alberta

Spring 2001



**National Library  
of Canada**

**Acquisitions and  
Bibliographic Services**

**395 Wellington Street  
Ottawa ON K1A 0N4  
Canada**

**Bibliothèque nationale  
du Canada**

**Acquisitions et  
services bibliographiques**

**395, rue Wellington  
Ottawa ON K1A 0N4  
Canada**

*Your file* *Votre référence*

*Our file* *Notre référence*

The author has granted a non-exclusive licence allowing the National Library of Canada to reproduce, loan, distribute or sell copies of this thesis in microform, paper or electronic formats.

The author retains ownership of the copyright in this thesis. Neither the thesis nor substantial extracts from it may be printed or otherwise reproduced without the author's permission.

L'auteur a accordé une licence non exclusive permettant à la Bibliothèque nationale du Canada de reproduire, prêter, distribuer ou vendre des copies de cette thèse sous la forme de microfiche/film, de reproduction sur papier ou sur format électronique.

L'auteur conserve la propriété du droit d'auteur qui protège cette thèse. Ni la thèse ni des extraits substantiels de celle-ci ne doivent être imprimés ou autrement reproduits sans son autorisation.

0-612-60490-X

**Canada**

**University of Alberta**

**Library Release Form**

**Name of Author:** Margaret Renaud-Young

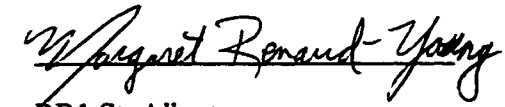
**Title of Thesis:** Structure Function Study of L-CAM: Insight into the Role of the  
First Extracellular Domain in the *trans* Cell-Cell Interaction.

**Degree:** Master of Science

**Year this Degree Granted:** 2001

Permission is hereby granted to the University of Alberta Library to reproduce single copies of this thesis and to lend or sell copies for private, scholarly or scientific research purposes only.

The author reserves all other publication and other rights in association with the copyright in the thesis, and except as herein before provided, neither the thesis nor any substantial portion thereof may be printed or otherwise reproduced in any material form whatever without the author's prior written permission.

  
RR1 St. Albert  
Alberta, T8N 1M8

Date Jan 30/2001

UNIVERSITY OF ALBERTA


FACULTY OF GRADUATE STUDIES

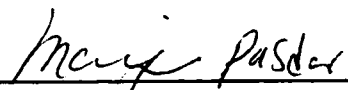
The undersigned certify that they have read, and recommend to the Faculty  
of Graduate Studies and Research for acceptance, a thesis entitled:

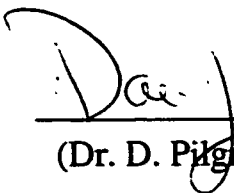
Structure Function Study of L-CAM:

Insight into the Role of the First Extracellular Domain in the *trans* Cell-Cell  
Interaction

Submitted by Margaret Renaud-Young in partial fulfillment of the  
requirements for the degree of MASTER OF SCIENCE.

  
\_\_\_\_\_  
(Dr. W. J. Gallin, Supervisor)

  
\_\_\_\_\_  
(Dr. M. Pasdar, Examiner)

  
\_\_\_\_\_  
(Dr. D. Pilgrim, Examiner)

Date: JAN 21, 2001

## **Abstract**

The state of cell-cell adhesion is important to processes such as cell differentiation, tissue function, and oncogenic progression. Cadherin proteins mediate adhesion via calcium dependent intercellular homophilic binding and intracellular linkage to the actin cytoskeleton. To test whether function of the putative binding site depends on the orientation and organization of the highly conserved tripeptide His-Ala-Val of the first domain, we mutated it to Val-Ala-His. To determine how different structural elements of the protein contribute to the adhesive interaction a deletion mutant of the first extracellular domain was constructed. Switching HAV to VAH did not eliminate adhesion, indicating that HAV is not an essential component of the adhesive interface. The HAV mutation may have disrupted the cadherin's ability to bind the unmutated L-CAM, therefore HAV/VAH was tested for its capacity to adhere to unmutated L-CAM. L-CAM adhered strongly with HAV/VAH, refuting the theory that HAV organization is important to the adhesive interface. Deletion of the first extracellular domain eliminated cell-cell adhesion, confirming previous observations that homophilic cadherin adhesion requires Domain I. However, the  $\Delta I$  mutants were able to interact with the unmutated L-CAM, in contrast to the theory that cadherin adhesion is restricted to the first extracellular domain.

## **Acknowledgement**

I would like to thank my supervisor Warren Gallin for his advice and support throughout the development of this thesis. He has given remarkable encouragement and important technical input that has enabled me to bring this work to completion. I would also like to thank the technicians and the other students in the Gallin lab that have offered valuable advice and friendship.

I would like to acknowledge the input of my committee members Dr. Dave Pilgrim and Dr. Manijeh Pashar. They have offered valuable recommendations and learning opportunities throughout the duration of the degree.

Lastly, this thesis could not have been completed without the loving support of my husband Jason, and my caring family. They and my friends have offered kindness and encouragement in the pursuit of this degree.



## **Table of Contents**

<b>Introduction.....</b>	<b>1</b>
<b>Methods and Materials.....</b>	<b>28</b>
<b>Results.....</b>	<b>35</b>
<b>Discussion.....</b>	<b>78</b>
<b>Bibliography.....</b>	<b>82</b>

## **List of Tables**

<b>Table 1: PCR Primers.....</b>	<b>29</b>
<b>Table 2: Analysis of Replicate Aggregation Assays.....</b>	<b>55, 56, 57</b>

## List of Figures

Figure 1: EMT-MET.....	5
Figure 2: Cadherin Involvement with Rac GTPase.....	8
Figure 3: Cadherin Structure.....	13
Figure 4: Models for <i>Cis</i> Dimerization.....	18
Figure 5: Cadherin Constructs Studied Using COMP.....	21
Figure 6: Models for <i>Trans</i> Interaction.....	25
Figure 7: Mutation of L-CAM.....	37,38,39,40
Figure 8: Western Blots of L-CAM Mutants.....	42
Figure 9: Immunofluorescence.....	45
Figure 10: Aggregation of HAV/VAH.....	48,49,50
Figure 11: Aggregation of $\Delta I$ .....	52,53
Figure 12: Coaggregation of HAV/VAH #1.....	60,61
Figure 13:Coaggregation of HAV/VAH #2.....	63,64
Figure 14:Coaggregation of HAV/VAH #4.....	66,67
Figure 15: Coaggregation of $\Delta I$ #1.....	70
Figure 16:Coaggregation of $\Delta I$ #2.....	72
Figure 17:Coaggregation of S180.....	74
Figure 18:Coaggregation of S180 L-CAM #11.....	76,77

## **List of Abbreviations**

<b>ECM</b>	<b>Extracellular matrix proteins</b>
<b>EMT</b>	<b>Epithelial-mesenchymal transition</b>
<b>MET</b>	<b>Mesenchymal-epithelial transition</b>
<b>EGF</b>	<b>Epithelial growth factor</b>
<b>GTPase</b>	<b>Guanosine triphosphatase</b>
<b>MEK</b>	<b>MAPK/ERK kinase</b>
<b>MAPK</b>	<b>Mitogen activated kinase</b>
<b>ERK</b>	<b>Extracellular regulated signal kinase</b>
<b>GEF</b>	<b>Guanosine exchange factor</b>
<b>IQGAP1</b>	<b>guanosine activating protein</b>
<b>GDI</b>	<b>Guanosine diphosphate dissociation inhibitor</b>
<b>L-CAM</b>	<b>Liver cell adhesion molecule</b>
<b>SH3</b>	<b>Src homology 3 (site that can bind the kinase src)</b>
<b>GSK-3<math>\beta</math></b>	<b>Glycogen synthase kinase</b>
<b>COMP</b>	<b>Cartilage oligomeric matrix protein</b>
<b>GST</b>	<b>Glutathione S transferase</b>
<b>CAR</b>	<b>Cell adhesion recognition</b>
<b>PPI</b>	<b>Proline, proline, isoleucine</b>
<b>GAD</b>	<b>Glutamic acid, alanine, aspartic acid</b>
<b>HAV</b>	<b>Histidine, alanine, valine</b>
<b>PCR</b>	<b>Polymerase chain reaction</b>
<b><math>\Delta</math>I</b>	<b>Deletion of domain 1</b>

# Introduction

## ***Cell Adhesion Background***

The spatial and functional separation of cell types is essential for the development and survival of multicellular organisms. This segregation requires molecules that allow cells to assume and maintain their spatial organizations within the organism, either through cell-cell adhesion or cell-matrix adhesion. Three major protein superfamilies are known to be important for these adhesive relationships: the immunoglobulins, the integrins, and the cadherins.

Immunoglobulins share a basic domain topology and are all involved in some form of adhesive interactions. Common to all immunoglobulins is a motif made up of two  $\beta$ -sheets in which hydrophobic side chains are sandwiched between anti-parallel 5-10 amino acid  $\beta$ -strands (Williams and Barclay, 1988). This conformation is further stabilized by an internal disulfide bond (Williams and Barclay, 1988). Between the faces of the  $\beta$ -sheets are the adhesive interfaces with which antibodies adhere to their antigens. (Williams and Barclay, 1988). Immunoglobulins and cadherins have similar extracellular repeats of a  $\beta$ -barrel structure, but the similarity in domain topology is a reflection of convergence not relatedness because of the dissimilarity in sequences (Shapiro et al., 1995b).

Proteins of the integrin superfamily are responsible for cell-matrix adhesion, and cell-cell adhesion. Integrins are dimeric transmembrane glycoproteins composed of  $\alpha$  and  $\beta$  subunits (Hynes, 1992). There are several different  $\alpha$  and  $\beta$  subunits, most of which are capable of pairing with a number of partners, creating a diverse assemblage of integrins. The extracellular regions of integrins are capable of interacting with specific ligands (ECM proteins), while the intracellular domains interact with partners that mediate cytoskeletal attachment and signal transduction (Hynes, 1992; Wu et al., 1998). Like cadherins, integrin activity is calcium dependent, although they utilize an entirely different mechanism of calcium coordination (calcium is contained within the core of the  $\alpha$ -subunit in integrins, whereas in cadherins it is located between domains) (Chothia and Jones, 1997).

The cadherin superfamily contains over 90 members (Marrs and Nelson, 1996; Wu and Maniatis, 1999), that can be grouped into three broad classes based on functional differences and sequence comparisons: classical cadherins, protocadherins, and desmosomal cadherins

## Classical Cadherin Background

Classical cadherins comprise the cadherin proteins that were first noted for their roles in development (Thiery et al., 1984) and the first to be isolated and sequenced (Gallin et al., 1987; Hyafil et al., 1981). The prototype of the classical cadherin likely arose from a primitive metazoan by the process of duplication of extracellular domains until there were five motifs present (Gallin, 1998). Later in the evolution of this primitive cadherin, introns were randomly inserted into the gene. The 16 inserted introns do not correspond to domain divisions, or any obvious division within the protein, although they occur in the same location in each class of classical cadherins (Gallin, 1998). After these events, formation of paralogue groups through gene duplication occurred producing the four recognized classes of classical cadherins: N-cadherin (neural), R-cadherin (retinal), E-cadherin (epithelial), and P-cadherin (placental) (Gallin, 1998). Within these four cadherin groups there is a more broad division between neural and nonneural cadherins, grouping together N- and R- cadherins, and E- and P-cadherins (Gallin, 1998). This grouping is consistent with the biological role of each type of cadherin. As the animal lineages split, the cadherins evolved to slightly different forms and expression levels, due to different selection pressures affecting different organisms (Gallin, 1998). For example, P-cadherin was named for the tissue in which it was discovered, mouse placenta (Nose and Takeichi, 1986), yet it has an orthologue B-cadherin in chicken, an animal that does not produce placenta (Napolitano et al., 1991). Also, P-cadherin is not prevalent in human placenta (Shimoyama et al., 1989). There are cases though where very little change has occurred between orthologues most notably N-cadherin (Gallin, 1998; Rimm and Morrow, 1994).

Cadherins are single-pass transmembrane glycoproteins that bind homophilically to cadherins of the same subtype expressed on other cells (Gallin et al., 1983; Yoshida-Noro et al., 1984). In epithelia, multiple cadherin cell-cell interactions are localized to the baso-lateral region in a manner that follows the circumferential dimensions of the cell, forming what is known as an adhesion belt (*zonula adherens*). This adhesion belt corresponds internally to a ring of actin filaments. Through modulation of the strength of cell-cell adhesion, classical cadherin junctions contribute to developmental processes such as the separation of cell layers and tissue types as well as cellular migration (Monier-Gavelle and Duband, 1997; Townes and Holtfreter, 1955). Throughout the course of development, classical cadherins are involved in the process of epithelial-mesenchymal transition (EMT): the disassembly of epithelium due to the loss of cadherin expression in epithelial cells, or mesenchymal-epithelial transition (MET): the formation of epithelium as a result of cadherin expression in mesenchyme (Prieto

and Crossin, 1995). An example of EMT and MET is the migration of neural crest cells in vertebrate embryos (Bronner-Fraser et al., 1992). After neural tube closure, N-cadherin is down-regulated in neural crest cells and they begin to migrate to their destinations. Upon reaching their destinations, the cells begin to re-express N-cadherin, form clusters at their destinations, and differentiate into their definitive tissues (Figure 1) (Bronner-Fraser et al., 1992). Adherens junctions are the first to form after epithelial cells have contacted each other (McNeill et al., 1993). After the initial contact provided by the cadherins, the membranes are adjacent to each other, allowing or inducing formation of other junctions (gap or desmosomal) (Mege et al., 1988). Cadherins facilitate segregation of different cell types through differential cadherin expression. Because they bind homotypically, cells that present different cadherins on their surfaces will not bind each other. An example of this is the process of neurulation in mammalian embryos, in which cells of the ectoderm stop expressing E-cadherin and begin to express N-cadherin permitting neural cells to separate from cells of the ectoderm (Hatta and Takeichi, 1986; Thiery et al., 1984).

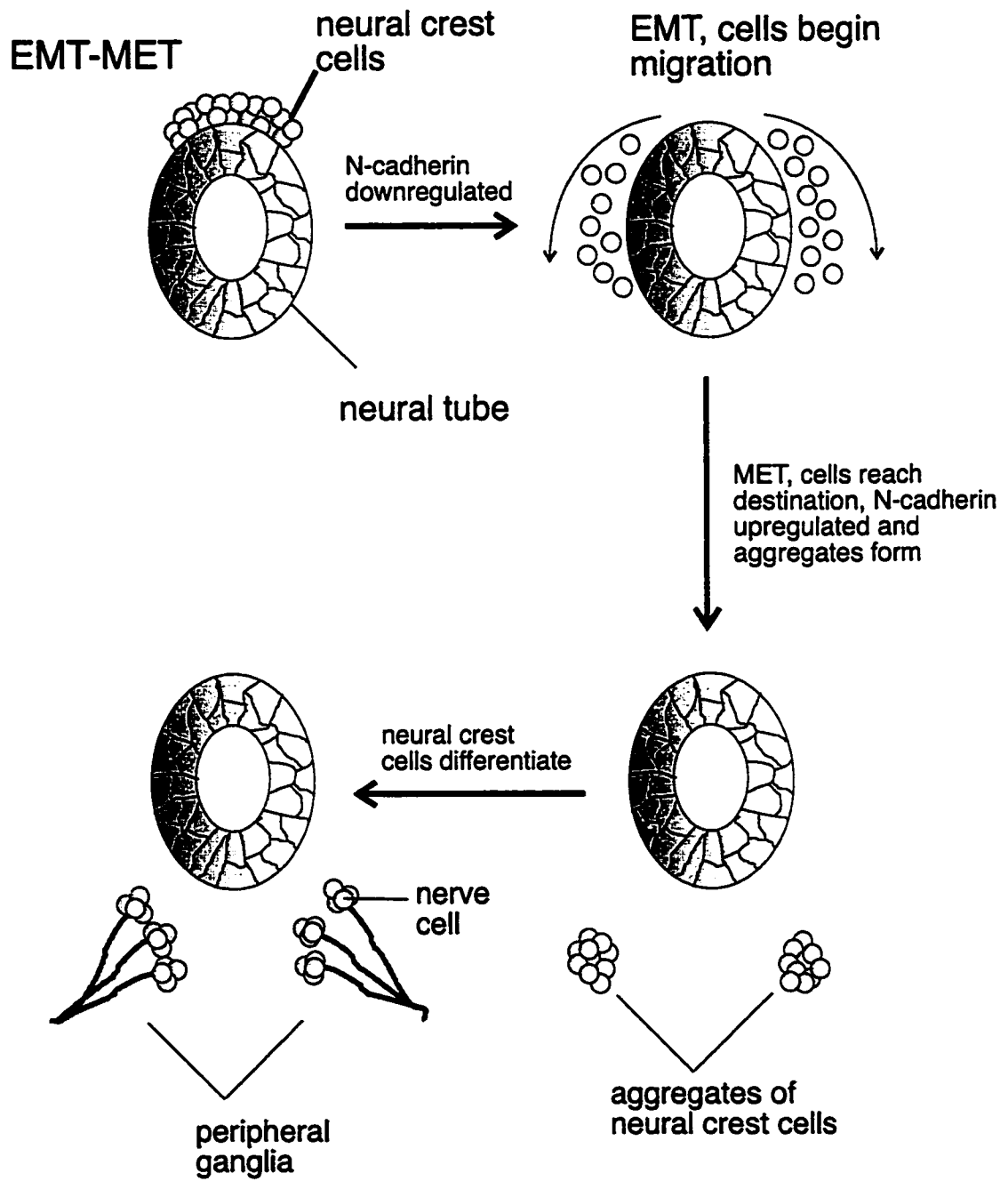
Cadherins are essential to the formation and maintenance of polarized epithelia (Prieto and Crossin, 1995), in their roles in cell adhesion and in their involvement in several signal transduction pathways that are important for cytoskeletal remodeling and cell cycle. Cadherin-mediated adhesion imposes controls on the cell cycle that restrict cell division (Li et al., 1998), and in some cases induce apoptosis (Hermiston and Gordon, 1995; Hermiston et al., 1996). Birchmeier and Behrens (Birchmeier and Behrens, 1994) review several cases in which invasiveness and uncontrolled cell division are abolished by E-cadherin transfection into tumors that do not express E-cadherin. Often invasiveness is not due to a lack of E-cadherin expression, but is the result of signaling events that lead to cadherin complex disassembly (Brady-Kalnay et al., 1998). An example of a mechanism of cadherin complex dissociation is tyrosine kinase phosphorylation of  $\beta$ -catenin (e.g. by EGF receptor, pp60<sup>src</sup>) (Hoschuetzky et al., 1994; Roura et al., 1999). Signaling events that occur downstream of the GTPase Ras also lead to cadherin complex dissociation. Ras is an oncogene that interacts with the mitogenic pathway through the serine/threonine kinase Raf, then MEK (a protein that phosphorylates mitogen-activated protein kinases) (Takai et al., 2001; Van Aelst et al., 1993). When sufficiently activated, MEK downregulates transcription of many proteins as part of the activation of the mitogenic pathways. Tiam 1, a protein down-regulated by MEK, is involved in the maintenance of cadherin based adhesion (Zondag et al., 2000). Tiam 1 is a guanosine exchange factor (GEF) that is specific to activation of the GTPase Rac (Figure 2). Rac is essential to cadherin activity through its modeling of the actin

### **Figure 1: EMT-MET**

Cadherin based adhesion induces controls on cellular migration and the cell cycle. An example of the processes EMT (epithelial-mesenchymal transition) and MET (mesenchymal-epithelial transition) is neural crest cell differentiation. These cells originate from the dorsal region of the embryonic neural tube. Before they migrate to their destinations, N-cadherin is down-regulated and cell-cell adhesion is disrupted (EMT). Neural crest cells proceed to migrate to where they will differentiate to their definitive forms. Once they reach their destinations they begin to express N-cadherin again and revert to the epithelial phenotype (MET).



# Figure 1



cytoskeleton and direct interaction with the cadherin complex (Fukata et al., 1999; Sander et al., 1999). Simultaneously, another GTPase, Rho, is being activated to a high level, sequestering actin to stress fibers at the basal region of the cell. Rac and Cdc42 are also capable of directly regulating cadherin based adhesion (Fukata et al., 1999; Kaibuchi et al., 1999). The Rac effector IQGAP1 is a GTPase activating protein (GAP) that attaches to Rac and activates it. When Rac is not at the membrane to attach to IQGAP1, the protein is situated at the cadherin complex attached to  $\beta$ -catenin in a region that overlaps its site of interaction with  $\alpha$ -catenin. Because Rac removes the IQGAP1 protein from the  $\beta$ -catenin, it allows formation of the cadherin-catenin complex and induces cadherin-based adhesion (Fukata et al., 1999). Cadherins also associate with the adapter protein Shc, which can be found in a complex with Ras (Shc binds Grb2, which binds Ras) (Xu and Carpenter, 1999).

### *L-CAM*

Liver cell adhesion molecule (L-CAM) is synthesized as a precursor of 135 kDa, which is cleaved to a size of 124 kDa and N-linked glycosylated at four sites along its extracellular surface before it is delivered to the plasma membrane (Gallin et al., 1987). In vivo, there are usually phosphoserine and phosphothreonine residues near the carboxy-terminus (Cunningham et al., 1984). Because L-CAM contains five extracellular domains, a transmembrane domain, and a cytoplasmic domain that is very similar to the other classical cadherins, it is a member of the classical cadherin subdivision of the cadherin superfamily.

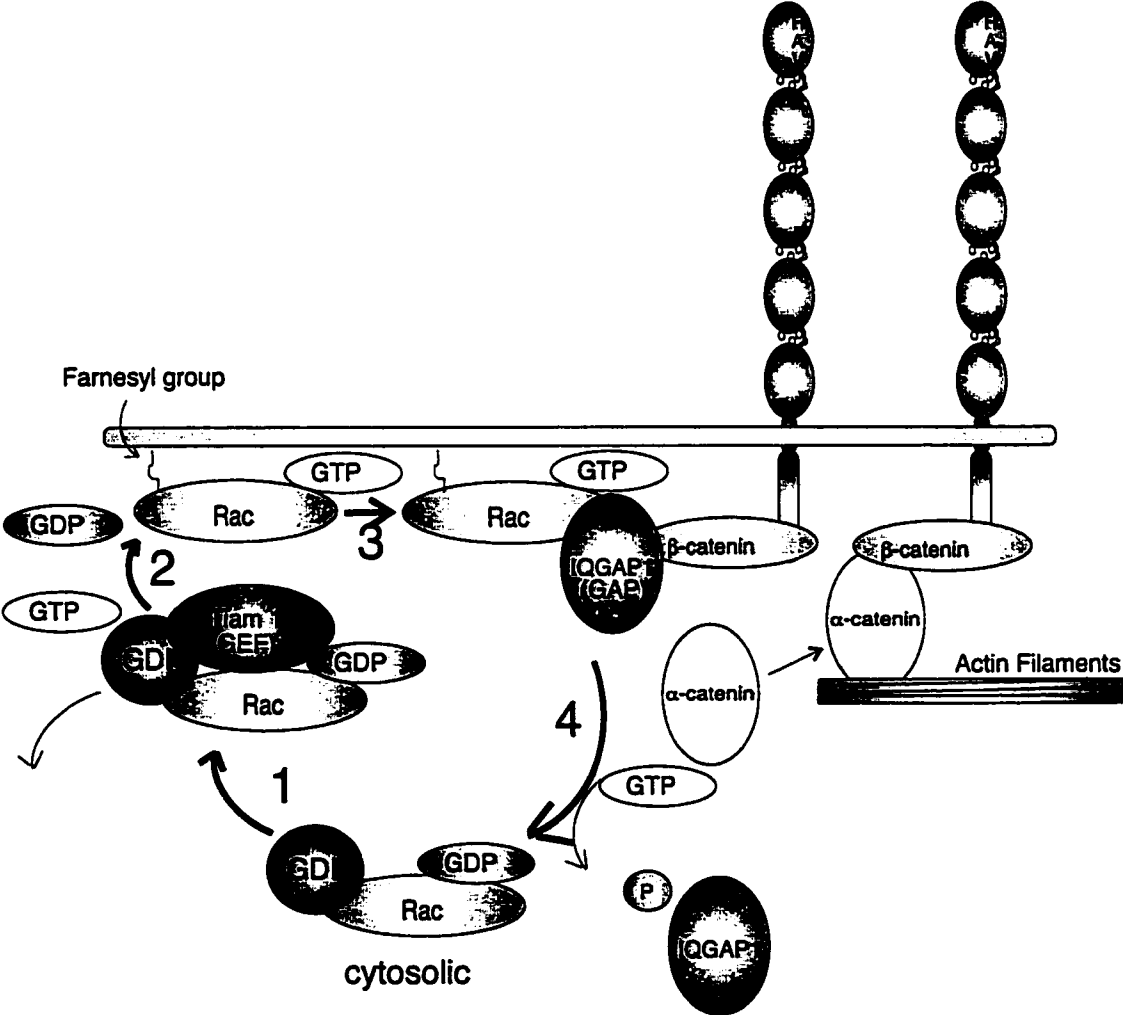
L-CAM was first purified from avian embryonic liver (Gallin et al., 1983), but it has since been found in most nonneuronal epithelial cells. When discovered, L-CAM was suggested to have been the chicken orthologue to E-cadherin in mammals. Convincing evidence for this is a 65.8% identity between L-CAM and mouse E-cadherin sequences, and L-CAM has a nearly identical tissue distribution throughout the organism (Edelman et al., 1983; Thiery et al., 1984). However, the proteins do not bind each other, and function-perturbing antibodies that deactivate L-CAM do not adhere or block the function of E-cadherin. A possible reason for this difference is that L-CAM and E-cadherin diverged as a result of gene conversion between L-CAM and B-cadherin at some point in the evolution of the two molecules in the avian lineage (Murphy-Erdosh et al., 1995). Gene conversion would make E-cadherin and L-CAM unable to bind to each other because the change in L-CAM would make it structurally incompatible with E-cadherin. However, because this mutation does not alter the placement of the gene on

## **Figure 2: Involvement with Rac GTPase**

Rac is a GTPase in the Ras superfamily that functions in cytoskeletal modification. These proteins are regulated by three different classes of proteins: GEFs (guanine exchange factors), GAPs (GTPase activating proteins), and GDIs (GDP dissociation inhibitors). The GEF exchanges GDP for GTP. The GAP induces the GTPase activity of Rac. The GDI binds the GDP inactive form and makes it soluble in the cytosol by covering its lipid group. Rac, Rho and Cdc 42 are post-translationally modified by attachment to a farnesyl geranylgeranyl group. When Rac is active the lipid is inserted into the plasma membrane. Inactivated Rac, bound to its GDI is soluble in the cytosol because the GDI shields the hydrophobic lipid modification. Whether Rac can remain attached to the membrane in its GDP bound form is not known. This figure depicts Rac interaction with the adherens junction based on current models:

1. GDP-Rac-GDI is bound by Tiam1 (a GEF).
2. Tiam1 facilitates GTP-GDP exchange for Rac and inserts the lipid farnesyl geranylgeranyl group into the plasma membrane.
3. GTP-Rac binds to IQGAP1, a GTPase activating protein that attaches to  $\beta$ -catenin. Because IQGAP1 is bound to  $\beta$ -catenin, it sterically inhibits  $\alpha$ -catenin association and formation of the adherens junction. GTP-Rac removes IQGAP1 from  $\beta$ -catenin, permitting adherens junction formation and stable cell-cell adhesion.
4. IQGAP1 induces GTP hydrolysis. GDP-Rac dissociates from IQGAP1, and the GDI binds Rac again. The GDI covers the farnesyl group, allowing GDP-Rac-GDI complex to move into the cytosol. Presumably the IQGAP1 mediates a specific activity once it has dissociated from Rac (it is likely involved in structural modification of the actin cytoskeleton).

Figure 2



the chromosome, it would not affect their patterns of expression because the promoters and transcription factors that lead to E-cadherin transcription have not been changed.

Li et al. (Li et al., 1998), and Mege et al. (Mege et al., 1988) transfected carcinomas lacking E-cadherin with cDNAs of full length L-CAM. As with E-cadherin transfections, the L-CAM protein caused a change in the cell morphology from squamous and pleiomorphic to epithelioid (Chen and Obrink, 1991; Navarro et al., 1991). In addition, similar to E-cadherin, L-CAM induced density-dependent growth inhibition. Because of the similarities between these proteins, information about the structure and function of L-CAM is also likely to be true for E-cadherin.

### Protocadherin Background

Protocadherins are characterized as having more than five extracellular cadherin domains, and variable cytoplasmic sequences (Marrs and Nelson, 1996; Wu and Maniatis, 1999). Some protocadherins can induce calcium dependent cell-cell adhesion (Sano et al., 1993) although it is not believed to be their primary function because they are not known to associate with the cytoskeleton (Suzuki, 1996). Protocadherins are distinct from the other cadherin subgroups in that the extracellular regions are encoded by unusually large, uninterrupted exons (Wu and Maniatis, 1999; Wu and Maniatis, 2000). All of the other known cadherin groups have at least two introns breaking up the sequences coding the extracellular region (Wu and Maniatis, 1999; Wu and Maniatis, 2000). Protocadherins are highly conserved in a variety of animal phyla, but an understanding of their functions has only recently begun (Sano et al., 1993; Suzuki, 1996). To date, most protocadherins have been found to function at synaptic junctions (Shapiro and Colman, 1999; Wu and Maniatis, 1999; Wu and Maniatis, 2000). The extensive variety of these proteins found in neural cells suggests a mechanism by which cells of the brain can segregate during development and maintain their specific synaptic connections (Shapiro and Colman, 1999). Protocadherins have roles in nonneural tissue as well. A novel  $\mu$ -protocadherin is essential to the branching of primordial kidney and lung in mice. Its structure is unusual in that it contains mucin-like repeats in its extracellular domain, and SH3 binding regions in its cytoplasmic domain (Goldberg et al., 2000).

Some cadherins that were classified as protocadherins have been assigned their own grouping. Fat proteins contain 34 cadherin ectodomains, and have sequences resembling the  $\beta$ -catenin binding region of the classical cadherins in their cytoplasmic domains (Wu and Maniatis, 2000). Their cadherin ectodomains more closely resemble

the protocadherins than the classical cadherins. However, unlike protocadherins, the sequences of ectodomains display variable intron/exon organization (Wu and Maniatis, 2000). Flamingo proteins have cadherin repeats that resemble the protocadherins, and their ecto-domain sequences lack introns. Flamingo is unique in having seven transmembrane domains, with very tight, hairpin turns between membrane passes (Wu and Maniatis, 2000). Another group of cadherins that are found in *Drosophila* are named after classical cadherins because their cytoplasmic domains interact with the catenin homologues (i.e. Armadillo and D $\alpha$ -catenin) (Oda et al., 1994). However, their extracellular domain sequences more closely resemble protocadherins than classical cadherins and they contain fewer introns. Also, both DN-cadherin and DE-cadherin have more than 5 ectodomains, although EC1 of DE-cadherin is cleaved during its maturation (Wu and Maniatis, 2000).

### Desmosomal Cadherin Background

Desmosomes form a distinct group of cell-cell junctions. They were first discovered by electron microscopy of epithelial cells and are noted for forming an electron-dense cytoplasmic plaque (Farquhar and Palade, 1965). Since their discovery, the group of proteins making up the plaque have been elucidated. Attaching to the desmosomal cadherins is plakoglobin, a catenin that is a homologue of the *Drosophila* protein Armadillo and the vertebrate catenins  $\beta$ -catenin and p120 catenin. Plakoglobin binds to desmoplakin, which can self associate to mediate clustering of desmoplakin-plakoglobin-cadherin complexes into a tightly packed plaque (Kowalczyk et al., 1997). Desmoplakin also binds to the intermediate filament cytoskeleton, which firmly anchors the plaque (Klymkowsky and Parr, 1995). Desmosomes are the adhesion junctions most capable of absorbing stress and distributing it throughout the epithelium (Legan et al., 1992). Because of their shape and durability, they are described as “riveting” cells together.

Desmosomal cadherins are similar to classical cadherins in their extracellular domains, but divergent in their cytoplasmic regions (Collins et al., 1991; Koch et al., 1990). There are two subclasses of desmosomal cadherins: desmogleins and desmocollins (Cowin et al., 1984). These desmosomal cadherin types differ from each other structurally, which likely reflects functional differences, since desmogleins and desmocollins are expressed in different tissue types and developmental stages. These cadherin groups have divergent sequences, and likely were only grouped together because of they form desmosomes (Buxton et al., 1993). Desmocollins have two

differentially spliced variants in their cytoplasmic domain sequences, with one variant closely resembling the classical cadherin cytoplasmic domain (Marrs and Nelson, 1996). Desmogleins are unique in that they contain an extra carboxy terminal domain of ~29 amino acids (Buxton et al., 1993).

### **Classical Cadherin Structure**

Most classical cadherins have a relative molecular mass of ~120kDa, and contain five potential glycosylation sites on their extracellular domains [Pouliot Y., 1992]. Classical cadherins have a common topology beginning with 10kDa cleaved pro-peptide, five extracellular domains, a transmembrane domain, and a cytoplasmic domain (Ranscht, 1994). The extracellular domains homotypically link cadherins to cadherins from other cells, while the intracellular domain forms a dynamic protein complex with the catenins and components of the actin cytoskeleton. Cadherins are believed to associate in two ways. The *cis* interaction is where cadherins of the same cell form homophilic dimers or groups via lateral or parallel interactions. The *trans* interaction is where cadherins of adjacent cells form multiple anti-parallel interactions that adhere cells to each other.

### **Common Characteristics of the Extracellular Domains**

The five cadherin extracellular domains share a basic folding topology: seven  $\beta$ -strands arranged in two  $\beta$ -sheets, such that the amino and carboxy termini emerge from opposite ends of the domain (Shapiro et al., 1995a). The five domains also contain large hydrophobic amino acids at each domain's center. Cadherin domains retain the same folding topology as a result of six highly conserved regions that are buried or in turns. They are essential for the  $\beta$ -sheets to fold back on themselves and create characteristic bulges in the  $\beta$ -barrel structure (Overduin et al., 1995).

Due to their overall shapes, the cadherin extracellular domains are known as  $\beta$ -barrels (Overduin et al., 1995). Regions of the cadherin domains that face an adjacent domain contain highly conserved calcium coordinating sequences (Figure 3) (Nagar et al., 1996; Overduin et al., 1995; Shapiro et al., 1995a). The binding region near the carboxy end of the domain contains the Pro-Glu-Asn-Glu (PENE) and Leu-Asp-Arg-Glu (LDRE) sequences. The other half of the calcium-binding region, which is near the amino end of the domain, contains the Asp-Ala-Asp (DAD) sequence. Calcium is essential to the structural integrity of the cadherin's extracellular region because it gives

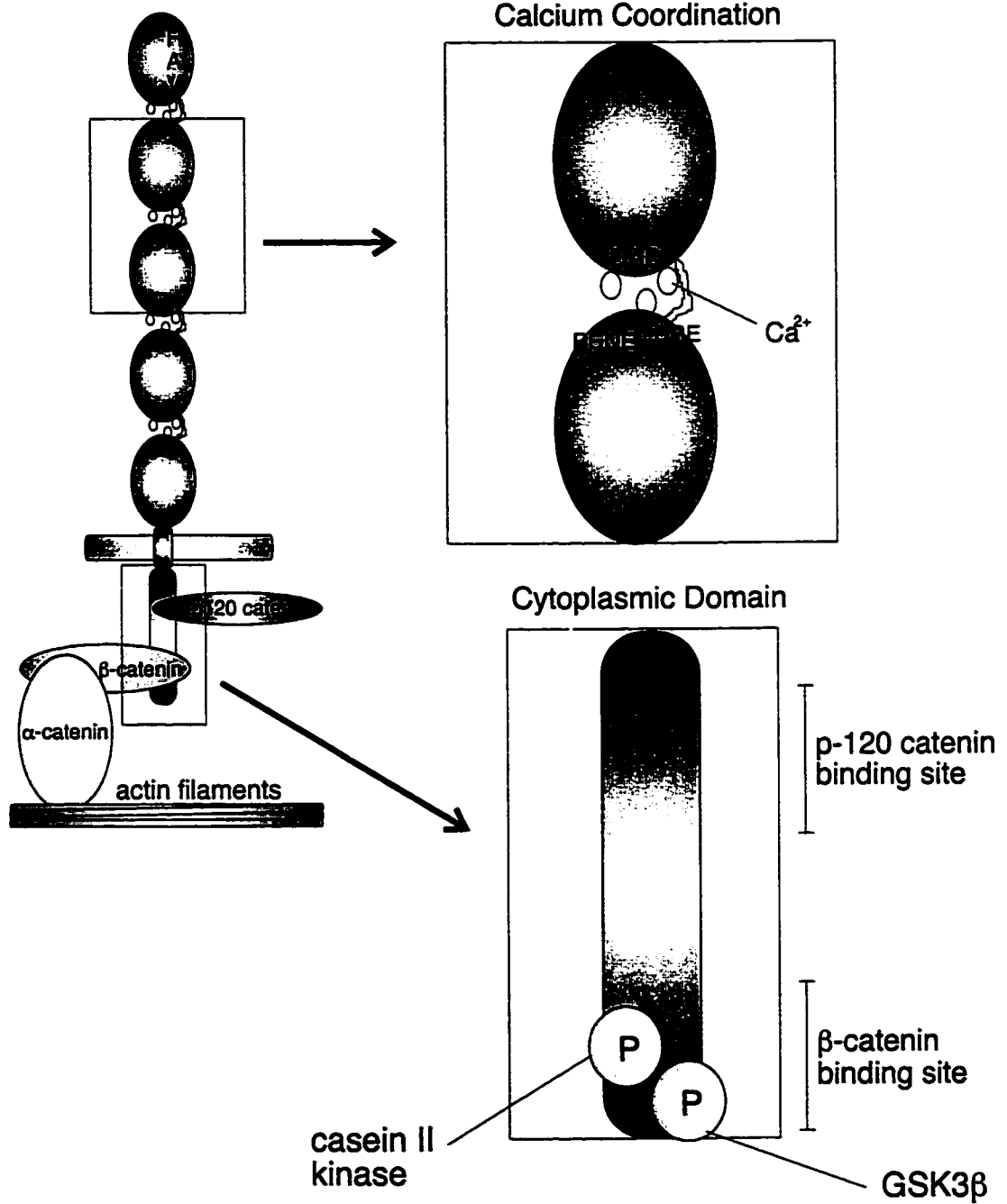
### **Figure 3: Cadherin Structure**

The structure of L-CAM is depicted as an integral membrane protein with 5 extracellular domains, a transmembrane domain and a cytoplasmic domain. Each domain is linked by a flexible stretch of amino acids centered on a proline residue (Gallin, 1998).

Regions of the extracellular domains that are adjacent to each other coordinate calcium ions, which maintain the protein in an active conformation that allows cell-cell adhesion, and protects it from proteolysis. The sequences involved in calcium coordination are highly conserved (DAD, PENE, and LDRE), and are consistent between each domain border in all classical cadherins. Classical cadherins bind to  $\beta$ -catenin and p120 catenin on the cytoplasmic domain. The p-120-catenin binding site is between amino acids 758-774 in E-cadherin (Thoreson et al., 2000). The role of p120-catenin is not fully understood, but it is believed to be involved in regulation of the adherens junction.  $\beta$ -catenin binds  $\alpha$ -catenin, which in turn binds to the actin cytoskeleton. The site of  $\beta$ -catenin binding is between amino acids 833-862 in E-cadherin (Lickert et al., 2000). Two phosphorylation sites have been discovered in this region that have been shown to increase the affinity of E-cadherin and  $\beta$ -catenin. The phosphorylations were at consensus sequences corresponding to casein II kinase and GSK 3 $\beta$  (Lickert et al., 2000)..



# Figure 3: Cadherin Structure



the protein a stable conformation that allows it to perform its function. Calcium also appears to maintain the domains in a configuration that partially protects the extracellular region from protease degradation (Stappert and Kemler, 1992). Cadherins are extremely sensitive to the loss of calcium binding, such that a single substitution in one calcium binding site is enough to abolish adhesion (Ozawa et al., 1990).

#### Extracellular domains 1-5

The first extracellular domain (EC1) has been studied extensively in the past because it is believed to contain the adhesive interfaces important to cell-cell adhesion and in some cases, lateral dimerization. Details of the first domain will be discussed with the models of cadherin based adhesion. The domains 2-4 have not been extensively studied, so their functional significance is unknown. However it is possible that these domains participate in weak adhesive interactions between cadherins of adjacent cells in fully or partially intercalated interactions (Sivasankar et al., 1999).

The fifth extracellular domain of classical cadherins is distinct from the others, in that it contains four characteristic cysteine residues (Suzuki, 1996). The function of these residues is not known, but they may act to strengthen the intra-domain structure of EC5 (Sivasankar et al., 1999). Reinforcement of the domain would imply that it must withstand a higher level of stress than its counterparts. A fully intercalated interaction may require that EC1 be tightly bound to EC5, and its unusual features may have evolved to accommodate those needs. Although it shares the general topology of the cadherin motif, this domain was not always considered to be like its counterparts because its sequence is quite different (Tanihara et al., 1994). Its calcium binding regions have occasional differences in their amino acid sequences when compared to the other highly conserved domains (Shapiro et al., 1995a). Because of this, domain 5 was not thought to bind calcium (Ranscht, 1994).

#### The transmembrane domain

The region that bridges the extracellular domains to the cytoplasmic domain is a stretch of ~25 amino acids that passes through the membrane once (Rimm and Morrow, 1994). The transmembrane segment (TMS) is well conserved among different cadherin family members (Huber et al., 1999). Its abundance of leucine residues has been shown to contribute to cadherin lateral dimerization. The transmembrane regions pack with each other, to facilitate clustering of cadherins (Huber et al., 1999). Mutations of a

stretch of leucines to prolines (to produce kinks in the structures) impaired adhesion in aggregation assays, implying that this packing is important to the formation of *trans* interactions that are stable and can withstand tension (Huber et al., 1999).

### Cytoplasmic Domain

The cytoplasmic segment links cadherins to the actin cytoskeleton. Because of the connection with the cytoskeleton, cells are firmly anchored to each other at the adherens junction. In an experiment where the effects of clustering on adhesive strength were assessed, the cytoplasmic domain was removed. Although cadherins were clustered, they could not withstand shearing forces of the magnitude that the full-length cadherin molecule could tolerate and the cells dissociated (Yap et al., 1997). Previous experiments where cadherin function was tested with aggregation assays revealed that cytoplasmic domain-deleted cadherins could not mediate cell adhesion (Nagafuchi and Takeichi, 1988; Ozawa and Kemler, 1998a; Ozawa and Kemler, 1998b). The cadherin cytoplasmic segment is more consistent among cadherin classes than EC1, implicating the importance of its conserved interaction with cytoplasmic binding partners (Rimm and Morrow, 1994). The cytoplasmic domain can be divided into three sub-domains: juxtamembrane, intermediate, and  $\beta$ -catenin binding. These regions are important for different aspects of cadherin function. The juxtamembrane region can bind p120 catenin (whose role in adhesion remains unclear) (Aono et al., 1999; Thoreson et al., 2000; Yap et al., 1998). The  $\beta$ -catenin binding region can be phosphorylated by casein II kinase, then GSK-3 $\beta$ . These phosphorylations lead to an increase in affinity between  $\beta$ -catenin and the cadherin and result in more stable cell-cell adhesion (Figure 3)(Lickert et al., 2000).

### Models of Adhesive Mechanisms

Several independent reports have arisen describing different mechanisms of *cis* and *trans* associations. Most of the lateral association theories are inconsistent with each other, and in this summary an attempt is made to clarify some of the observations.

#### ***cis* Interaction**

Although there are several contradictory models of *cis* interaction, it is a widely accepted phenomenon. The collective association of many closely clustered cadherins

would more effectively mediate adhesion to an adjacent cell than scattered independent cadherins along a broad surface of the plasma membrane. There are three main models to which most of the data can be grouped: strand exchange, calcium sharing, and catenin bridge (Figure 4).

#### *Strand Exchange Dimers*

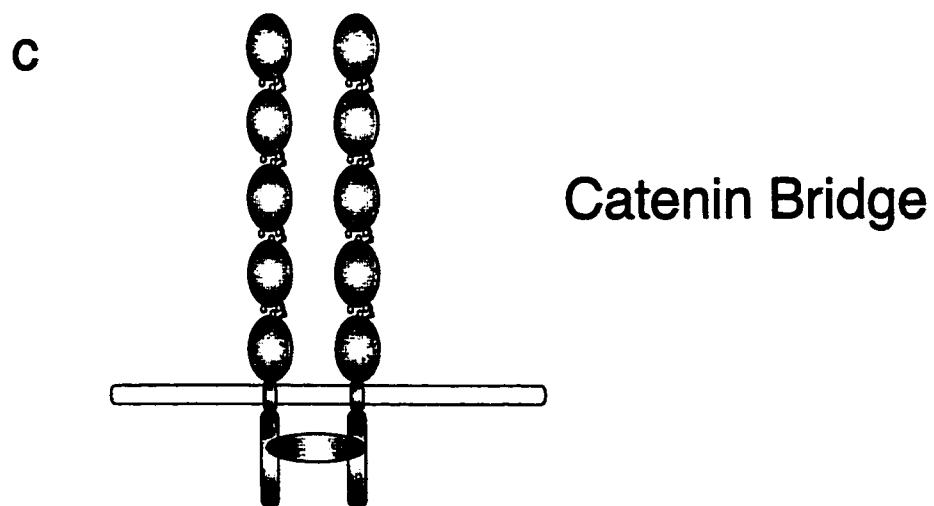
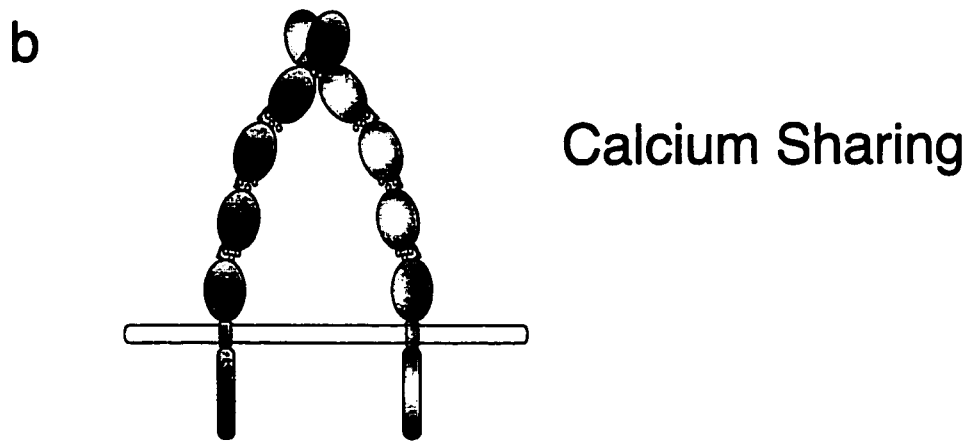
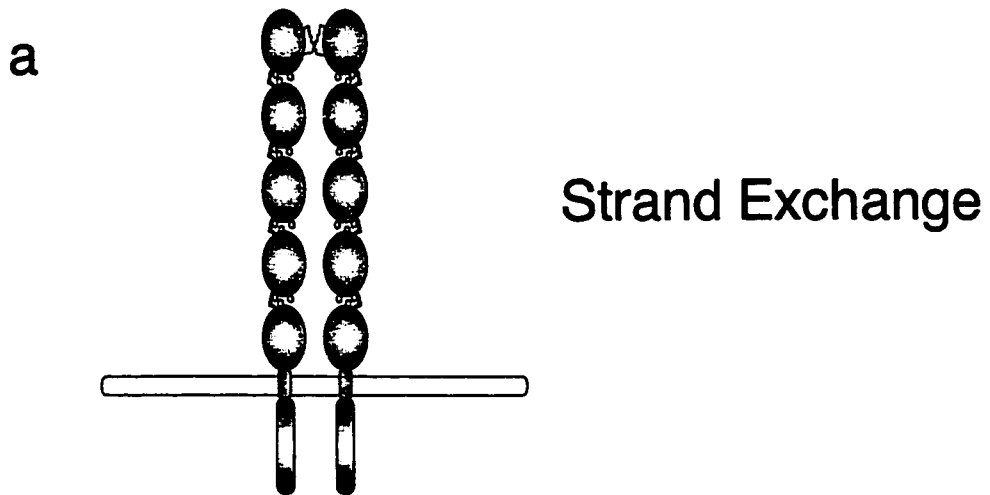
The strand exchange model proposes a crossover of cadherin ligands, forming pairs of cadherins on surface of the cell (Shapiro et al., 1995a; Tamura et al., 1998). Using crystallographic structural analysis, Tamura et al. (Tamura et al., 1998) have visualized N-cadherin's first extracellular domain and noted a depression lined with small hydrophobic residues proximal to the protruding Trp 2. The amino terminus of one cadherin is proposed to insert its Trp 2 into a hydrophobic pocket of the adjacent cadherin's first domain. Mutation of the Trp2 to Tyr and Ala abrogated adhesion. Another mutation of a small Ala residue that lines the pocket, to a larger Met residue disrupted cell-cell adhesion (Tamura et al., 1998). Strand exchange interactions between each domain are also thought to occur along the entire extracellular surface of the cadherins. The dimers formed on the plasma membrane could then associate with dimers of an adjacent cell to form an adhesion zipper (Figure 4) (Shapiro et al., 1995b).

Calcium independent dimerization has been shown previously by Brieher et al. (Brieher et al., 1996). They constructed a C-cadherin peptide of the entire extracellular sequence that could form dimers in the presence and absence of calcium. Dimers that formed in the absence of calcium as well as monomeric peptides were adhered to beads, and exposed to calcium in an aggregation assay. Only the beads with dimers aggregated extensively, leading them to conclude that the calcium independent interaction was the *cis* interaction and the calcium dependent dimers formed the *trans* interaction.

#### **Figure 4: Models for *Cis* Dimerization**

Cadherin lateral dimerization is not fully understood. There are three models for the mechanism of this interaction. The first of these models suggests that Trp2 of the cadherin amino terminus is inserted into a hydrophobic pocket of an adjacent cadherin. The adjacent cadherin, in turn, inserts its Trp2 into the pocket of the first cadherin. This exchange of strands mediates grouping of cadherins (A). The second model depicted proposes that the interdomain calcium coordination can be shared between two cadherins. This sharing of calcium would mediate dimerization (B). The third model reveals a mechanism of dimerization that involves one or more cytoplasmic proteins that group cadherins via the cytoplasmic domain (C).

## Figure 4: Models for Cis Dimerization



### *Calcium Sharing*

The model proposed by Nagar et al. (Nagar et al., 1996) suggests dimerization is mediated by two cadherins coordinating calcium ions between extracellular domains 1 and 2. The studies performed by this group used X-ray crystallographic analysis, and NMR to study EC1 and EC2 of E-cadherin. The conformation of cadherins that share calcium is kinked, and will only allow a dimerization association between the first and second domain.

Tomschy et al. (Tomschy et al., 1996) support the theory of a calcium dependent lateral association with experiments that propose that EC1 is the site of both parallel and anti-parallel associations. They constructed two mutants: E-cadherin extracellular region and E-cadherin extracellular domains connected to cartilage oligomeric matrix protein (E-cadherin-COMP). In solution, the E-cadherin-COMP constructs would associate with each other at the COMP region (Figure 5). Tomschy et al. (Tomschy et al., 1996) suggested these complexes represented E-cadherin behavior on the membrane surface due to the close association of many E-cadherin molecules. Analytical ultracentrifugation revealed that the monomeric extracellular E-cadherins failed to associate with each other, while E-cadherin-COMP complexes formed aggregates, based on a broad sedimentation profile. E-cadherin molecules that were examined with negative staining electron microscopy demonstrated that extracellular domain E-cadherin remained in monomers, while the E-cad-COMP bound to other E-cad-COMP complexes (Tomschy et al., 1996). On the E-cad-COMP molecule, the E-cadherin domains point away from the COMP domains in a conformation resembling a star. Within the star structure the E-cadherin molecules appear to form rings, indicative of a lateral dimers. Dimer formation of E-cad-COMP complexes occurs where two rings appear joined. The joining of these rings represents the anti-parallel interaction that occurs between cadherins of adjacent cells. While the proof seems adequate, conformation of the E-cad-COMP would have made it difficult for lateral associations involving EC2-EC5 to occur. This data supports an interaction between EC1s of different cadherins in lateral and anti-parallel associations, but because of potential strain of the molecule, it cannot be assumed that EC1 is the only cadherin domain involved in the cell-cell interaction.

Pertz et al. (Pertz et al., 1999) offer supporting data to the mechanism of lateral association proposed by Nagar et al. (Nagar et al., 1996). E-cad-COMP peptides were exposed to increasing calcium concentrations. In low calcium there were no rings of dimers or anti-parallel interactions, but as the calcium concentration increased, lateral dimers formed. When the concentration reached physiological levels, many E-cad-

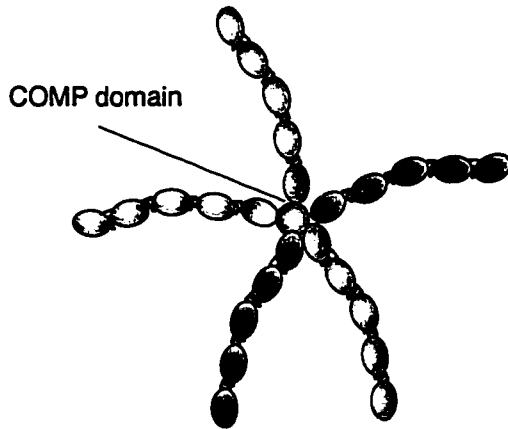
**Figure 5: Cadherin Constructs Interactions Studied Using Cartilage Oligomeric Matrix Protein**

Tomschy et al. [1996] constructed an E-cadherin chimera involving the COMP molecule. They substituted the transmembrane and cytoplasmic domains with COMP and observed the complexes it formed in solution by negative staining TEM. Cadherins associated via the COMP complexes whereby the COMP regions cross-linked with each other in the centre of the complex and the cadherin extracellular regions pointed outward resembling a star (A). Lateral dimers were believed to form when they observed a ring within an E-cad-COMP complex (B). *Trans* associations were observed when two or more E-cad-COMP complexes were in association with each other (C).

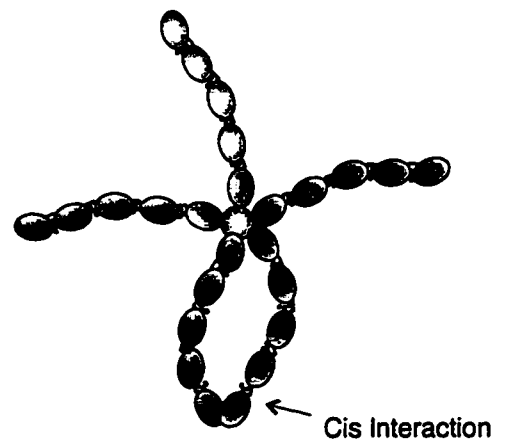


# Figure 5: Cadherin Interactions Studied Using Cartilage Oligomeric Matrix Protein (COMP)

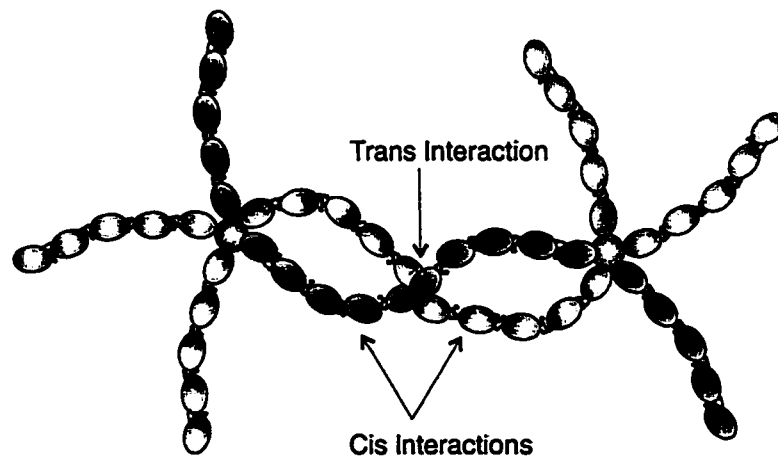
**a** Association of Cadherins via COMP Molecules



**b** Dimer Formation within the E-cad-COMP complex



**c** Association of Two E-cad-COMP Complexes



COMP complexes had formed dimers and anti-parallel interactions. From this they proposed a two step interaction to the adhesion process where the *cis* association, must precede the *trans* association. Pertz et al. (Pertz et al., 1999) confirm the necessity of Trp 2 and the hydrophobic pocket described by Tamura et al. (Tamura et al., 1998), although they do not support strand exchange between cadherins. Instead of fitting into a hydrophobic pocket on an adjacent cadherin, Trp 2 is proposed to fit into the pocket on its own first domain. This implies that calcium dependent dimers form and cause a conformational change that induces Trp 2 to fit in the pocket of EC1, initiating the exposure or activation of the adhesive interface and permitting the cadherins to form the *trans* interaction.

### *Catenin Bridge*

This model for a *cis* interaction proposes that lateral adhesion is mediated by a catenin linking two cadherins. Yap et al. (Yap et al., 1998) constructed a C-cadherin construct with its cytoplasmic domain replaced with three repeats of the FK506-binding protein. Lateral cadherin aggregates were induced by the addition of the drug FK1012 to the cell medium, which bridges the binding proteins together bringing the cadherins into close association on the plasma membrane. Association was then measured with a sensitive laminar flow assay. Their analysis revealed that clustering confers an increase in binding strength, and that cadherins could maintain a substantial degree of binding even in the absence of interaction with the cytoskeleton. Because this interaction could not occur without addition of the binding protein to the medium, they concluded that the surface of lateral dimerization was not located on the extracellular domain and that some portion of the cytoplasmic domain is responsible for this association (Yap et al., 1998). To test which region is responsible for lateral association they created constructs that substituted defined regions of the cytoplasmic domain with myc tag regions. They found that cadherins that retained the juxtamembrane region of the cytoplasmic domain without the  $\beta$ -catenin binding region mediated adhesion. Only cadherins containing the juxtamembrane region could cluster. Yap et al. (Yap et al., 1998) then tested by blot overlay whether the juxtamembrane region could associate with itself. Because it could not self associate they used GST-associated juxtamembrane peptides to seek potential binding partners. The protein p120 catenin (Reynolds et al., 1996) co-precipitated with the construct, raising the possibility that p120 catenin forms a bridge between cadherins (Yap et al., 1998). If lateral dimerization must be mediated by another protein whose association with the cadherin can be controlled, then their evidence supports their

original theory that cells can control the degree of clustering through dimerization in order to achieve a gradation of strength of cadherin adhesiveness.

### ***trans Interactions***

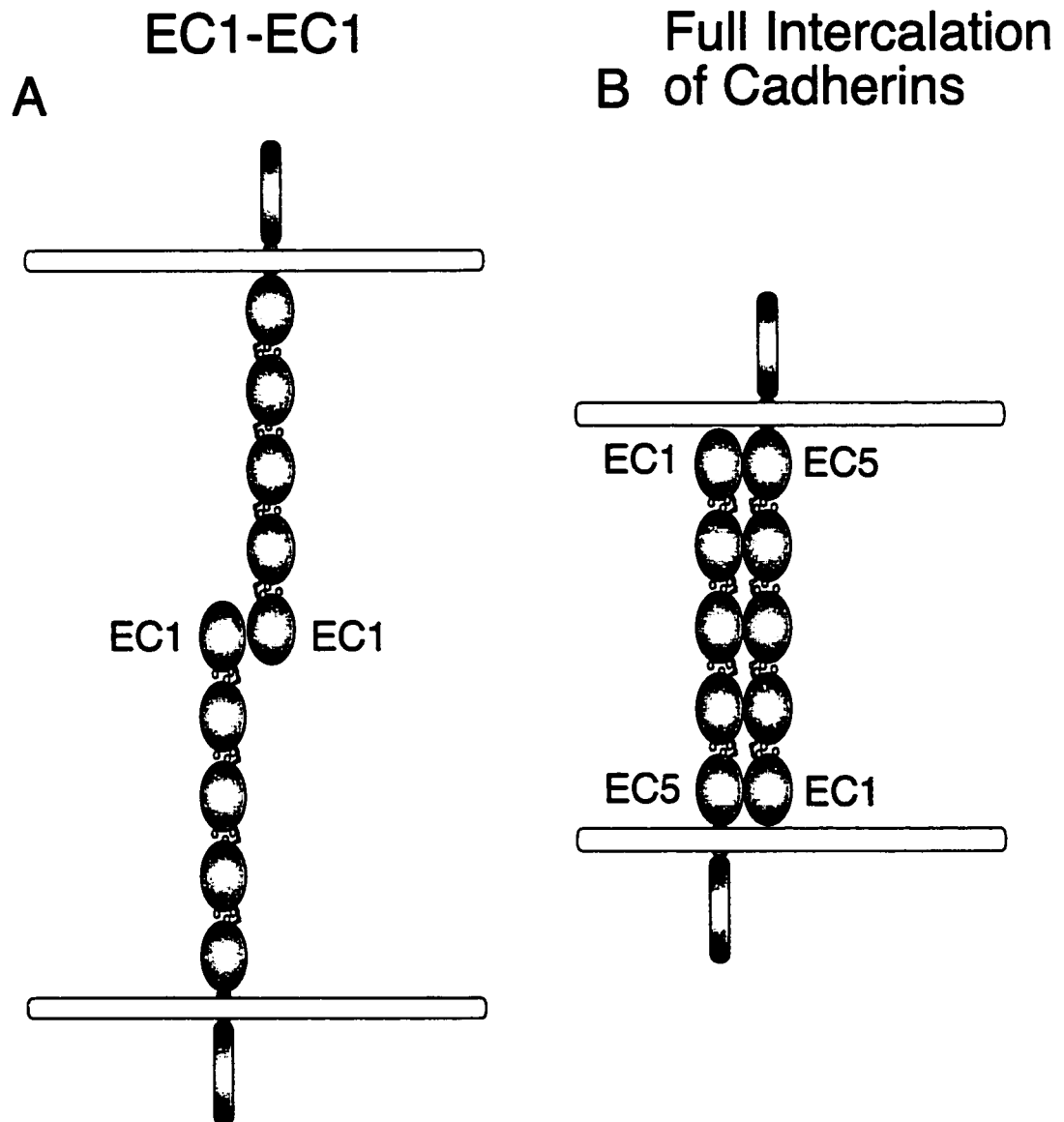
The anti-parallel interaction is a bond between cadherins of different cells, and the presumptive site of homotypic binding. This adhesive site is characterized by the tripeptide His-Ala-Val (HAV). The mechanism of this interaction has yet to be deciphered. Most current evidence indicates that cell-cell adhesion is restricted to the EC1 domain. The first extracellular domain is believed to contain the most important region of homophilic cadherin binding (Nose et al., 1990). Chimeras of E- and P-cadherin were constructed and their adhesion was tested against full length E- and P-cadherins. Binding specificity to the full-length protein was only altered when the contribution of the other protein consisted of the first extracellular domain, or small regions within it (Nose et al., 1990). The specificity determining sites were found to lie within first 113 residues of the first extracellular domain. Two of the chimeras that were altered within this region were capable of adhering with E- and P-cadherin. Altering some residues allowed the mutant cadherin to bind a cadherin whose sequence contained the same residues, but because other specific sequences necessary for binding the original cadherin type were left unaltered, the mutant cadherin could still bind its parent molecule (Nose et al., 1990). Also, this region contained the binding sites for function blocking antibodies to E- and P-cadherins. Overduin et al. (Overduin et al., 1995) have proposed that the homophilic binding sequence is surrounded by amino acids that project from the cadherin domain, restricting access to only the cadherin that can provide the perfect fit. Only the same cadherin type would have the complimentary sequence that can access the region of the adhesive interface (Figure 6).

Although the exact regions of the first domain that cause strong and specific binding in classical cadherins are unknown, there is a highly conserved sequence of three amino acids (His-Ala-Val) that are thought to be important to homophilic cell-cell adhesion (Overduin et al., 1995; Shapiro et al., 1995a). Arrival at the theory that HAV mediates cadherin cell-cell adhesion stems from an observed sequence similarity between classical cadherins and hemagglutinins from influenza strain A. Hemagglutinins are integral membrane proteins that mediate attachment and fusion of influenza virus to upper respiratory tissue in mammals and birds (Blaschuk et al., 1990a). This protein forms a homotrimeric complex: each subunit is composed of two covalently linked chains HA1 and HA2. These chains are characterized by the presence

### **Figure 6: Models for *Trans* Interaction**

There are two main models regarding the cell to cell or *trans* interaction. One model is that cell-cell adhesion is mediated by interactions of the first extracellular domains (EC1) (A). Support for this model stems from numerous function-blocking antibodies that are specific to the first extracellular domain, and specificity determining sites found in the first extracellular domain. The other model suggests that cadherins interact in a manner in which each domain participates in the adhesive interaction (B). Support for this model was obtained with an experiment that measured molecular forces of multiple adhesive interactions. The point of greatest adhesion corresponded to the length of one cadherin extracellular region, insinuating that the adhesive interaction is mediated by all five extracellular domains.

Figure 6: Models of Trans Interaction



of the dipeptide HA followed by a Val or Asn. Crystallographic analysis of the hemagglutinin indicates that the His of HA1 forms hydrogen bonds with two Ile of HA2, causing the amino terminus of HA2 to be buried in the homotrimeric complex. Blaschuk et al. (Blaschuk et al., 1990a) draw attention to what they believe is a significant similarity between amino acid sequences of cadherins and hemagglutinins. However, one cannot assume this sequence similarity reflects a functional similarity. There were large gaps in the hemagglutinin sequence between regions that shared the most similarity, implying that the match was more coincidental than a reflection of relatedness [sequence comparison in Blaschuk, 1990 #104]. Seeking to verify the significance of HAV to cadherin based adhesion, Blaschuk et al. (Blaschuk et al., 1990b) tested a variety of CAR sequences (cell adhesion recognition) of three or more residues that were common to the first extracellular domains of the classical cadherins L-CAM, N-cadherin, P-cadherin, and E-cadherin. An example of a known CAR sequence is RGD, which is known to mediate adhesion for ECM proteins such as fibronectin. Three possible CARs were found that were consistent within this group of cadherins: PPI, GAD, and HAV. Only HAV-containing peptides prevented compaction in the eight-cell stage mouse embryo (Blaschuk et al., 1990b). However, it should be noted that the peptide sequences they used consisted of 10 amino acid residues. The shorter sequence of 6 residues inhibited compaction in 30% fewer embryos than the 10 amino acid peptide. There is doubt that HAV is absolutely crucial to binding since many non-classical cadherins do not have HAV, yet are still capable of adhesion (Tanihara et al., 1994). In some cases these cadherins contain amino acids in that region that are structurally similar to the ones in classical cadherins (e.g. Leu for Val, Arg for His, Gln for His).

Although the theory behind HAV mediating cadherin binding is weak, the evidence presenting HAV peptides as cadherin inhibitors has been supported (Noe et al., 1999; Sander et al., 1998). If HAV mediates the *trans* interaction of cadherin based adhesion, then it acts in one of two ways. One mechanism of HAV-mediated binding may be through a direct connection of the HAV sequences: i.e. HAV of both cadherins interact with each other, and the amino acids surrounding the sequence merely permit the HAVs to come within close proximity. Adhesion may also be mediated through HAV interacting with entirely different residues from another region of the binding partner's extracellular domain: HAV binds to a region that is closer to the carboxy terminal than the HAV of the other cadherin. Based on the proposed mechanism of HAV-mediated binding by the influenza hemagglutinins, the mechanism of HAV mediated *trans* interaction would likely be the latter because the His-Ala side chains are

proposed to hydrogen bond to two Ile in the amino terminus of the other chain (Pouliot, 1992).

The theory that cadherins might fully intercalate has only recently begun to be investigated. Sivasankar et al. (Sivasankar et al., 1999) bound C-cadherin extracellular domains to a substrate and spaced two plates at a distance equal to the length of one cadherin extracellular region. They then proceeded to gently pull the plates apart and measure the points of maximum resistance. Distances with the maximum resistance can be inferred to correspond to the points of the strongest cadherin-cadherin interaction. Full intercalation of the extracellular region had the highest resistance (Sivasankar et al., 1999). It is possible that the unusual features of the fifth extracellular domain are evolved to interact with EC1. All previous evidence has proven the importance of the first extracellular domain. The possibility of a *trans* interaction occurring with any other extracellular domain had not been investigated (Figure 6).

### **Objectives**

The objective of this project is to determine how each portion (or domain) contributes to specific aspects L-CAM function. Many experiments testing the function of the cadherins have shown that the first domain is important to adhesive function, but the contribution of the other domains has yet to be elucidated. The effect of deletion of the first extracellular domain on cell-cell adhesion was examined, and the results of aggregation and coaggregation experiments have lead to insight about the adhesive roles of the other cadherin domains.

Point mutations within a domain make it possible to focus on the precise part of the molecule that is essential for its function. For this reason, the presumptive site of homophilic cadherin binding has been altered to read Val-Ala-His instead of His-Ala-Val, to determine whether these three amino acids are the regions of homophilic cadherin binding.

Aggregation assays were performed to determine if the mutated cadherins' can cause cells to aggregate in a manner comparable to the unmutated protein (Hoffman, 1992). Coaggregation assays were used to find out if the mutant cadherins could aggregate with unmutated protein (Hoffman, 1992). Changing the protein may not have disabled the interaction with the same mutant, but may have rendered it unable to bind the wild type protein. Also, if the mutation disabled the protein's ability to interact with itself, it may still have regions that can interact with the unmutated L-CAM.

## Methods and Materials

### *Cell Line*

The S180 cell line was obtained from the axial tip of a transplanted mouse sarcoma (Dunham and H.L., 1952). S180 cells are spindle shaped and resemble fibroblasts. They do not express any known cadherins, making them ideal for observing the effects of cadherin transfection.

### *Construction of L-CAM expression plasmid*

The 5' end of the L-CAM reading frame was amplified from the original L-CAM cDNA clone (Gallin et al., 1987) using primers WJG1003 and WJG1004 (Table 1) and digested with NheI and KpnI. The KpnI/BamHI fragment containing the 3' half of the reading frame was isolated from plasmid L-CAM KB4 (Gallin et al., 1987). pBK-CMV expression vector was modified by digestion with EcoRI and KpnI followed by polishing with Mung Bean nuclease and ligation to remove part of the polylinker. The resulting vector (pBK-CMV  $\Delta$ E/K) was digested with NheI and BamHI and a three fragment ligation was performed. The entire insert of the resulting plasmid was completely sequenced to confirm that no PCR errors had been introduced. The plasmid construct is depicted in Figure 7B.

### *Construction of HAV/VAH plasmid*

The HAV/VAH mutant was created by overlapping PCR mutagenesis. Two fragments were amplified from L-CAM plasmid template using (a) primers WJG1034 and WJG1045 and (b) primers WJG1058 and WJG1042. The resulting PCR products were gel purified and a mixture was used as a template, amplified with primers WJG1034 and WJG1042 (Table 1). The resulting PCR product was digested with XhoI and KpnI, ligated into the wild-type pBK-CMV-LCAM plasmid that had also been digested with XhoI and KpnI and transformed into *E. coli* and a cloned plasmid was isolated. The sequence of the resulting insert was determined to confirm that only the designed mutation had been introduced into the L-CAM sequence. The plasmid construct is depicted in Figure 7B.



**Table 1: PCR Primers**

<b>Primer</b>	<b>Description</b>	<b>Sequence</b>
WJG1003	L-CAM 5' end, sense, for expression	GGGCTAGCGGCCCGGTCCCTGAGCC
WJG1004	L-CAM 5' end, antisense, for expression	TTGTTGGATTTGATCTGCACC
WJG1006	L-CAM 5' end, antisense	CGTTCTCCTCGATGTAGCC
WJG1034	LCAM359-376	CAGCTTCACCATCTACGC
WJG1035	LCAM828-846	GACCAGAACGACAACAAGC
WJG1036	LCAM1219-1240	TGGAAGAGAATAAGCCAGGTAC
WJG1037	LCAM2129-2146	AGGGACAGCCAAGAAGCTG
WJG1038	LCAM2481-2498	ATCGGGAAGCTTCATCGAC
WJG1039	LCAM618-599	TGTCCTTGTTGGATTTGATC
WJG1040	LCAM1029-1010	GGTCAATGGTGAACATCTGG
WJG1041	LCAM1459-1442	GACAGGGGCACTTTGTTC
WJG1042	LCAM1950-1930	CCTTGAAGGGGTAGGTATGTG
WJG1043	LCAM2337-2316	CCTCCTCGTCGTAGTTGTAGAC
WJG1045	HAV-VAH AS	GTGGGCCACGGATAAGAGGGTGTAGCGA
WJG1058	HAV-VAH SII	CTCTTATCCGTGGCCCACTCGGCCAGCGGGCA
WJG1046	D1A	TGAACACGGGCTCTTCTGCCTCGGGAG
WJG1047	D2B	GCAGAAGAGGCCCGTGTTCATCAAGGAGG

**Table 1**

List of primers used to make the wild-type L-CAM as well as the HAV/VAH and  $\Delta I$  mutants. These primers were also used for sequencing the plasmids and PCR products for confirmation of identity. The location of the corresponding sequences in the expression plasmid are marked on Figure 7B.

### *Construction of $\Delta I$ plasmid*

The  $\Delta I$  mutant was created by overlapping PCR mutagenesis. Two fragments were amplified from L-CAM plasmid template using (a) primers WJG1034 and WJG1046 and (b) primers WJG1047 and WJG1042. The resulting PCR products were gel purified and a mixture was used as a template, amplified with primers WJG1034 and WJG1042 (Table 1). The resulting PCR product was digested with XhoI and KpnI, ligated into the wild-type pBK-CMV-LCAM plasmid that had also been digested with XhoI and KpnI transformed into *E. coli* and a cloned plasmid was isolated. The sequence of the resulting insert was determined to confirm that only the designed mutation had been introduced into the L-CAM sequence. There were two undesigned mutations found, one converting an arginine to a proline in the pro-peptide sequence and the other converting valine to isoleucine in the second extracellular domain (see Figure 7D). The plasmid construct is depicted in Figure 7B.

### *Transfection*

S180 cells were grown in DMEM (Dulbecco's Modified Eagle's Medium) supplemented with 15% (v/v) FBS (Fetal Bovine Serum) and 10 $\mu$ g/mL Gentamicin from Gibco (Gaithersburg, MD) and maintained at 37°C with 10% (v/v) CO<sub>2</sub>. Cells were transfected with plasmids by the calcium coprecipitation method (Xia et al., 1996). After overnight incubation, cells were incubated in normal medium. Plasmid selection was initiated the following day by supplementing the medium with 400 $\mu$ g/mL Geneticin (G418, Gibco BRL). Two weeks following transfection, cells were selected for their abilities to express high levels of cadherin. Drug resistant cells were screened for abundant L-CAM expression using Magnetic Activated Cell Sorting (Miltenyi Biotec). Cells were incubated with rabbit anti-L-CAM antibody (1:250) in 2mM EDTA/Phosphate Buffered Saline (150mM NaCl, 2mM NaH<sub>2</sub>PO<sub>4</sub>, 10mM Na<sub>2</sub>HPO<sub>4</sub>, pH 7.4)/0.5%(w/v) BSA (Bovine Serum Albumin), then with magnetic beads coupled to goat-anti-rabbit antibody (20 $\mu$ l per 10 million cells). The cells were passed through a high gradient magnetic separation column (Miltenyi Biotec). Cells expressing cadherin were retained in the column during the first passage, then rinsed from the column in the absence of the magnetic field. Limiting dilution of the separated cells was performed to isolate clonal cultures. Positive expression of L-CAM was confirmed with immunofluorescence with the polyclonal rabbit anti-L-CAM antibody. Only a single clone from each transfection plate was saved, ensuring that the clones are independently

derived. Cultures were maintained at a level of 200 $\mu$ g/mL of G418 in DMEM 15% (v/v) FBS.

#### *Verification of the Transfectants*

Nearly confluent 10cm dishes of S180, S180 L-CAM #11, HAV/VAH #1, HAV/VAH #2, HAV/VAH #4,  $\Delta$ I #1 and  $\Delta$ I#2 cells were scraped into Tris/EDTA (100mM NaCl, 25mM EDTA, 10mM Tris-HCl, pH 8.0) buffer and DNA was extracted by overnight Proteinase K digestion (8.2 $\mu$ L of 10mg/mL Proteinase K, 42 $\mu$ L 10% (w/v) SDS) incubated at 65°C, followed by phenol/chloroform extraction (Moore, 1998). Transfected unmutated and mutated L-CAM sequences were amplified by PCR using PCR primers WJG1034 and WJG1042. PCR products were purified using "GeneClean," a commercial kit (Bio101), prior to sequencing (Amersham Thermosequenase I). Primers used for the sequencing reaction were WJG1034, WJG1035, and WJG1040.

#### *Antibodies*

Polyclonal goat and rabbit anti-L-CAM IgG had been raised against a fusion protein encompassing most of the L-CAM extracellular region. For aggregation experiments, Fab fragments were made by overnight digestion of the whole IgG, with pepsin and subsequent treatment with  $\beta$ -mercaptoethanol and iodoacetamide to produce monovalent Fab fragments (Acheson and Gallin, 1992).

### *Immunofluorescence*

Cells were grown on glass coverslips. Confluent and subconfluent cultures were fixed with 4% paraformaldehyde (wt/vol) in PBS at room temperature for 15 min. and quenched with 0.1M (w/v) glycine in PBS for 15 min. to inactivate residual aldehyde. Cells were permeabilized and further blocked in carageenan Triton-X 100 (41mM Tris Base, 4.4mM Na<sub>2</sub>HPO<sub>4</sub>, 1.8mM NaH<sub>2</sub>PO<sub>4</sub>, 120mM NaCl, 5g/L (w/v) Triton X-100, 7g/L (w/v) Lambda Carageenan, 30mM NaN<sub>3</sub>) and 3% (v/v) goat serum, followed by primary incubation with rabbit anti-L-CAM (1:250 dilution) in carageenan Triton-X solution, and secondary incubation with FITC-conjugated goat anti-rabbit IgG (1:250) or Texas Red-conjugated goat anti-rabbit IgG (1:400). Coverslips were mounted on slides with Mowiol/DABCO or Vectashield (Vector Laboratories) and Anti-fade (Molecular Probes) and examined by confocal microscopy.

### *Western Blotting*

Confluent cultures of each mutant were harvested with boiling 2% SDS in 125mM Tris (pH 6.8) buffer and analyzed for protein concentration using the BCA method (Pierce).  $\beta$ -mercaptoethanol and 2X Sample Buffer (125mM Tris-HCl, 4% (w/v) SDS, 20% (w/v) glycerol, 0.0002% (w/v) Bromophenol Blue, pH 6.8) was added just prior to loading 42.5, 75, and 150 $\mu$ g of each of the extracts onto a 7.5% polyacrylamide gel (Laemmli, 1970). Proteins were electrophoretically transferred to nitrocellulose, blocked with 5% (w/v) skim milk, and incubated with the rabbit anti-LCAM antibody at a concentration of 1:1000 in 5% (w/v) skim milk/TTBS (50mM Tris-HCl, 150mM NaCl, 0.1% Tween 20, pH 8.0) for 2 hours and washed 5 times with TTBS. The blot was then incubated with 5 $\mu$ Ci of <sup>125</sup>I coupled to Protein A for 4 hours and exposed to a phosphoimager screen for 7 days. Blots were visualized using Imagequant (Molecular Dynamics).

### *Aggregation Assays*

Aggregation assays were performed according to Hoffman (1992). Cells were released with 5mM EDTA/2% (v/v) FBS/PBS and incubated on ice in Spinners Minimal Essential Medium (Gibco, BRL) for one hour to allow full dissociation. Aliquots of 2 million cells were incubated with anti-LCAM or nonimmune Fab fragments (3mg of 10mg/mL Fab fragments per 2 million cells) in HDF buffer (137mM NaCl, 5mM KCl, 5.5mM glucose, 4 mM NaHCO<sub>3</sub>, 2mM EDTA, pH 7.5) for

a minimum of 30 minutes on ice. The assay was initiated by suspending the cells in pre-warmed Eagles medium, transferring them to glass scintillation vials and shaking at ~80rpm at 37°C. At the times 0, 20, 40 and 60 minutes, aliquots of cell suspension were combined with 1% glutaraldehyde in PBS (pH 7.5). Cells were counted by diluting the glutaraldehyde cell suspension into Isoton II (Beckman/Coulter Electronics) and counting particles within the range of single suspended S180 cell sizes (10 and 20µm) with a Z2 Coulter Counter. Percentage aggregation for each vial was calculated by the formula  $(N_0 - N_t)/N_0$ ; where  $N_0$  equals number of particles at time 0, and  $N_t$  is the number of particles at the time the cells were sampled. Each point on the graph represents the average of three separate vials, treated with the same Fab.

### *Coaggregation Assays*

Coaggregation was performed with slight modifications according to Friedlander et al. (Friedlander et al., 1989). Cells were loaded with 3mg/mL of either Texas Red labeled fixable dextran, or FITC labeled fixable dextran via the Influx method (Molecular Probes). Dyes were added to a sterile hypertonic medium containing FBS. Briefly, cells are exposed for 20 minutes to a hypertonic solution containing the dyes in which the cells will pinocytose surrounding medium. The cells are then exposed to a hypotonic lysis medium comprised of a 6:4 ratio of Eagles Medium (Gibco, BRL) and water. The hypotonic medium is added to induce rupturing of the pinocytic vesicles, allowing the dye to be spread throughout the cytoplasm. Cells are then exposed to recovery medium of normal DMEM until the experiment is about to proceed (usually ~8 hrs.).

Labeled cells were released with 5mM EDTA / PBS. After counting, cells were diluted to 100 000 cells/50µL in HDF with appropriate Fab fragments (0.8mg/100 000 cells). The assay is initiated when both cell types are combined with the MEM and incubated in 24 well plates coated with PolyHEMA (PolyHEMA saturated in 95% (v/v) EtOH is allowed to evaporate from each well) on a rotary shaker at ~80rpm. Cells were fixed after the 60 min. incubation period by addition of the aliquots to 4% (w/v) paraformaldehyde PBS (pH 7.5). The number of Texas Red labeled cells in a cluster and the total number of cells in that cluster were counted and recorded as a percentage of Texas Red labeled cells (TR/total cells). Comparisons of percentages of the three replicate wells were performed using single factor ANOVA to test whether or not they should be grouped together (the null hypothesis is that the groups are not significantly different from each other). In all but three analyses of 62, there was no significant difference between groups indicating that grouping data from the 3 wells together was

not making an unsupported assumption. Data from twenty coaggregates from three replicate wells were pooled and were graphed in a histogram with bin sizes of 10%. Clusters were also photographed using confocal microscopy. To calculate levels of aggregation, aliquots were taken from each well at times 0 and 60. Past experiments revealed that if the level of aggregation was low (less than 20%), then there was likely an insignificant number of clusters in the sample, and not enough to obtain a full data set. For this reason, clusters were not counted in data sets that had less than 20% aggregation. For instance, I did not seek to count clusters from wells which the cells were pre-incubated with anti-L-CAM Fab fragments because their aggregation was less than 20%. Also, pairings of  $\Delta I$  with itself,  $\Delta I$  with S180, and S180 with itself aggregated to levels that were consistently lower than 20%. If S180 aggregation happened to be high, it was usually attributable to excess cellular debris adhering cells in a cadherin independent manner. When the negative control was contaminated in this way, the experiment was abandoned because any of the other wells could be contaminated in the same way.

## Results

Mutations of L-CAM were created to test which regions are involved in cadherin homophilic interactions and signaling. S180 cells were transfected with the plasmids containing wild-type L-CAM (S180L), the mutant His-Ala-Val/Val-Ala-His (HAV/VAH), and Deletion of Domain 1 ( $\Delta$ I) (Figure 7). Figure 7A is a structural diagram of L-CAM and the two mutants. Several clonal cultures of HAV/VAH transfectants were isolated and three were used for experimentation. PCR was used to confirm the insertion of the sequence in the genome (Figure 7C). The PCR product from HAV/VAH co-migrated with the wild-type L-CAM PCR product, as expected. The first four sequences shown in Figure 7D are the first 153 amino acids in the unmutated L-CAM and HAV/VAH mutants (the first 20 amino acids shown in the sequence are part of the precursor sequence). These sequences confirm that the clones said to contain the HAV/VAH mutation do in fact express the deviation in the sequence.

Two  $\Delta$ I clones were isolated and PCR was used to confirm that the sequence was present in the genome (Figure 7C). The PCR product from the cells transfected with  $\Delta$ I migrated faster than the unmutated L-CAM and HAV/VAH sequences due to its shorter sequence. Figure 7D confirms through sequencing that the PCR product is the  $\Delta$ I mutation. It should be noted that two other mutations have been found in the sequence that were not deliberately induced. In the precursor sequence a Pro was substituted for an Arg residue. This may have an effect on processing of the protein and transport to the membrane. The proline's pentagonal rigid side chain may have altered the tertiary structure of the precursor sequence. As shown in the Western blot, there is a distinct higher molecular weight form of  $\Delta$ I which may be the precursor. Immunofluorescence supports the possibility of processing differences, in that  $\Delta$ I cells were filled with punctate intracellular staining resembling vesicles. The second mutation is the 44th amino acid in the second domain in which Ile is substituted for Val. This mutation is unlikely to be significant since the residue that was substituted has similar properties to the one that was replaced (a short, nonpolar side chain). The side chain faces outwards, so there is no effect on side-chain packing in the interior of the domain. Also the mutated residue is at a site that is highly variable in other domains and other cadherins [alignment not shown].

Western blots were performed to compare protein expression between the mutant cadherins and unmutated L-CAM (Figure 8). Unmutated L-CAM co-migrates with the three HAV/VAH clones. This indicates that the mutation did not interfere with the post-translational modification of the protein (ordinarily there are four glycosylation

### **Figure 7: Mutation of L-CAM, the Avian Orthologue of Mammalian E-cadherin**

The two mutants being investigated are depicted to the right of the unmutated L-CAM (A). HAV/VAH was constructed to test the importance of the residues HAV in the binding of cadherins of adjacent cells (Blaschuk et al., 1990a and 1990b).  $\Delta$ I was constructed to test the importance of the first cadherin domain to cell-cell interactions. Part B is a diagram of the plasmid construct used to create the mutants HAV/VAH and  $\Delta$ I from the L-CAM cDNA. Listed within the ring are the primers referenced in the *Materials and Methods* section, the location of the CMV promoter, the L-CAM cDNA (EC1, EC2, EC3, EC4, EC5, and HAV), the SV40 poly (A) promoter, and the G418 resistance sequence. The presence of the plasmids that were transfected into the clones was verified through PCR of the genomic DNA with primers WJG1034 and WJG1042 (C). HAV/VAH migrated at the same rate as the unmutated L-CAM construct.  $\Delta$ I migrated slightly faster than the full length L-CAM, reflecting its shorter sequence which is a result of deletion of the first domain. PCR products from Fig. 1C were sequenced (D). The first 21 amino acids listed comprise part of the precursor region, the remainder of residues encompass domain 1 and part of 2. The transversion of HAV to VAH is verified at amino acids 78, 79, and 80 of the first domain. The deletion of the full first domain is also confirmed by the alignment of the  $\Delta$ I clones.



Figure 7A

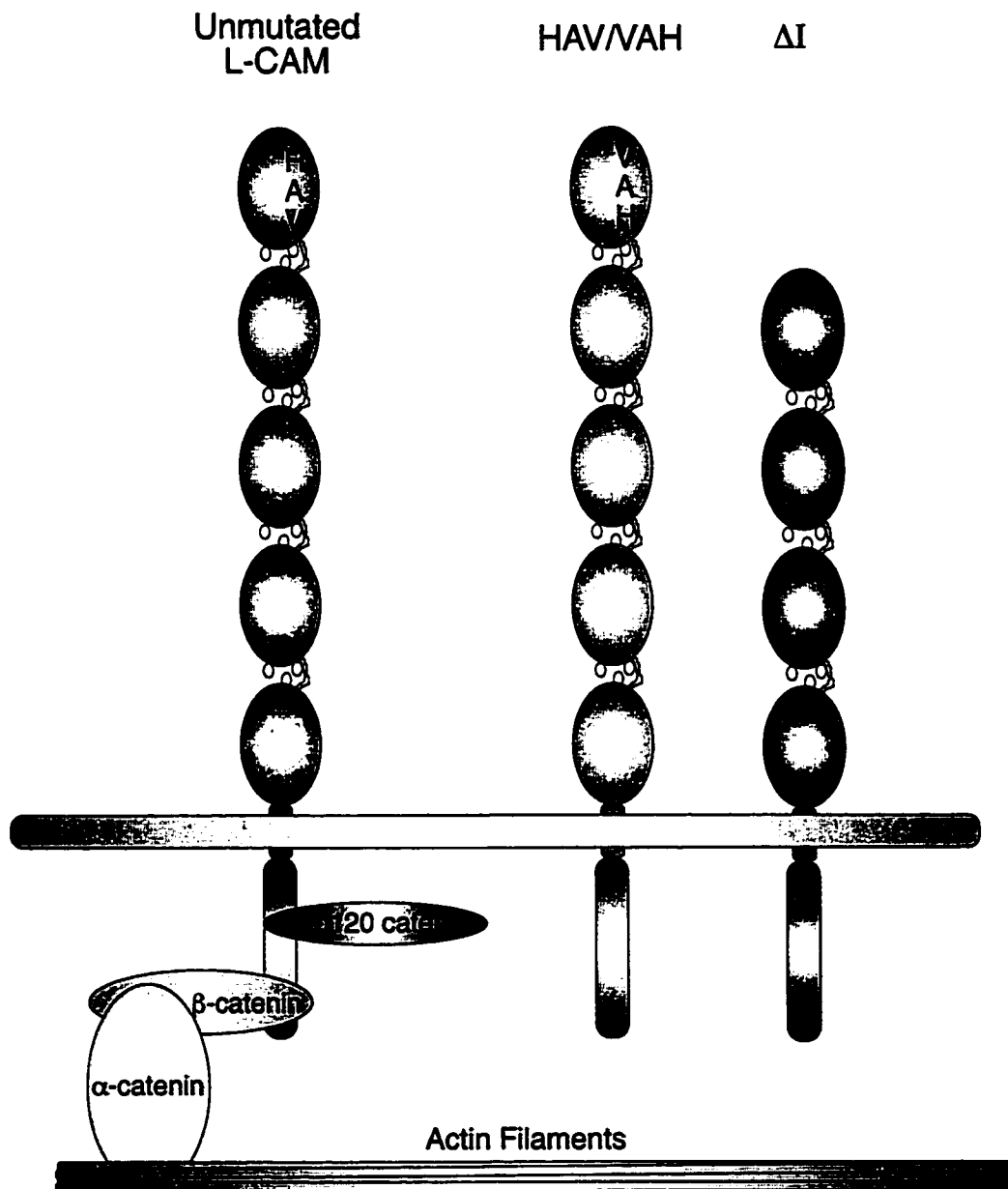


Figure 7B

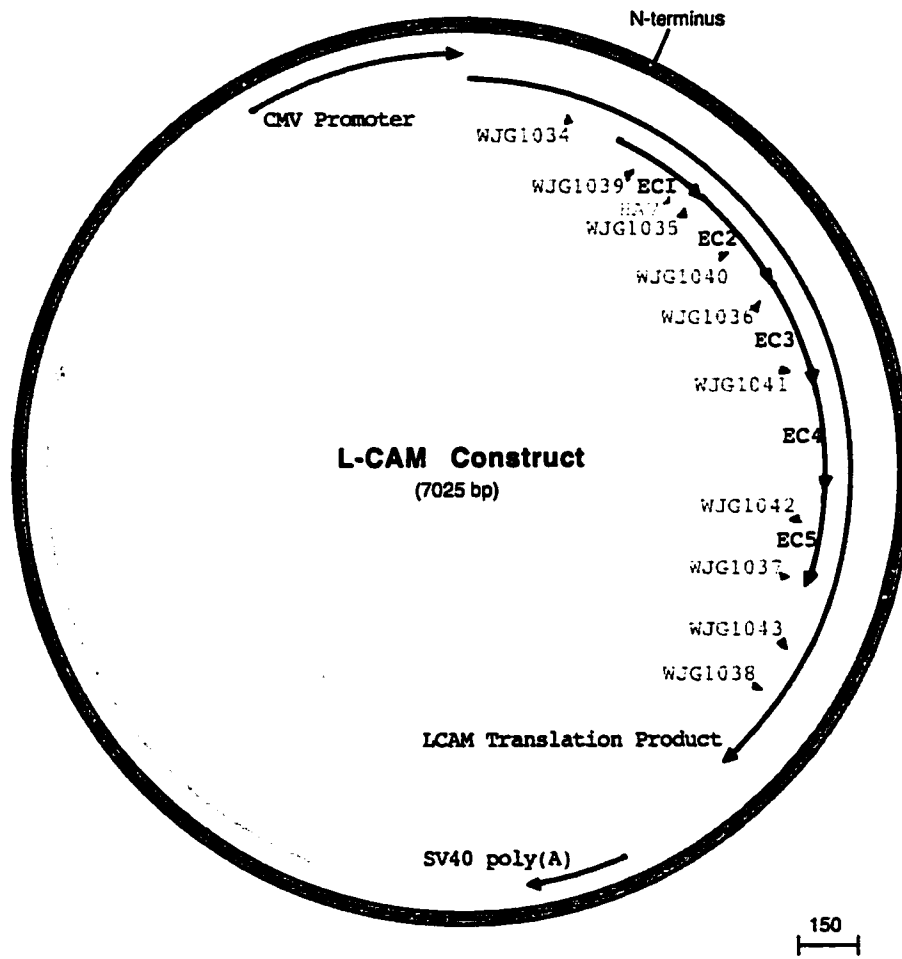
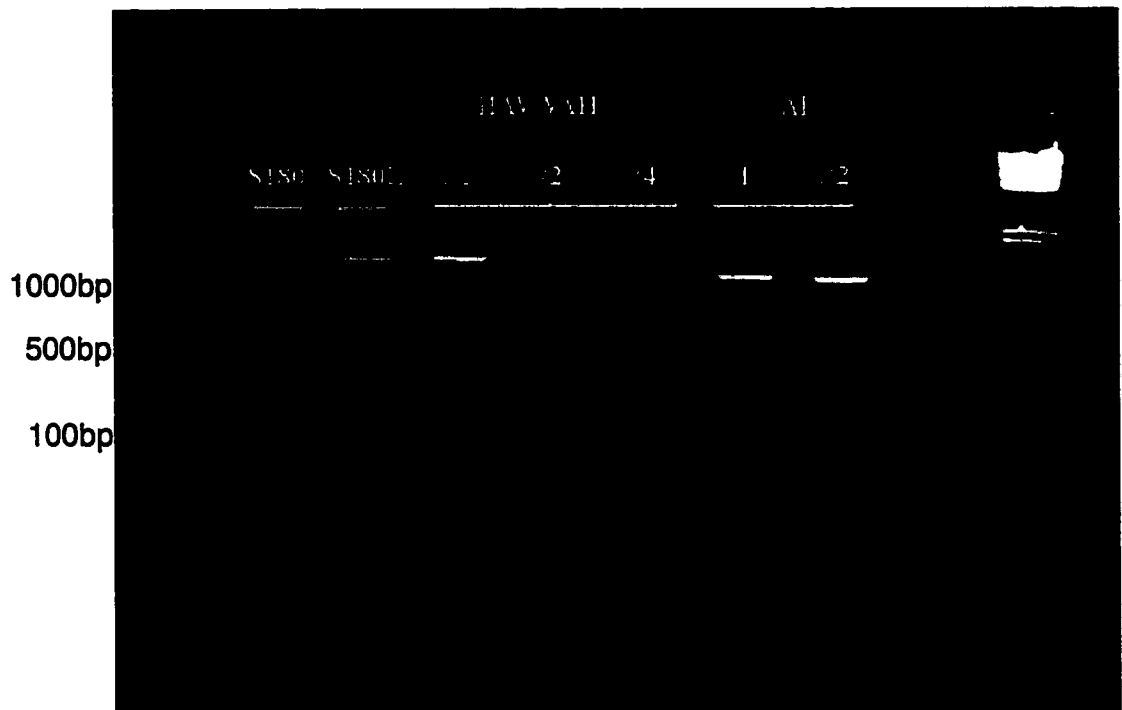


Figure 7C



# Figure 7D

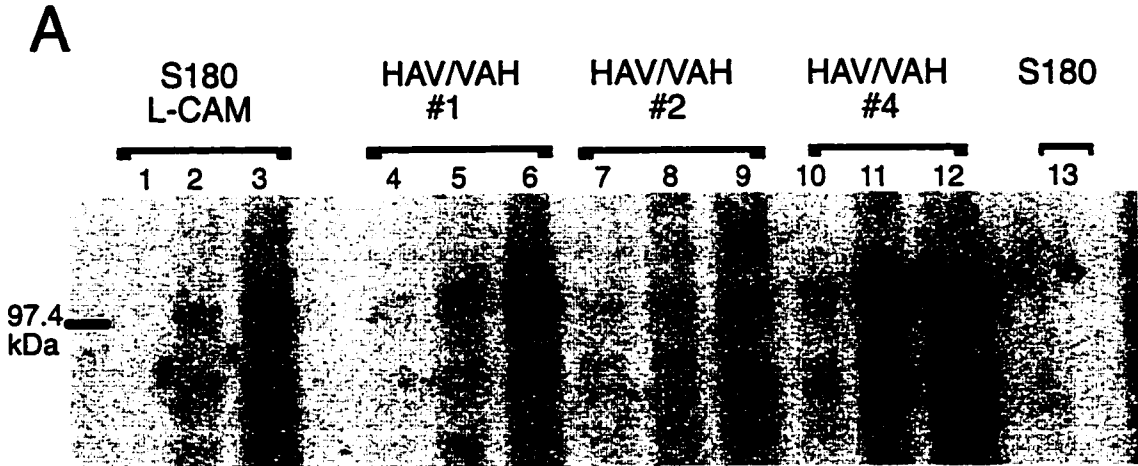
	precursor sequence	EC1	
HAV/VAH#2	<b>MTPAVLTFPKHDPGFLRRQKRDWVIPPISCLENHRGPYPMRLVQIKSNKD</b>		50
HAV/VAH#1	[Redacted]		50
wt	[Redacted]		50
HAV/VAH#4	[Redacted]		50
ΔI#2	[Redacted] P [Redacted] -----		21
ΔI#1	[Redacted] P [Redacted] -----		21
	<b>EC1</b>		
HAV/VAH#2	[Redacted] SV		100
HAV/VAH#1	[Redacted] SV		100
wt	[Redacted] H		100
HAV/VAH#4	[Redacted] SV		100
ΔI#2	-----		21
ΔI#1	-----		21
	<b>EC1</b>	<b>EC2</b>	
HAV/VAH#2	[Redacted] SV		150
HAV/VAH#1	[Redacted] SV		150
wt	[Redacted] SV		150
HAV/VAH#4	[Redacted] SV		150
ΔI#2	[Redacted] SV		45
ΔI#1	[Redacted] SV		45
	<b>EC2</b>		
HAV/VAH#2	[Redacted] SV		200
HAV/VAH#1	[Redacted] SV		200
wt	[Redacted] SV		200
HAV/VAH#4	[Redacted] SV		200
ΔI#2	[Redacted] SV		95
ΔI#1	[Redacted] SV		95

### **Figure 8: Western Blots of L-CAM Mutants**

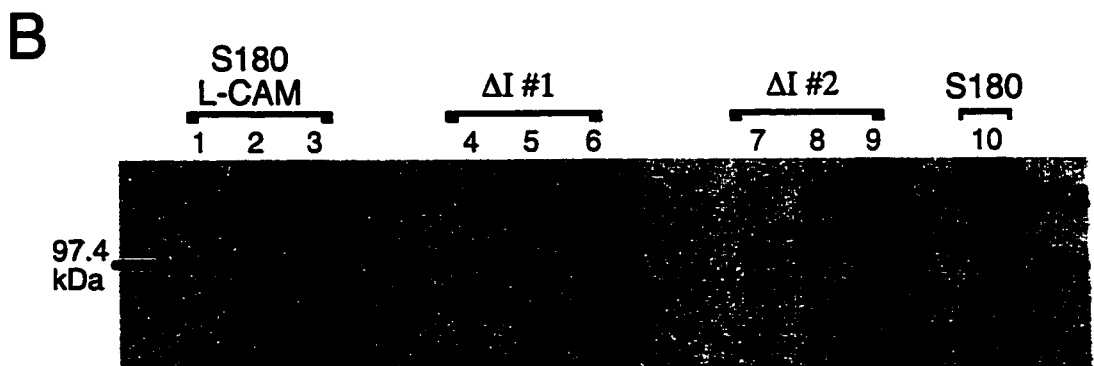
Part A is a Western Blot showing the expression levels of HAV/VAH (lanes 4-12) mutants and comparing them with the S180 L-CAM #11 clone (lanes 1-3). Proteins were separated on a 7.5% acrylamide gel, and transferred to nitrocellulose. The blot was incubated with rabbit anti-L-CAM antibody then coupled to <sup>125</sup>I-protein A. Phosphoimaging analysis was used to visualize the blot, and Imagequant was used to quantify differences in band intensities. HAV/VAH #4 expressed the highest level of cadherin (2.15 the level of S180 L-CAM #11). HAV/VAH #1 had a slightly higher level of expression than wild-type L-CAM (lanes 1-3)(1.15 the level of S180 L-CAM #11) and HAV/VAH #2 had the lowest level of expression (0.85 the level of S180 L-CAM #11). Lane 13 represents 150µg of untransfected S180 extract, added as a negative control. Part B depicts the expression levels of ΔI transfectants (lanes 4-9) compared with unmutated L-CAM (lanes 1-3). Blots were treated as described in A. The ΔI clones migrated to two levels. One form migrated faster than unmutated L-CAM, representing what is likely the fully processed cadherin. It is expected to be slightly faster than L-CAM because of the domain deletion. The slower migrating form likely represents the ΔI precursor sequence. ΔI #1 has the highest expression levels of the two clones. When the faster migrating bands were compared to S180L #11, ΔI #1 was 0.95, and ΔI #2 was 0.84. Both ΔI mutants had slightly higher levels of faster migrating band than S180 L-CAM #11(ΔI #1: 1.03, and ΔI #2: 1.01), possibly indicating differences in the efficiency of protein processing. Lane 10 represents 150µg of untransfected S180 extract, added as a negative control.

Figure 8

Western Blot Comparing Expression of HAV/VAH to Unmutated L-CAM



Western Blot Comparing Expression of  $\Delta I$  to Unmutated L-CAM



sites) (Gallin et al., 1987). The highest expressing clone is HAV/VAH #4, with a band intensity 2.15 times the level of S180 L-CAM #11 (Figure 8A). HAV/VAH #1 expresses slightly higher amounts of transfected protein than the full length clone S180 L-CAM #11 (1.15 times the level of S180 L-CAM #11). HAV/VAH #2 expresses slightly lower levels than L-CAM on the blot (0.85 times the level of S180 L-CAM #11).

Two distinct bands are visible in both  $\Delta$ I cadherin transfectants. One migrates faster than wild-type L-CAM, and likely represents the fully processed protein that is faster due to the deletion of the first domain sequence (Figure 8B). The slower migrating species of  $\Delta$ I essentially co-migrates with full-length L-CAM, and likely represent  $\Delta$ I precursors.  $\Delta$ I #1 expresses slightly more protein than  $\Delta$ I #2 with band intensities of 0.95 and 0.83 times the level of S180 L-CAM #11, respectively. When comparing the slower migrating species with that of S180 L-CAM #11, it was found that the  $\Delta$ I clones expressed slightly higher protein levels ( $\Delta$ I #1: 1.03,  $\Delta$ I #2: 1.01). If the slower migrating species is the precursor sequence, then possibly the unintentional substitution of Pro for Arg in the precursor sequence has affected  $\Delta$ I post-translational processing.

S180 cells appear spindle-shaped, or spread on the substrate. When the concentration of cells on a culture dish is confluent, they appear squamous, forming more than one layer of cells on a substrate. S180 cells transfected with L-CAM retain the tendency to form multiple layers, but the layers tend to be sheets of cells that are connected through cadherin mediated adhesion. Immunofluorescence reveals that wild type L-CAM localizes to the plasma membrane at sites of cell-cell interaction (Figure 9). Contact regions are somewhat flattened, suggesting that they are extended sites of interaction between adjacent cells. HAV/VAH #1, #2, and #4 have the same morphology as S180 L-CAM cells in that the fluorescence is most intense, and membranes are flattened at points between adjacent cells (Figure 9).

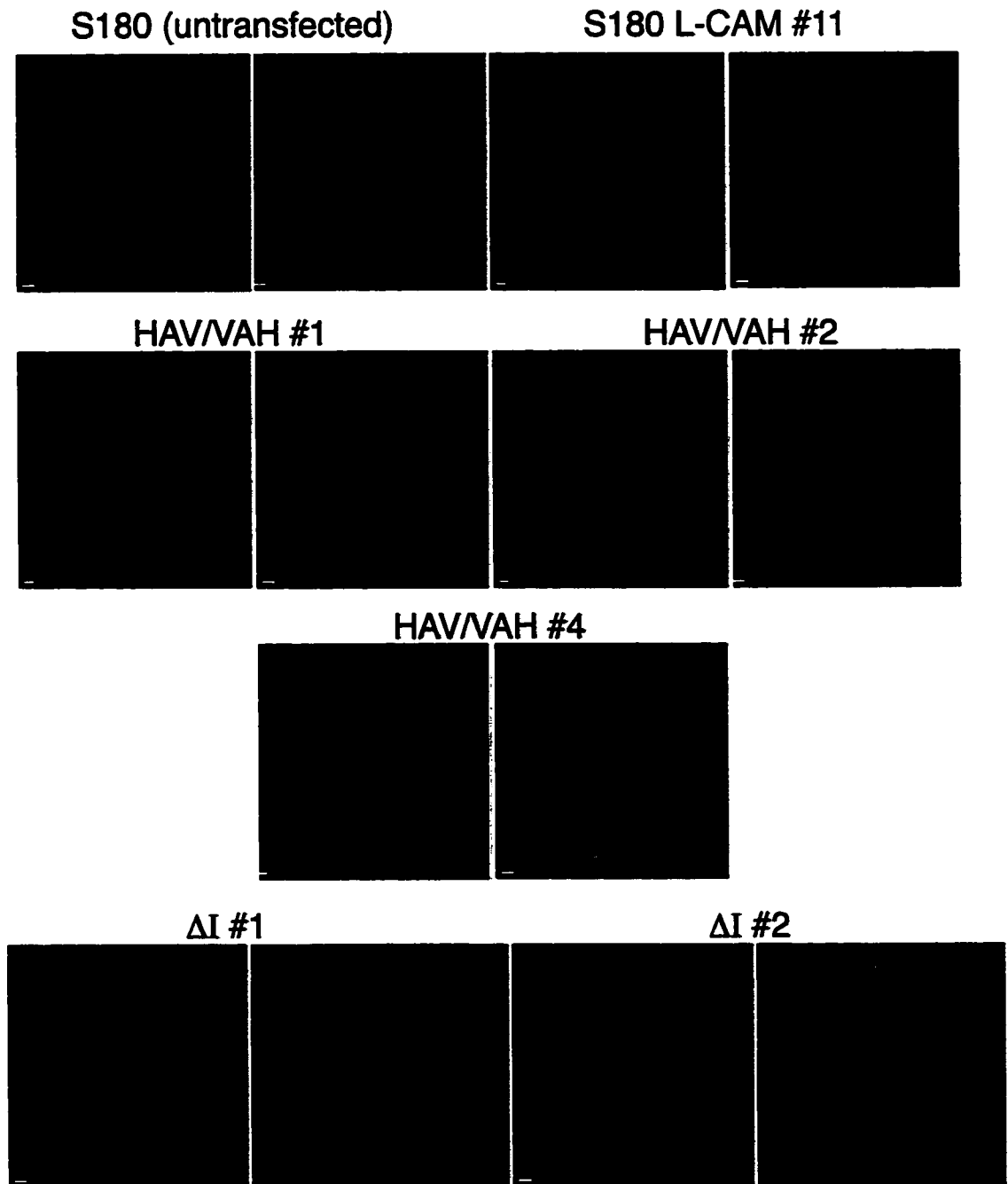
$\Delta$ I cadherins are not as intensely localized to the plasma membrane at points of contact as the unmutated L-CAM and HAV/VAH clones (Figure 9). Much of the staining was to what appeared to be intracellular vesicles, indicating that a significant amount of the  $\Delta$ I cadherin transcribed is not transported to the plasma membrane or it quickly recycles. This may be attributable to the mutation in the precursor sequence of Arg to Pro (Figure 7C). Although there may be inefficient transport to the membrane, it is probable that sufficient protein is transported to the plasma membrane to mediate

### **Figure 9: Immunofluorescence**

The top left panels reveal two different magnifications of untransfected S180 cells that were processed the same as the other cells that were scanned. Although there appears to be some nonspecific staining, it is not as intense as the specific staining of S180 L-CAM #11, HAV/VAH, or  $\Delta I$  transfectants. In S180 L-CAM #11 and HAV/VAH cells, the most intense cadherin staining is where two cells are adjacent, indicating that the cadherins are mediating cell-cell adhesion. The three HAV/VAH clones also stain most intensely at the plasma membrane, demonstrating that the proteins are delivered to the membrane. The staining resembles the wild-type L-CAM, implying that the mutation did not impair the cadherin's function. Immunofluorescence of the  $\Delta I$  clones demonstrate that cadherin staining is noticeable at points of cell-cell contact as well as in what appear to be intracellular vesicles. The sizes of each scale-bar are as follows: a is 10 $\mu$ m; b, d, f, h, j, k, and m are 5 $\mu$ m; c, e, g, and i are 2 $\mu$ m. Panels l and o do not have scale bars shown, but they were taken at the same magnification as panels k and m.



# Figure 9: Immunofluorescence



weak adhesive interaction. Staining with FITC reveals a concentration of protein at points of cell-cell contact (Figure 9).

Short-term aggregation assays are functional tests of cell adhesion activity. Although staining is informative regarding localization of the cadherin to the lateral region of the plasma membrane, it is uninformative about the ability of the cells to initiate and maintain stable adhesive contact under the stress of shearing forces. Immunofluorescence of  $\Delta I$  and HAV/VAH L-CAM mutants reveal that both mutant cadherins concentrate at the lateral region of the plasma membrane. In both mutants, membranes of adjacent cells are flattened, which implies that they can mediate cadherin-based adhesion (Figure 9). The more stringent aggregation assay is necessary to differentiate the functional capacity of the two mutants.

HAV/VAH cells are highly adhesive, usually aggregating to the level of wild type L-CAM clones or higher (Figure 10, Table 2). Figure 4 depicts aggregation of HAV/VAH cells relative to unmutated L-CAM (S180L #11) and untransfected S180 cells. All three clones aggregated to consistently high levels as shown by the graphs in Figure 10Aa, 10Ba, and 10Ca (HAV/VAH #1 at ~55%, HAV/VAH #2 at 69%, and HAV/VAH #4 at ~55% respectively). The wild type L-CAM transfectant demonstrated assay to assay variation in aggregation between ~35% and ~55%. Nonspecific S180 aggregation was usually between 10-20%. The observed adhesion in all three clones was L-CAM specific, because pre-incubation of the cells with anti-LCAM Fab fragments reduced aggregation to a level comparable to the nontransfected S180 cells (~10%). The lower panels of Figure 10Ab, 10Bb, and 10Cb are photographs of the suspensions fixed at times 0 and 60 minutes. They confirm the data depicted in the graphs, showing an increase in clusters over time in suspensions containing S180L and HAV/VAH cells. Table 2 shows the levels of aggregation at 60 minutes in the replicate experiments of each clone. Pair-wise comparisons of the mutant transfectants to S180 and unmutated L-CAM were made incorporating data from the three repeats of the experiments for each clone (Haber and Runyon, 1973). These comparisons support the conclusions that can be interpreted from the graphs. If HAV was a crucial segment of the putative interface of cadherin homoassociation, then reversing the sequence would likely have compromised its function. These results imply that the orientation of HAV sequence is not crucial to the function of L-CAM.

Unlike HAV/VAH,  $\Delta I$  does not profusely aggregate in an aggregation assay. Its level of aggregation was comparable to nontransfected S180 cells, regardless of whether the cells were preincubated with anti-LCAM or nonimmune Fab fragments (Figure 11Aa with  $\Delta I$  #1 at ~8%, and 11Ba with  $\Delta I$  #2 at 12% with nonimmune Fab fragments).

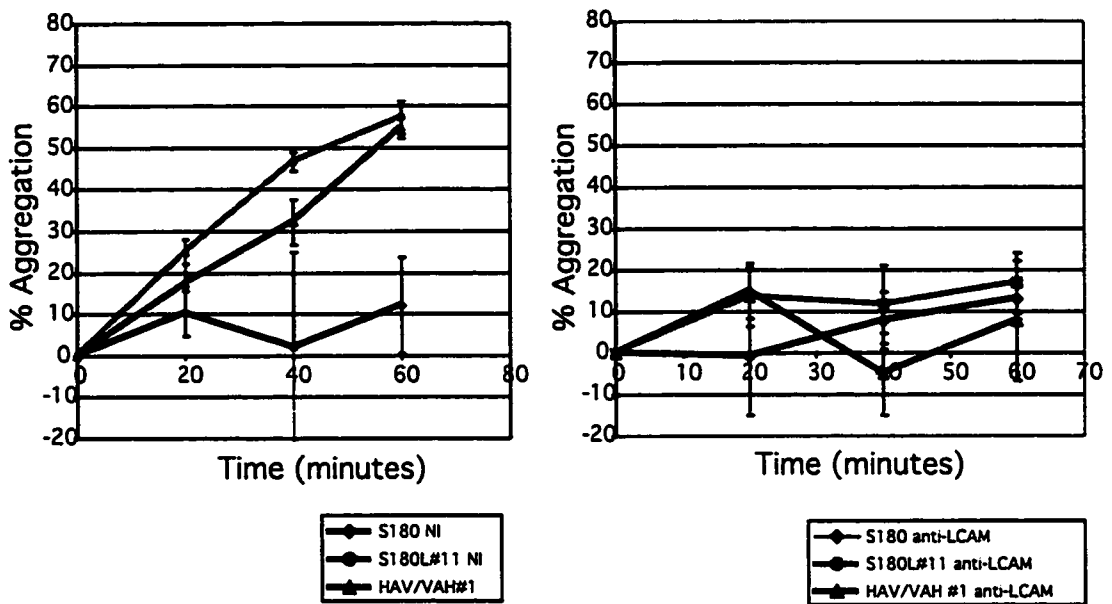
### **Figure 10: Aggregation of HAV/VAH**

Aggregation assays of HAV/VAH clones (A: #1, B: #2, C: #4). Each assay was performed with the wild-type L-CAM transfectant (S180 L-CAM #11) as a positive control and untransfected S180 cells as a negative control. The three cell types were also incubated with anti-L-CAM Fab fragments to show that the observed adhesion was cadherin mediated. The three HAV/VAH clones aggregated to similar levels (55-70% aggregation). The lower panels (b) reveal a change in the appearance of cells during the course of the assay. In essence, HAV/VAH and S180 L-CAM cells formed clusters in medium that contained nonimmune Fab fragments, while S180 cells and the cells exposed to anti-LCAM Fab fragments did not form significant sized clusters (usually less than 20 cells).

# Figure 10A

## Aggregation Assay of HAV/VAH #1

**a**



**b**

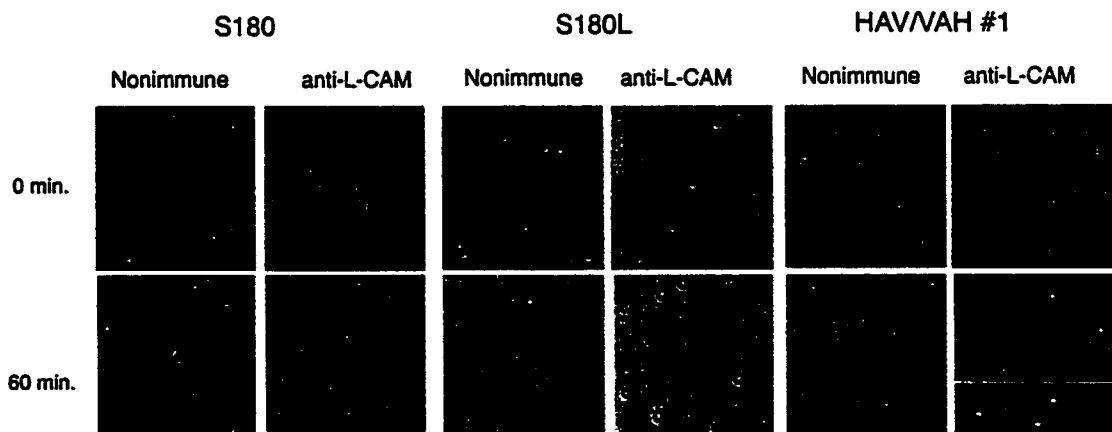
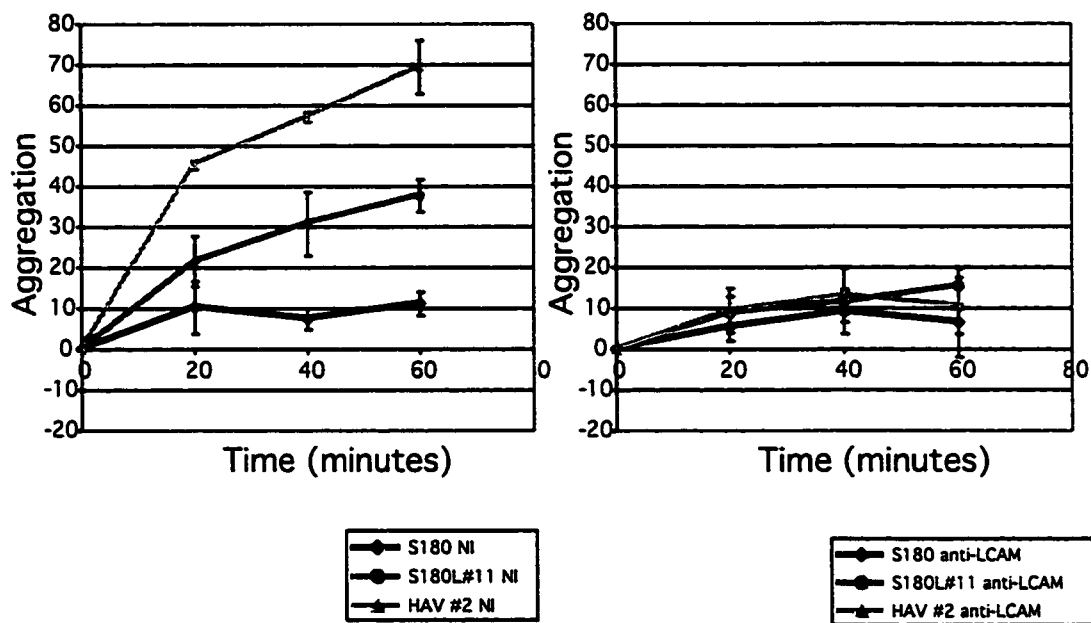


# Figure 10B

## a Aggregation Assay of HAV/VAH #2



## b

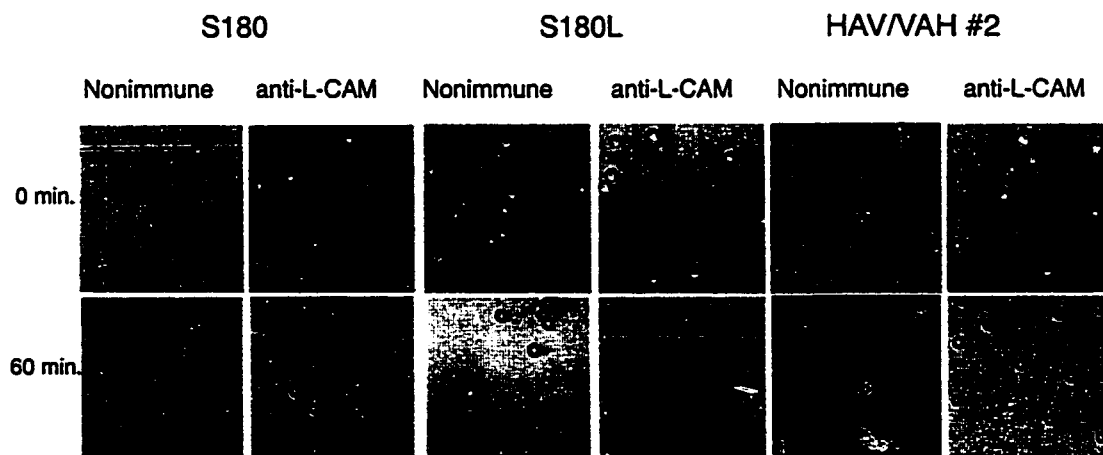
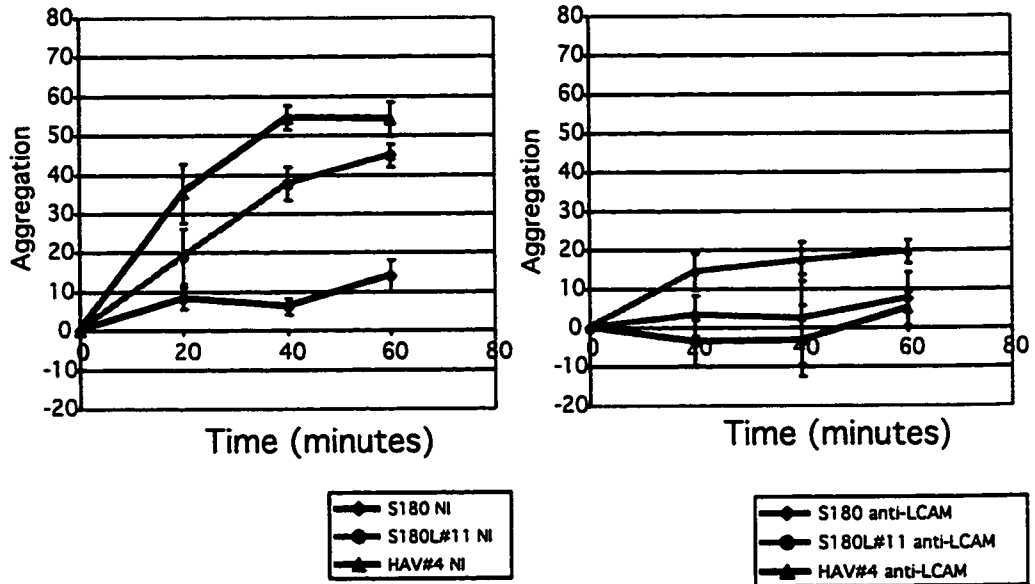


# Figure 10C

## Aggregation Assay of HAV/VAH #4

**a**



**b**

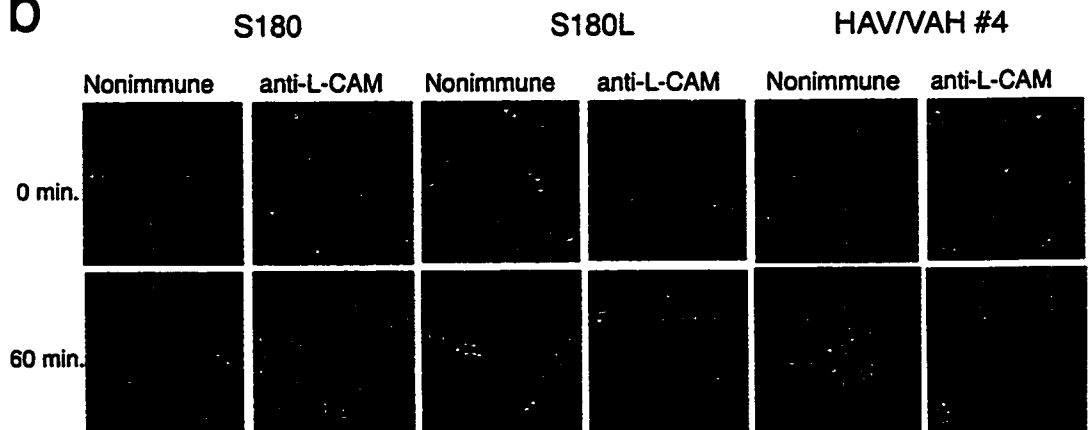
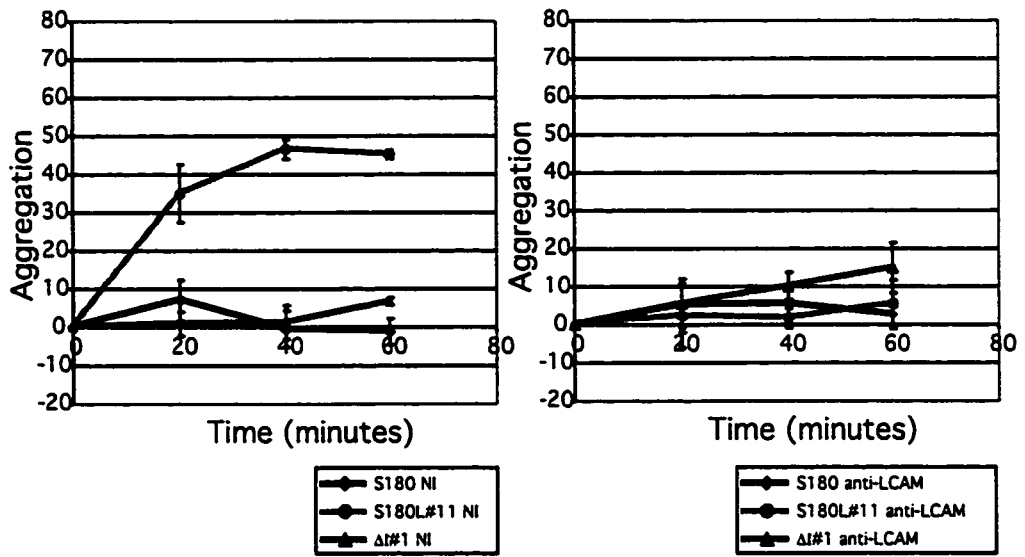


**Figure 11: Aggregation of  $\Delta I$**

Aggregation of  $\Delta I$  clones (A: #1, B: #2). Assays were performed as described for Figure 4. Essentially,  $\Delta I$  did not aggregate more than the S180 negative control (A, a: B, a).  $\Delta I$ 's inability to aggregate was not due to experimental error because the unmutated L-CAM transfectant aggregated, and its aggregation was inhibitable by anti-LCAM Fab fragments. The lower panels depict the appearance of the cells before and after the experiment was initiated.  $\Delta I$  cells did not form aggregates after one hour of incubation while S180L cells formed clusters.

# Figure 11A

## a Aggregation Assay of $\Delta I$ #1



## b

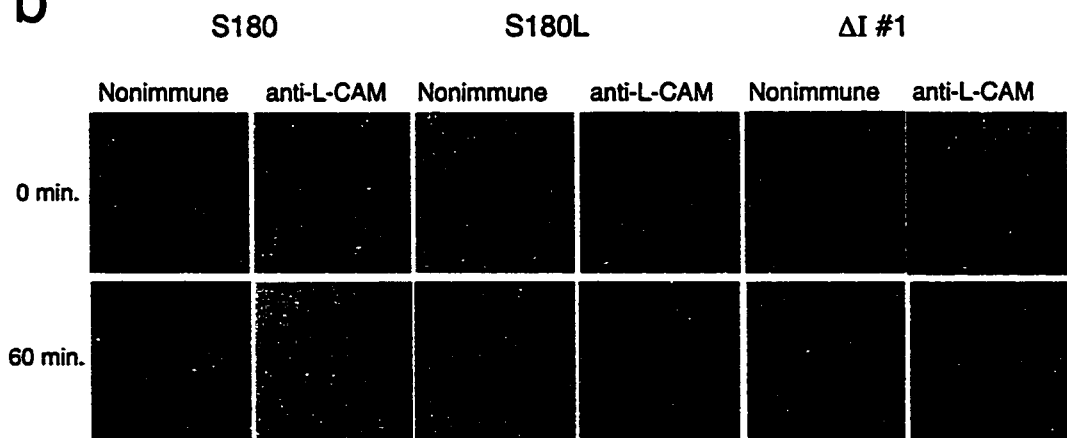




# Figure 11B

## a Aggregation Assay of $\Delta I$ #2

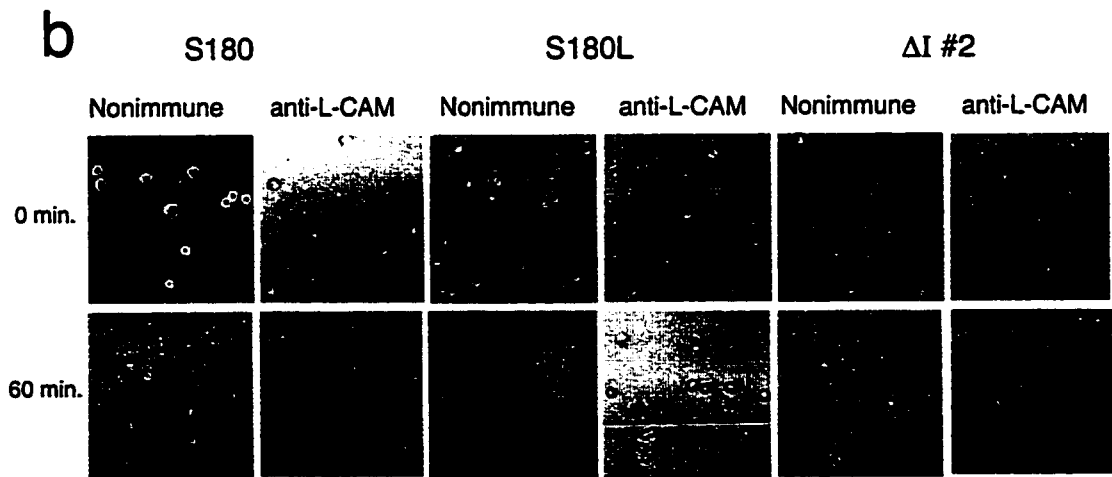
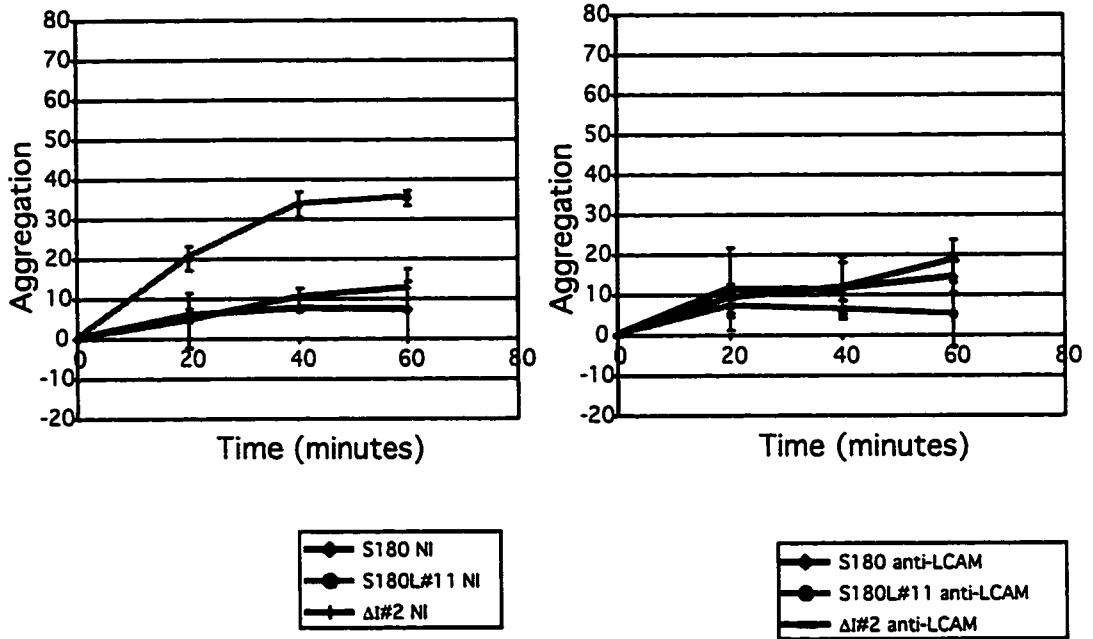


## **Table 2: Analysis of Replicate Aggregation Assays**

Replicates of the aggregation assays were subjected to analysis by two factor ANOVA. This form of analysis takes into account the amount of variation observed between the three replicates of a single cell type (i.e. unmutated L-CAM, or S180), as well as comparing the values obtained over three trials between one cell type and another. The *between group variance* reflects the magnitude of difference between and/or among group means. The *within group variance* reflects the dispersion of scores within each treatment group. F-ratios represent the *between group variance* divided by *within group variance*. If the F-ratio is lower than the **F-critical value**, then it can be assumed that the two independent variance estimates may be regarded as estimates of the same population value [Haber and Runyan, 1973].

Due to the amount of variation within each experiment, the F-ratios often exceeded the F-critical values, even though they represented % aggregation of the same cell type. However, the within group F-ratios did not exceed F-critical values as much as the between group F-ratios (e.g. the within sample comparison of  $\Delta I\#1$  with S180L was 19.2, but the between sample comparison is 157.6). Also, when the between group ratio is compared between different Fab treatments, an enormous difference in F-value can be observed (e.g.  $\Delta I\#1/S180L$  exposed to nonimmune Fabs produced an F-ratio of 157.6, but comparison of the same cells treated with Fab fragments produced an F-ratio of only 1.4.). For this reason the F-values are an informative derivation of the data to allow comparison of aggregation levels between the three different cell types tested in each assay.

**Table 2: Analysis of Replicate Aggregation Assays**

<b>Transfectant</b>	<b>% Aggregation after 60 minutes</b>	<b>F-values/ F-critical Within Sample Comparison</b>	<b>F-values/F-critical Between Sample Comparison</b>
<b>ΔI #1</b> Nonimmune Fabs	1. 37.9, 20.5, 26.4 2. 6.8, 10.7, 16 3. 5.9, 7.9, 6.2	ΔI #1/S180L: 19.2/3.9 ΔI #1/S180: 14.7/3.9	ΔI #1/S180L: 157.6/4.7 ΔI #1/S180: 19.1/4.7
	1. 33.6, 25.4, 32.4 2. 25.4, 15.1, -2.7 3. 22.4, 12, 10.4	ΔI #1/S180L: 8.7/3.9 ΔI #1/S180: 9.8/3.9	ΔI #1/S180L: 1.4/4.7 ΔI #1/S180: 15.8/3.9
<b>S180L</b> Nonimmune Fabs	1. 45.9, 55.9, 56.4 2. 33.1, 40.1, 38.6 3. 44.2, 44.7, 46.3	S180L/ΔI #1: 19.2/3.9 S180L/S180: 10.4/3.9	S180L/ΔI #1: 157.6/4.7 S180L/S180: 352.3/4.7
	1. 37.3, 24.6, 18.8 2. 17.7, 11.1, 5.7 3. -1.7, 9, 9.1	S180L/ΔI #1: 8.7/3.9 S180L/S180: 17.1/3.9	S180L/ΔI #1: 1.4/4.7 S180L/S180: 9.8/4.7
<b>S180</b> Nonimmune Fabs	1. 16.3, 6, 8.7 2. 9.9, -2.1, 1.4 3. -4.2, -1.5, 2.6	S180/ΔI #1: 14.7/3.9 S180/S180L: 10.4/3.9	S180/ΔI #1: 19.1/4.7 S180/S180L: 352.3/4.7
	1. 15.8, 17.5, 13.2 2. 2.6, 0.6, 1.1 3. -0.7, 1.8, 6.3	S180/ΔI #1: 9.8/3.9 S180/S180L: 17.1/3.9	S180/ΔI #1: 15.8/4.7 S180/S180L: 9.8/4.7
<b>ΔI #2</b> Nonimmune Fabs	1. 16.9, 16.2, 23.6 2. 13.1, 17.1, 7.1 3. 29.2, 13, 20.4	ΔI #2/S180L: 8.3/3.9 ΔI #2/S180: 3.2/3.9	ΔI #2/S180L: 135.1/4.7 ΔI #2/S180: 5.6/4.7
	1. 7.9, 22.2, 17.7 2. 24, 17.8, 13.4 3. 20.9, 8, 5.2	ΔI #2/S180L: 1.6/3.9 ΔI #2/S180: 3/3.8	ΔI #2/S180L: 0.7/4.7 ΔI #2/S180: 3.4/4.7
<b>S180L</b> Nonimmune Fabs	1. 43.9, 41.9, 44.7 2. 36.7, 33.3, 36 3. 47, 44.8, 50.7	S180L/ΔI #2: 8.3/3.9 S180L/S180: 8.4/3.9	S180L/ΔI #2: 135.1/4.7 S180L/S180: 269.5/4.7
	1. 19.8, 22.8, 23.4 2. 14, -1.7, 3.4 3. 29.2, -5.2, -5.7	S180L/ΔI #2: 1.6/3.9 S180L/S180: 2.2/3.9	S180L/ΔI #2: 0.7/3.9 S180L/S180: 0.1/4.7
<b>S180</b> Nonimmune Fabs	1. 11.5, 19.8, 19.4 2. 15.3, 4.2, 2 3. 5.7, 10.8, 11.2	S180/ΔI #2: 3/3.8 S180/S180L: 8.4/3.9	S180/ΔI #2: 3.4/4.7 S180/S180L: 269.5/4.7
	1. 0.9, 12.7, 18.9 2. 11.1, 18.6, 13.5 3. 3.8, -1.8, 6.7	S180/ΔI #2: 3/3.8 S180/S180L: 2.2/3.9	S180/ΔI #2: 3.4/4.7 S180/S180L: 0.1/4.7

Transfectant	% Aggregation after 60 minutes	F-value/ F-critical Within Sample Comparison	F-value/Fcritical Between Sample Comparison
<b>HAV/VAH #1</b> Nonimmune Fabs	1. 52.7, 57.4, 54 2. 31, 25.6, 33.9 3. 45.2, 27.7, 28.3	HAV#1/S180L: 25.2/3.8 HAV#1/S180: 2.7/3.9	HAV#1/S180L: 8.5/4.7 HAV#1/S180: 36/4.7
	1. -6.2, 22.5, 7 2. -4.3, 17.1, 15 3. 22.4, 4.5, 6.7	HAV#1/S180L: 0.4/3.9 HAV#1/S180: 0.4/3.9	HAV#1/S180L: 0.7/4.7 HAV#1/S180: 0.02/4.7
<b>S180L</b> Nonimmune Fabs	1. 59.3, 52.7, 59.3 2. 41.7, 29.8, 39.6 3. 47, 44.7, 50.6	S180L/HAV#1: 25.2/3.8 S180L/S180: 1.1/3.9	S180L/HAV#1: 8.5/4.7 S180L/S180: 67.7/4.7
	1. 23.1, 8.7, 18.7 2. 25.8, 13.9, 20.2 3. 29.2, -5.2, -5.7	S180L/HAV#1: 0.4/3.9 S180L/S180: 2.7/3.9	S180L/HAV#1: 0.7/4.7 S180L/S180: 0.8/4.7
<b>S180</b> Nonimmune Fabs	1. -0.2, 13.8, 22.7 2. 20.7, 33.4, 1.9 3. 5.7, 10.8, 11.1	S180/HAV#1: 2.7/3.9 S180/S180L: 1.1/3.9	S180/HAV#1: 36/4.7 S180/S180L: 67.7/4.7
	1. 18, 12, 8.6 2. 4.7, 20.2, 18.7 3. 3.8, -1.8, 6.7	S180/HAV#1: 0.4/3.9 S180/S180L: 2.7/3.9	S180/HAV#1: 0.02/4.7 S180/S180L: 0.8/4.7
<b>HAV/VAH #2</b> Nonimmune Fabs	1. 46.4, 49.6, 40.1 2. 70.9, 75.1, 62.1 3. 59.5, 59.5, 51.6	HAV#2/S180L: 5.9/3.9 HAV#2/S180: 4.4/3.9	HAV#2/S180L: 46.3/4.7 HAV#2/S180: 205.6/4.7
	1. 10, 19.6, 17 2. 15.4, 13.6, 2.8 3. 15.5, 18.1, 18.3	HAV#2/S180L: 6/3.9 HAV#2/S180: 1.7/3.9	HAV#2/S180L: 5.2/4.7 HAV#2/S180: 5.3/4.7
<b>S180L</b> Nonimmune Fabs	1. 59.4, 52.7, 59.3 2. 37.7, 33.9, 41.9 3. 35.4, 31.2, 32.2	S180L/HAV#2: 5.9/3.9 S180L/S180: 7/3.9	S180L/HAV#2: 46.3/4.7 S180L/S180: 117.9/4.7
	1. 23.1, 8.8, 18.7 2. 16.1, 19.4, 10.5 3. -15, 0.2, -8.3	S180L/HAV#2: 5.9/3.9 S180L/S180: 10.2/3.9	S180L/HAV#2: 5.2/4.7 S180L/S180: 0.02/4.7
<b>S180</b> Nonimmune Fabs	1. -0.2, 13.8, 22.7 2. 9.2, 9.6, 14.4 3. 18, 5, 12.4	S180/HAV#2: 4.4/3.9 S180/S180L: 7/3.9	S180/HAV#2: 205.6/4.7 S180/S180L: 117.9/4.7
	1. 18.4, 12.2, 8.7 2. 4.8, -0.9, 15.8 3. 5.5, 3.1, 9.3	S180/HAV#2: 4.4/3.9 S180/S180L: 10.2/3.9	S180/HAV#2: 5.3/4.7 S180/S180L: 0.02/4.7

<b>Transfectant</b>	<b>% Aggregation after 60 minutes</b>	<b>F-values/ F-critical Within Sample Comparison</b>	<b>F-value/F-critical Between Sample Comparison</b>
<b>HAV/VAH #4</b> Nonimmune Fabs	1. 34.2, 27.8, 41.3 2. 34.4, 38.4, 30.5 3. 58.5, 54.2, 49.7	HAV#4/S180L: 24.5/3.9 HAV#4/S180: 12.7/3.9	HAV#4/S180L: 1.8/4.7 HAV#4/S180: 150/4.7
	1. -4, 6.5, -4.3 2. -34, -37, 15.3 3. 9.2, 4.9, 0.6	HAV#4/S180L: 5.6/3.9 HAV#4/S180: 2/3.9	HAV#4/S180L: 2.8/4.7 HAV#4/S180: 5.4/4.7
<b>S180L</b> Nonimmune Fabs	1. 33.1, 40.1, 38.6 2. 35.4, 31.2, 32.2 3. 41.6, 45.6, 47.4	S180L/HAV#4: 24.3/3.9 S180L/S180: 6.8/3.9	S180L/HAV#4: 1.8/4.7 S180L/S180: 180/4.7
	1. 14, -1.7, 3.4 2. -15.3, 0.2, -8.4 3. 22.7, 16.5, 19.3	S180L/HAV#4: 5.6/3.9 S180L/S180: 9.8/3.9	S180L/HAV#4: 2.8/4.7 S180L/S180: 1.7/4.7
<b>S180</b> Nonimmune Fabs	1. 9.9, -2.1, 1.4 2. 18, 5, 12.4 3. 9.5, 15.6, 17	S180/HAV#4: 12.7/3.9 S180/S180L: 6.8/3.9	S180/HAV#4: 150/4.7 S180/S180L: 180/4.7
	1. 11.1, 18.6, 13.5 2. 5.5, 3.1, 9.3 3. 5.8, 1.5, 15.1	S180/HAV#4: 2/3.9 S180/S180L: 9.8/3.9	S180/HAV#4: 5.4/4.7 S180/S180L: 1.7/4.7

The low aggregation depicted was not due to unusual experimental conditions, since S180L cells aggregated to 45% and 35% respectively with the same treatment as  $\Delta$ I clones. Figure 11Ab and 11Bb are photographs of cell suspensions fixed at time 0 and 60 minutes. Only the S180L cell suspensions have clusters, confirming that only S180L aggregated, while the  $\Delta$ I mutants did not. Data analysis that incorporates the repeats of these experiments confirms these conclusions (Table 2). The inability of  $\Delta$ I to aggregate supports previous data implicating a crucial role for the extracellular domain 1 (EC1) in cell-cell adhesion.

Although cells expressing the HAV/VAH mutation are capable of homotypic interaction resulting in aggregation, the mutation may have impaired their ability to cross-adhere with the wild-type L-CAM. Mutation of HAV to VAH may not have disrupted the ability of the cadherins to mediate adhesion because the HAV binding surface is still complementary (i.e. His of one cadherin can still bind Val of another, Figure 10). If the complementary binding of HAV/VAH mutant is not disrupted, then theoretically HAV/VAH would not bind unmutated L-CAM. Deletion of the first extracellular domain disabled the  $\Delta$ I mutation from binding other  $\Delta$ I expressing cells in an aggregation assay. This indicates that EC1 is essential to cadherin-cadherin interaction. However, some models of cadherin adhesion predict that cadherins do not interact solely by EC1 but bind along the entire surface of the extracellular domain. Possibly the full-length cadherin molecule may be able to partially rescue  $\Delta$ I aggregation. EC1 of the unmutated L-CAM may bind  $\Delta$ I along part of its extracellular domains.  $\Delta$ I cannot reciprocate the complete binding, possibly making the adhesion less strong.

Coaggregation experiments were used to assess each mutant clone's ability's to cross-adhere with S180, S180L, and the other mutants. Cells were differentially labelled with the pinocytic loading method using dyes Texas red dextran 10W and fluorescein dextran 10W. To numerically verify aggregation, samples were taken at times 0 and 60 minutes and their concentrations were determined through counting on a hemacytometer. Coaggregates were analyzed in samples whose concentration differences from times 0 and 60 min. were calculated to be higher than 30% aggregation.

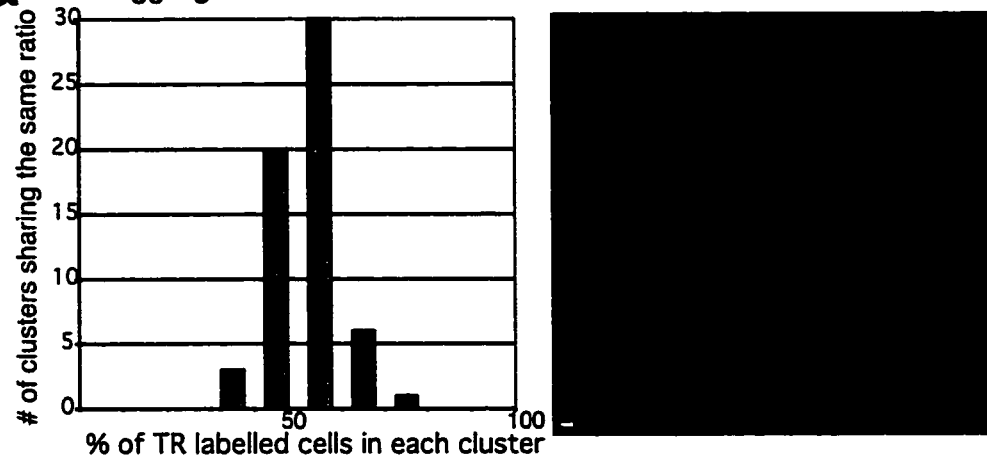
The HAV/VAH clones were able to aggregate with S180L and with  $\Delta$ I. They did not coaggregate with S180 (Figures 12c, 13c, and 14c). Aggregation with S180L and  $\Delta$ I was inhibitable by anti-LCAM Fab fragments, showing that this aggregation was cadherin dependent (data not shown). HAV/VAH coaggregated with S180L in a ~50%

## Figure 12

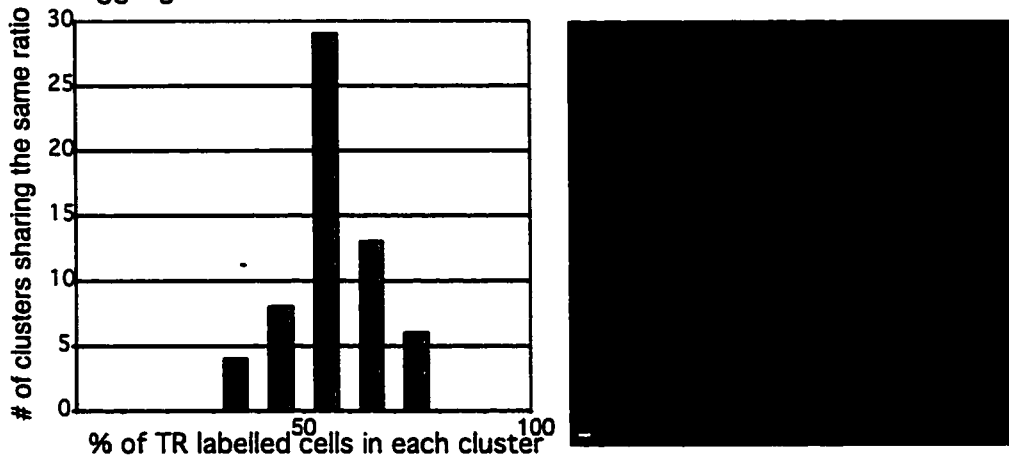
Coaggregation experiments were performed to test the mutant's abilities to cross adhere with the unmutated L-CAM and each other. This figure demonstrates coaggregation of Texas Red labelled HAV/VAH #1 with fluorescein labelled HAV/VAH #1 (a), S180 L-CAM #11 (b), untransfected S180 (c),  $\Delta I$  #1 (d), and  $\Delta I$  #2 cells (e). The ratio of Texas Red labelled HAV/VAH #1 cells in coaggregation with itself and unmutated L-CAM was mostly between 50 and 60%. In coaggregation with S180, HAV/VAH #1 cells comprised 80-100% of the cluster. In coaggregation with  $\Delta I$ #1 and #2, HAV/VAH #1 formed approximately 70% of the clusters. Each scale-bar represents 2 $\mu$ m.

# Figure 12

**a** Coaggregation of Texas Red Labeled HAV/VAH #1 with itself



**b** Coaggregation of Texas Red Labeled HAV/VAH #1 with S180 L-CAM #11



**c** Coaggregation of Texas Red Labeled HAV/VAH #1 with S180

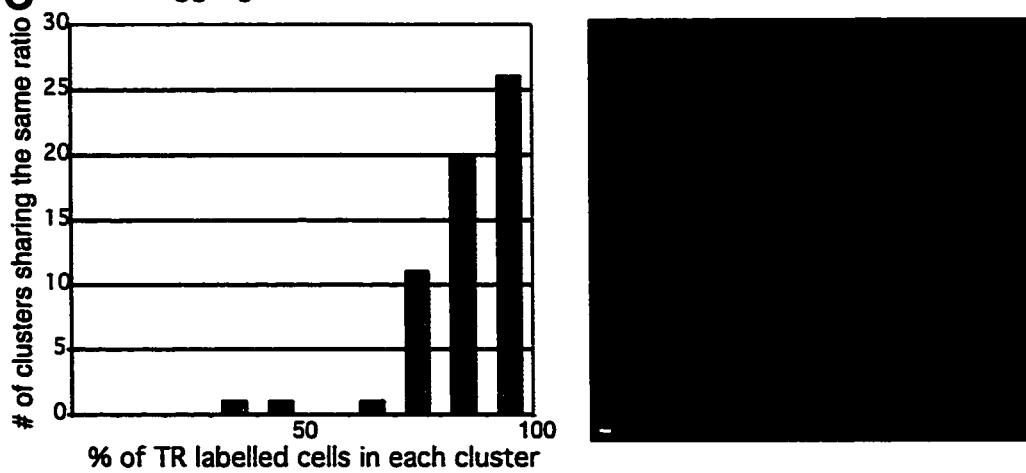
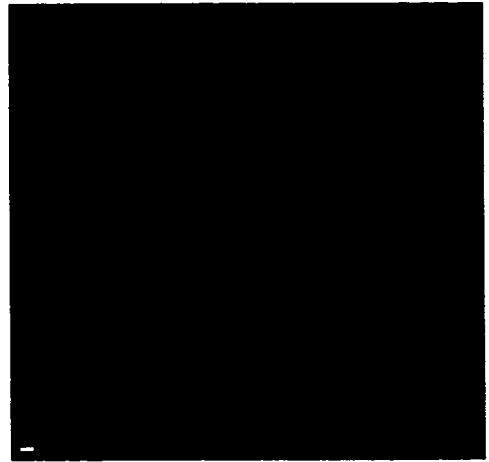
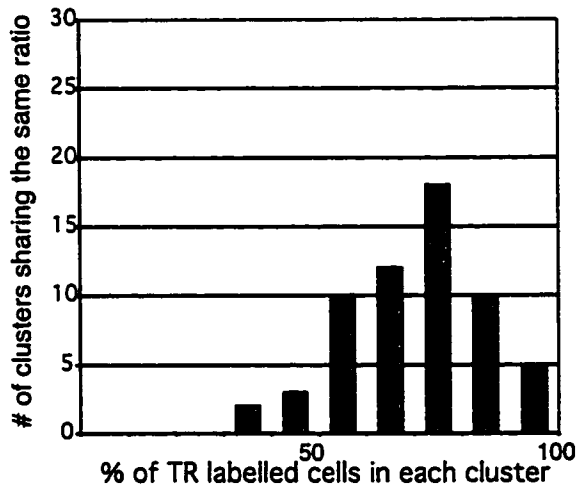




# Figure 12

**d** Coaggregation of Texas Red Labeled HAV/VAH #1 with  $\Delta I$  #1



**e** Coaggregation of Texas Red Labeled HAV/VAH #1 with  $\Delta I$  #2

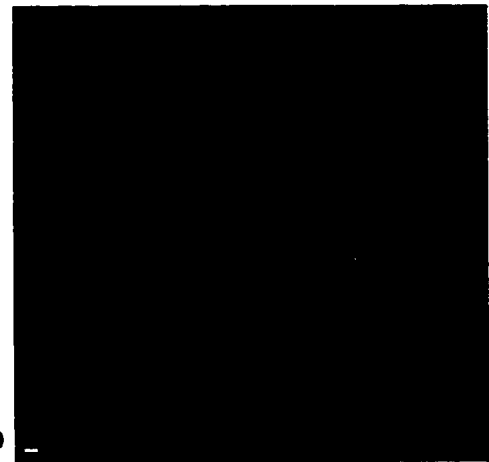
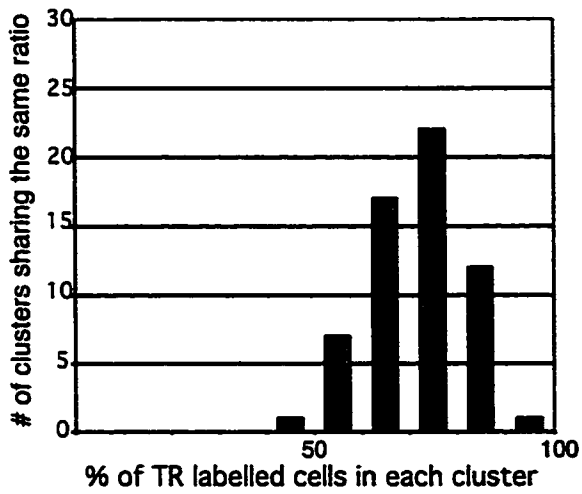


### **Figure 13**

Coaggregation of HAV/VAH #2 is depicted in the same manner as HAV/VAH #1 coaggregation in Figure 6. This figure demonstrates coaggregation of Texas Red labelled HAV/VAH #2 with fluorescein labelled HAV/VAH #2 (a), S180 L-CAM #11 (b), untransfected S180 (c),  $\Delta I$  #1 (d), and  $\Delta I$  #2 cells (e). Essentially, the ratios of HAV/VAH #2 to the cells that it coaggregated with are consistent between the two clones. The scale-bars represent: 2 $\mu$ m for a and d, 5 $\mu$ m for b and c, and 10 $\mu$ m for e.

# Figure 13

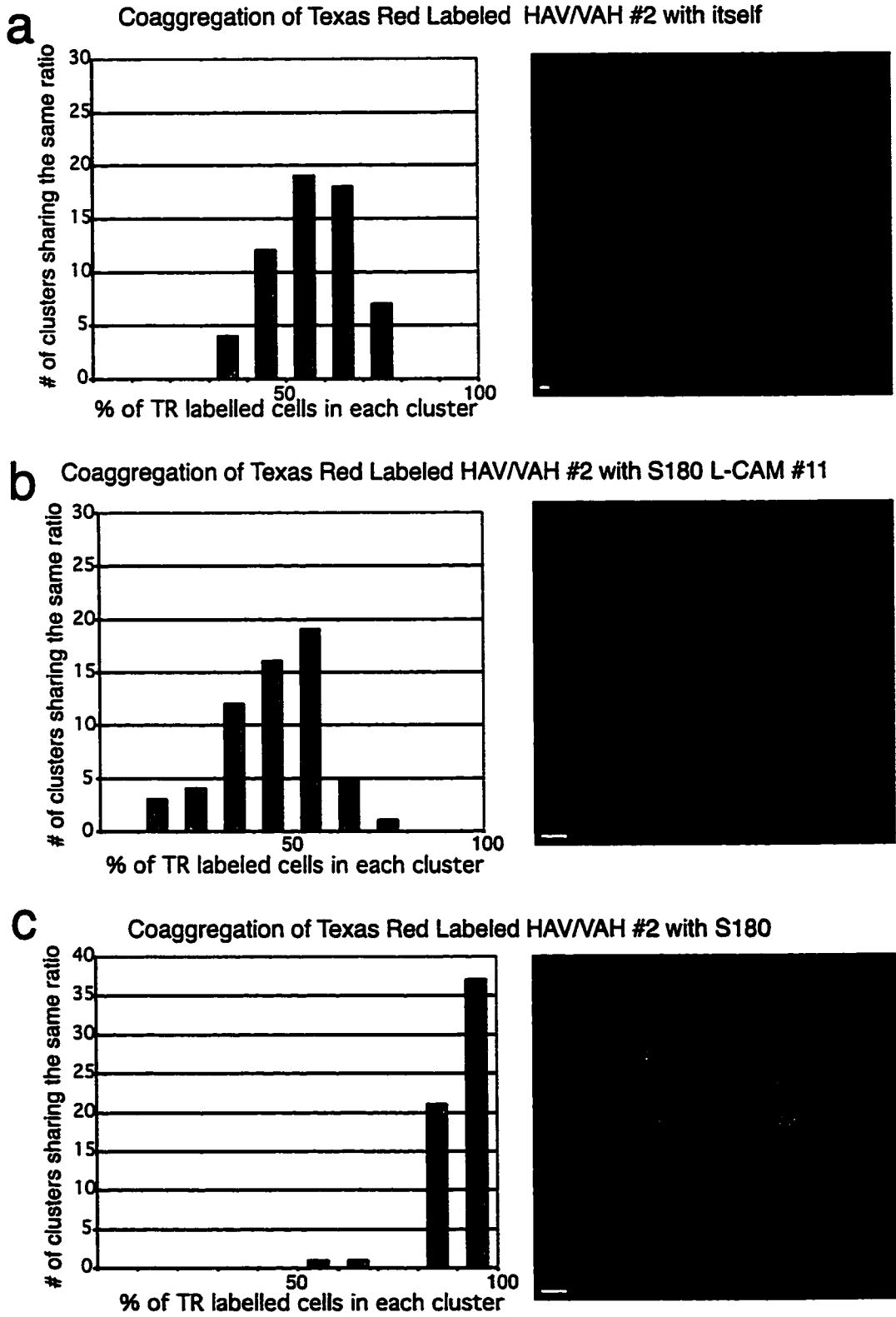
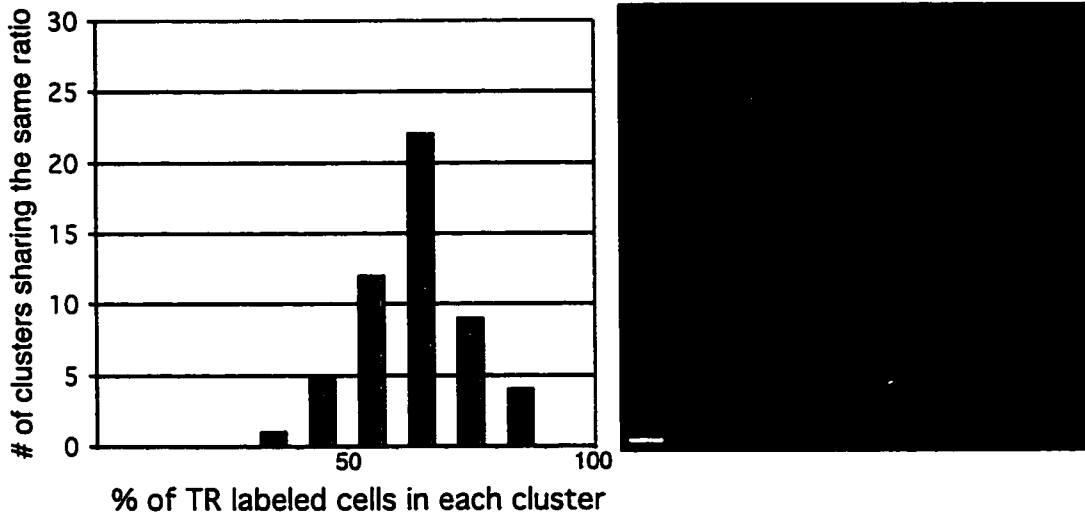


# Figure 13

**d** Coaggregation of Texas Red Labeled HAV/VAH #2 with  $\Delta I$  #1



**e** Coaggregation of Texas Red Labeled HAV/VAH #2 with  $\Delta I$  #2

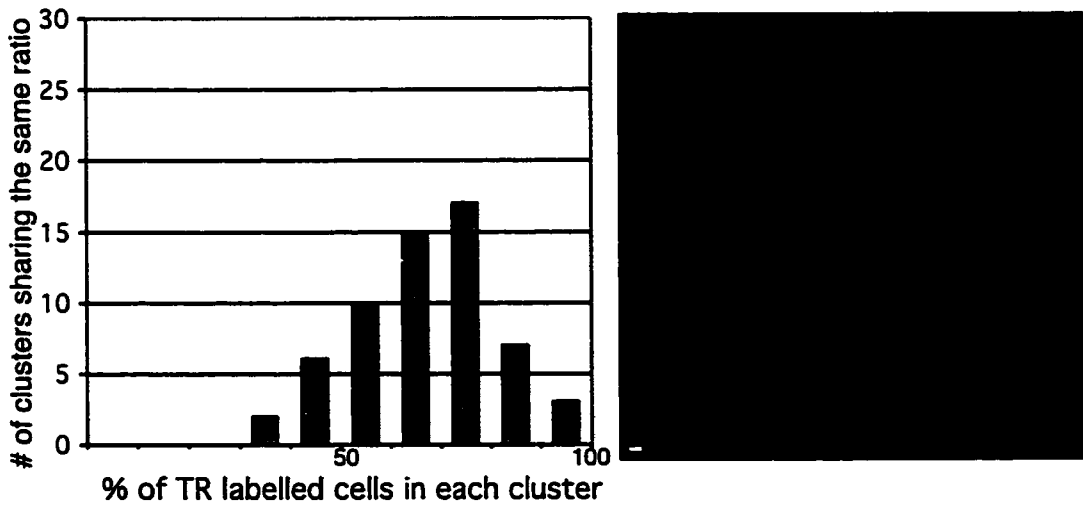


#### **Figure 14**

Coaggregation of HAV/VAH #4 is depicted in the same manner as HAV/VAH #1 coaggregation (Figure 6), and HAV/VAH #2 coaggregation (Figure 7). This figure demonstrates coaggregation of Texas Red labelled HAV/VAH #4 with fluorescein labelled HAV/VAH #4 (a), S180 L-CAM #11 (b), untransfected S180 (c),  $\Delta$ I #1 (d), and  $\Delta$ I #2 cells (e). The ratios of HAV/VAH #4 to the cells it was coaggregated with are consistent with the results of the other HAV/VAH clones. The scale-bars represent: 2 $\mu$ m for a and 5 $\mu$ m for b and c. Panels d and e do not have scale bars showing, but were taken at the same magnification as b and c.

# Figure 14

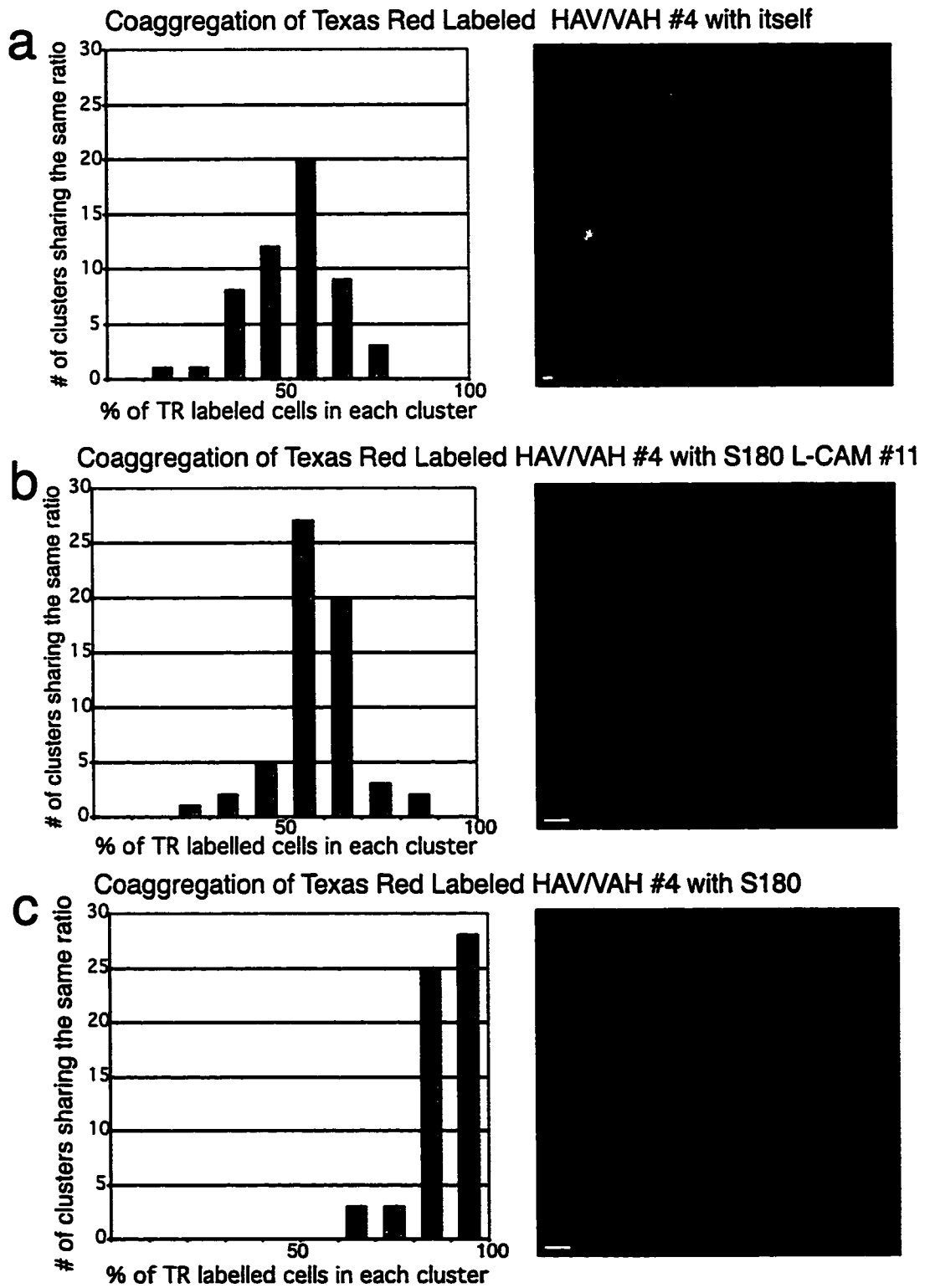
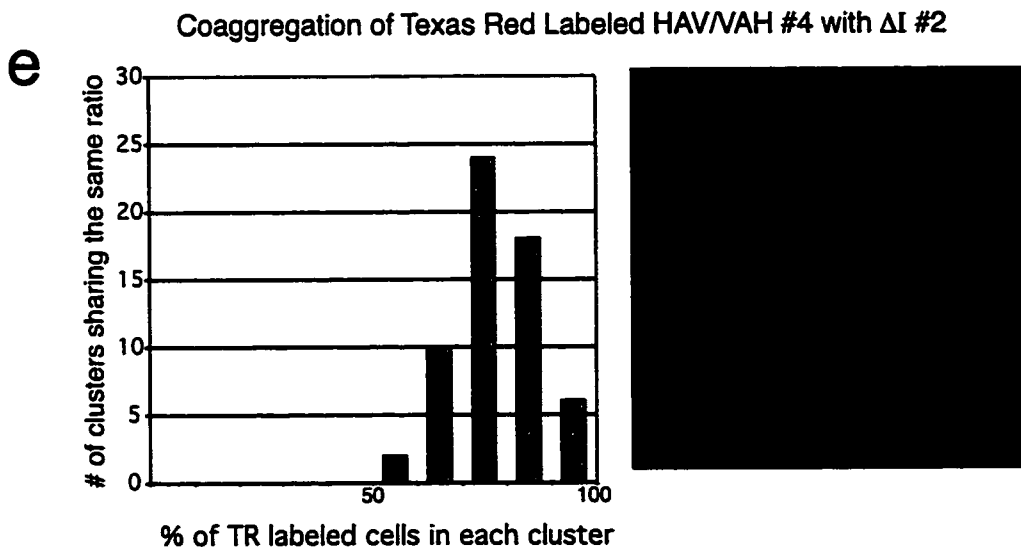
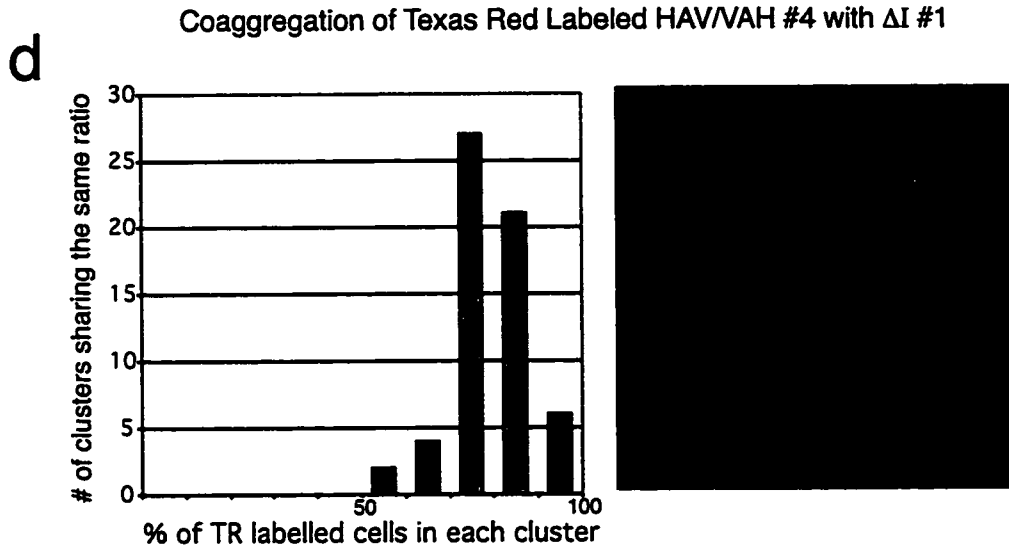


# Figure 14



ratio, demonstrating there is no difference in probability between one or both cell types joining in a cluster (Figure 12b, 13b, 14b, and 18b,c,d). For all clones, the ratio of HAV/VAH to S180 cells peaked in the 90-100% range (a reciprocal relationship of S180/HA V/VAH can be observed in Figure 17). The ability of HAV/VAH to cross-adhere with unmutated L-CAM implies that the orientation of the HAV sequence is not important to the *trans* interaction, since the HAV/VAH mutant functionally aggregates both homotypically and heterotypically with wild type LCAM.

Cell-cell adhesion is believed to be due to a *trans* interaction between the first domains of cadherins of adjacent cells. However, recent evidence suggests that the *trans* interaction is between domains 1 and 5, implicating the possibility of two or more adhesive surfaces between cadherins of two cells (Leckband and Sivasankar, 2000; Sivasankar et al., 1999). Interestingly  $\Delta$ I coaggregates with S180L and HAV/VAH cells (Figure 15 and 16). Unlike HAV/VAH, the clusters  $\Delta$ I formed with S180L contained approximately 10-40%  $\Delta$ I cells. The probability of  $\Delta$ I cells joining in a cluster is less favorable than the wild-type, implying the interaction between  $\Delta$ I and wild type L-CAM is not as strong or stable as the interaction between two wild-type cells. This supports the model of Sivasankar et al. (Sivasankar et al., 1999), in which cadherins interact along the entire extracellular sequence.  $\Delta$ I is unable to interact homotypically because it is lacking domain 1. However, it can interact a little with the full length protein because the full-length cadherin domain 1 can interact with  $\Delta$ I's other extracellular domains.  $\Delta$ I interacts with HAV/VAH to approximately the same ratio as wild-type L-CAM (peaks range from 10% to 40%  $\Delta$ I in a cluster). Coaggregation of the clones of HAV/VAH with the mutants of  $\Delta$ I showed more variation than homotypic HAV/VAH association and association between HAV/VAH and S180L. Essentially the peaks in distribution ranged from 60-80% HAV/VAH cells in an aggregate (Figure 12d, 12e, 13d, 13e, 14d, and 14e). Coaggregation of HAV/VAH with  $\Delta$ I has a peak range that is distinct from the negative control, S180 and the positive control, HAV/VAH. It is therefore unlikely that this event is an artifact, but represents true adhesion. Replicates of experiments testing coaggregation of S180, S180 L-CAM #11, HAV/VAH #1 and  $\Delta$ I #2 with each other has yielded consistent results with the data that is shown.



### **Figure 15**

Coaggregation of Texas Red labelled  $\Delta$ I #1 with fluorescein labelled S180 L-CAM #11 (a), HAV/VAH #1 (b), HAV/VAH #2 (c), and HAV/VAH #4 cells (d). There are no histograms or pictures shown for coaggregation of  $\Delta$ I with  $\Delta$ I or S180 cells because these samples failed to aggregate to a level of 20% or higher. There is a broad range of peak ratios of  $\Delta$ I #1 with full-length L-CAM and HAV/VAH clones (lowest is 10-20%, highest is 30-40%). These ratios are close to the reciprocal of S180L/  $\Delta$ I and HAV/VAH/ $\Delta$ I coaggregation, confirming that  $\Delta$ I cells comprise ~20-30% of the cells in a cluster. Each scale-bar represents 2 $\mu$ m. Panel d was taken at the same magnification as a, b and c.

# Figure 15

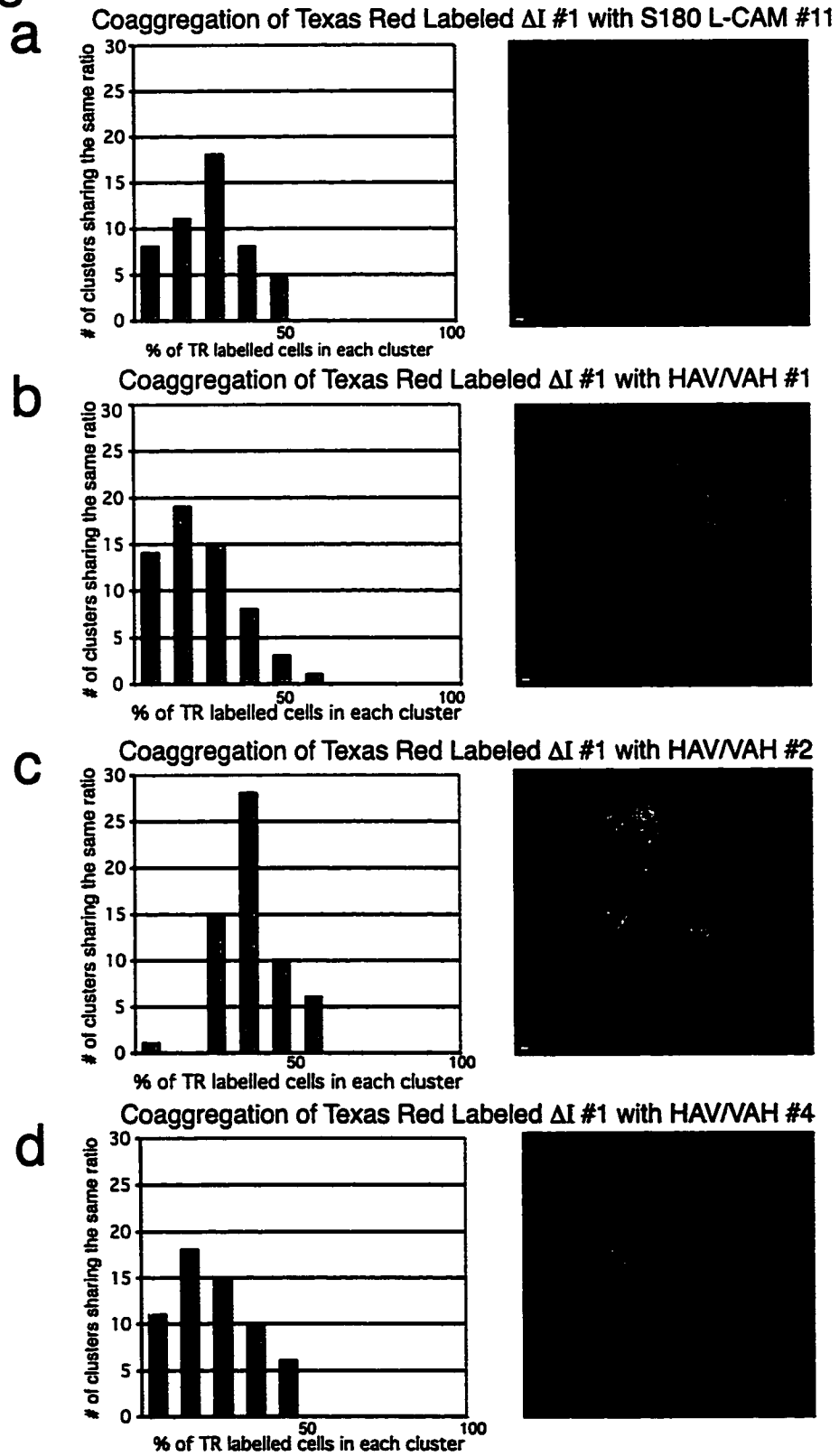
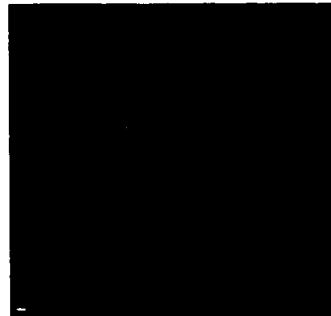
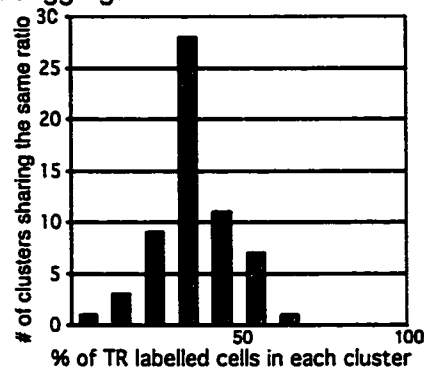


**Figure 16**

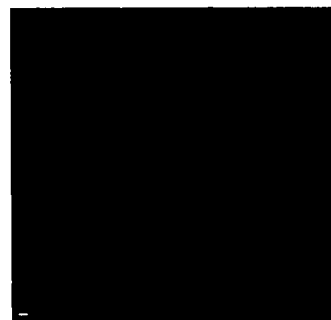
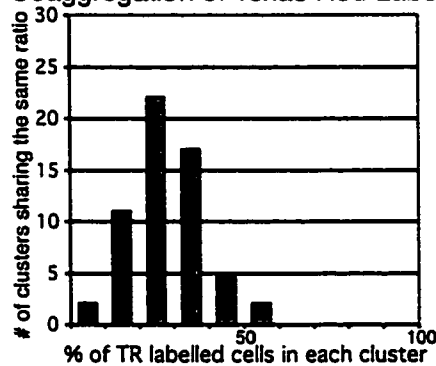
Coaggregation of Texas Red labelled  $\Delta$ I #2 with fluorescein labelled S180 L-CAM #11 (a), HAV/VAH #1 (b), HAV/VAH #2 (c), and HAV/VAH #4 cells (d).  $\Delta$ I #2 cells seem to comprise a higher percentage of clusters than  $\Delta$ I #1 (the peak ratios range between 20-40%). However, this small difference likely only reflects experimental variation. As with  $\Delta$ I #1, the values of these ratios are close to the reciprocal of S180L/  $\Delta$ I and HAV/VAH/ $\Delta$ I coaggregation. Each scale-bar represents 2 $\mu$ m. Panel d was taken at the same magnification as a, b and c.

# Figure 16

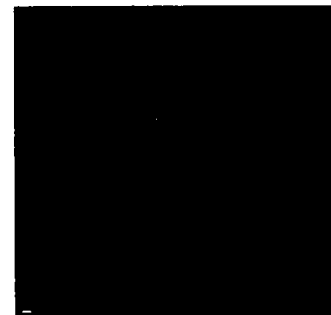
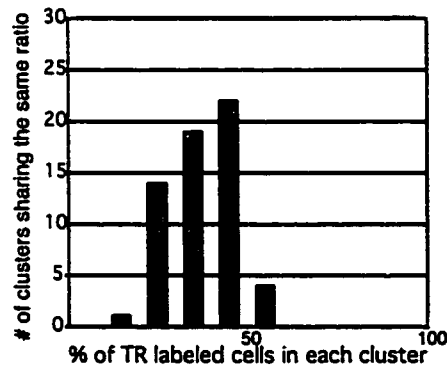
**a** Coaggregation of Texas Red Labeled  $\Delta I$  #2 with S180 L-CAM #11



**b** Coaggregation of Texas Red Labeled  $\Delta I$  #2 with HAV/VAH #1



**c** Coaggregation of Texas Red Labeled  $\Delta I$  #2 with HAV/VAH #2



**d** Coaggregation of Texas Red Labeled  $\Delta I$  #2 with HAV/VAH #4

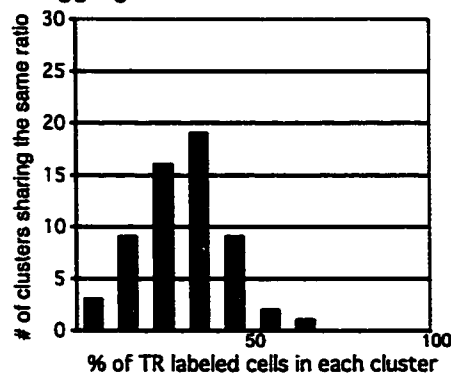
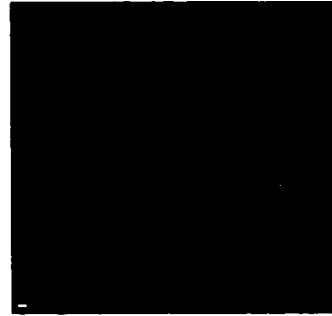
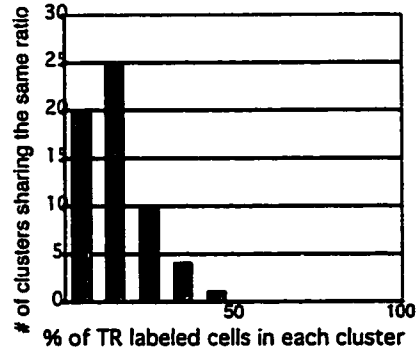


**Figure 17**

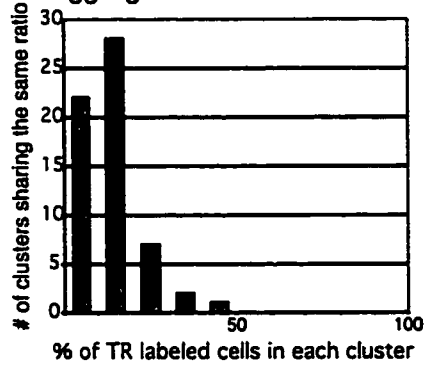
Coaggregation of Texas Red labelled S180 cells with fluorescein labelled S180 L-CAM #11 (a), HAV/VAH #1 (b), HAV/VAH #2 (c), and HAV/VAH #4 cells (d). There are no histograms or pictures shown for coaggregation of S180 with S180 or  $\Delta I$  cells because they failed to aggregate to a level of 20%. In all assays depicted, S180 cells comprised mostly 0-20% of the coaggregates. These ratios are also the reciprocal of S180L/S180 and HAV/VAH/S180. Each scale-bar represents 2 $\mu$ m. Panel d was taken at the same magnification as a, b and c.

# Figure 17

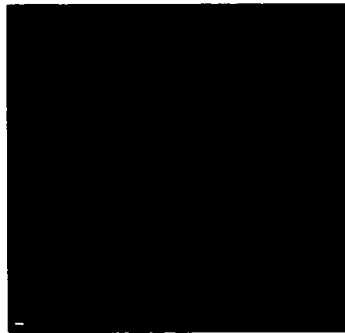
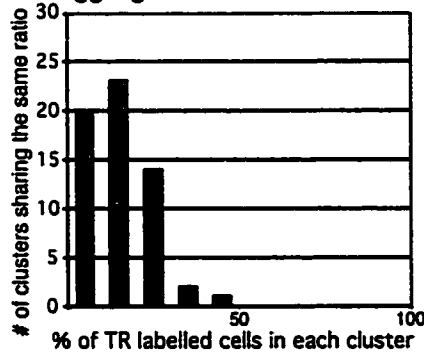
**a** Coaggregation of Texas Red Labeled S180 with S180 L-CAM #11



**b** Coaggregation of Texas Red Labeled S180 with HAV/VAH #1



**c** Coaggregation of Texas Red Labeled S180 with HAV/VAH #2



**d** Coaggregation of Texas Red Labeled S180 with HAV/VAH #4

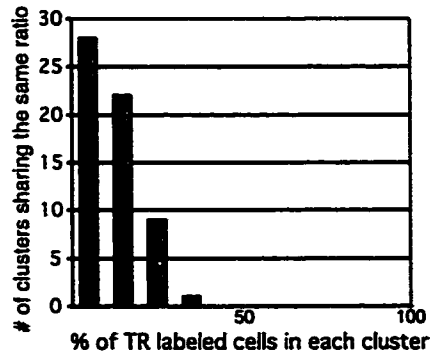
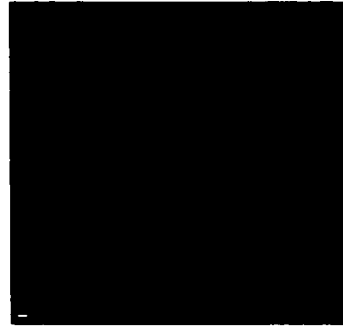
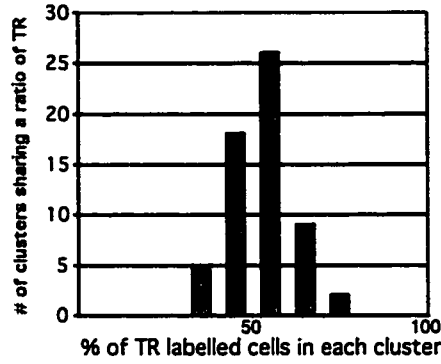


**Figure 18:**

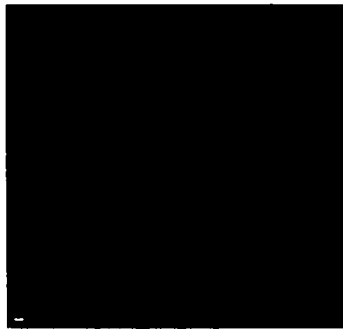
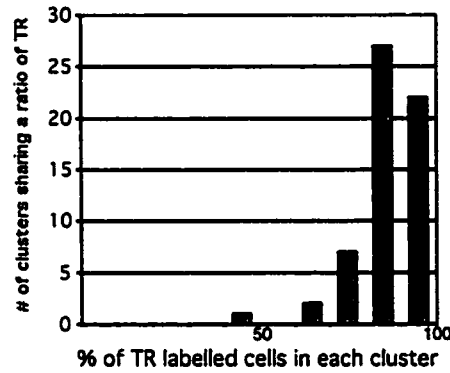
Coaggregation of Texas Red labelled S180 L-CAM #11 with fluorescein labelled S180 L-CAM #11 (a), S180 (b), HAV/VAH #1 (c), HAV/VAH #2 (d), HAV/VAH #4 (e),  $\Delta I$  #1 (f), and  $\Delta I$  #2 cells (g). Coaggregation with fluorescein labeled S180 L-CAM and the HAV/VAH clones was roughly 50%. S180 L-CAM cells comprised 80-100% of the clusters formed with S180 cells. Full-length L-CAM made up about 70% of the coclusters with  $\Delta I$  mutants. These ratios are the reciprocal of what the previous figures have shown, supporting the relationships previously depicted. Each scale-bar represents 2 $\mu$ m, except for panel d, which represents 10 $\mu$ m.

# Figure 18

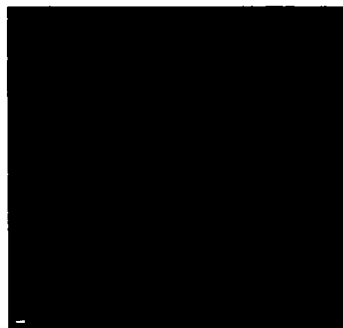
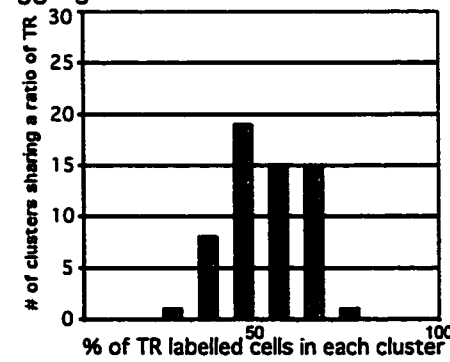
**a** Coaggregation of Texas Red Labeled S180 L-CAM #11 with itself



**b** Coaggregation of Texas Red Labeled S180 L-CAM #11 with S180



**c** Coaggregation of Texas Red Labeled S180 L-CAM #11 with HAV/VAH #1



**d** Coaggregation of Texas Red Labeled S180 L-CAM #11 with HAV/VAH #2

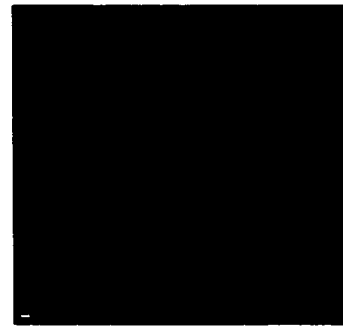
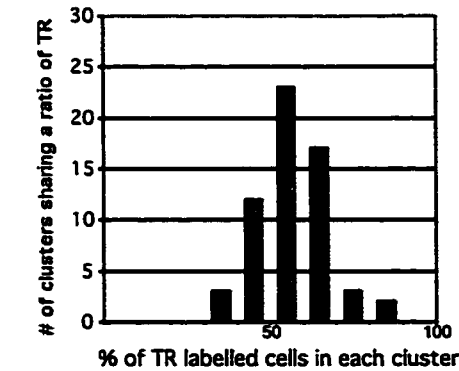
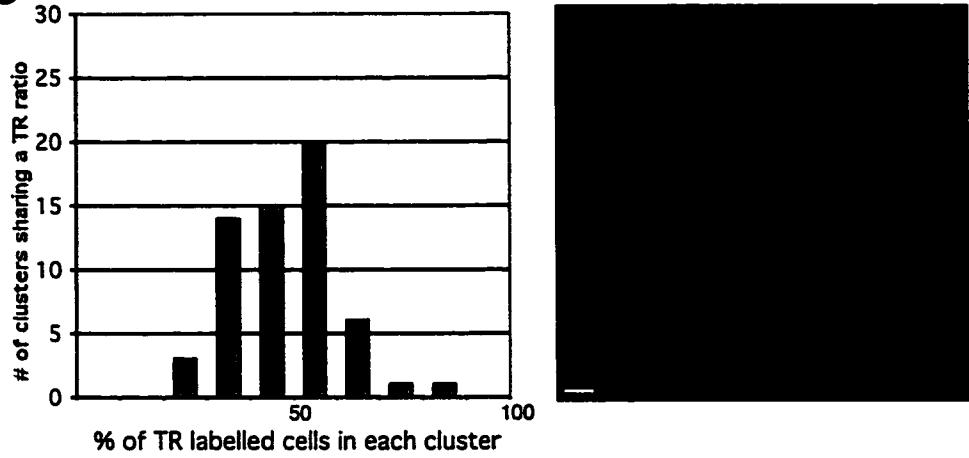


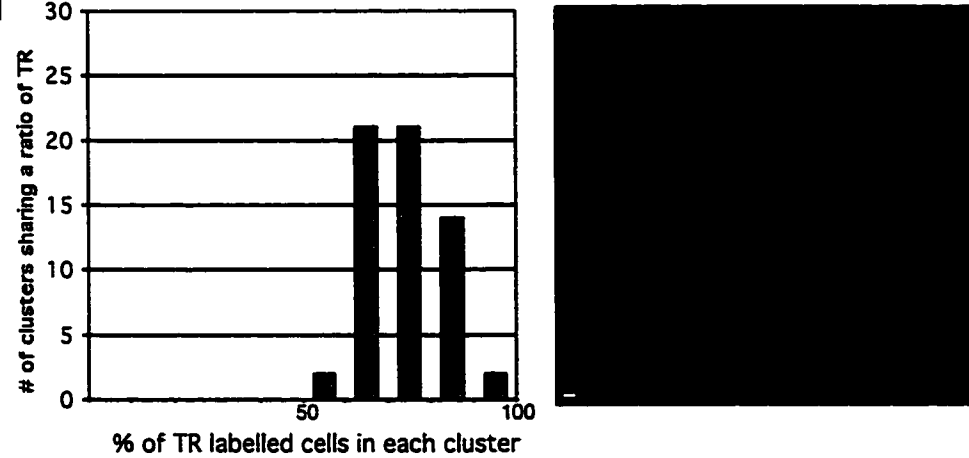


# Figure 18

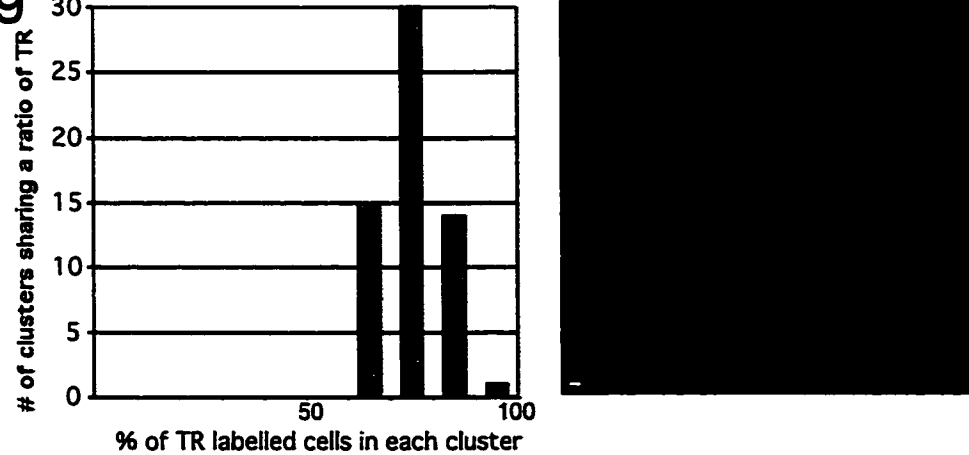
**e** Coaggregation of Texas Red Labeled S180 L-CAM #11 with HAV/VAH #4



**f** Coaggregation of Texas Red Labeled S180 L-CAM #11 with  $\Delta I$  #1



**g** Coaggregation of Texas Red Labeled S180 L-CAM #11 with  $\Delta I$  #2



## Discussion

Although much is being learned about the intracellular signals that modulate cadherin based adhesion, little is still known about how the extracellular domains mediate *trans* and *cis* interactions. There are no inherent clues about the topology of the cadherin extracellular structure that implicates a concrete mechanism of protein-protein interaction (i.e. it does not contain sequences resembling known adhesive interfaces). A region of the protein that has been shown to be important to the *trans* interaction is the first extracellular domain [Nose et al., 1986]. Some groups proposed that the presumptive binding site is the tripeptide HAV, located in the first domain [Blaschuk et al., 1990a and 1990b], although the importance of this sequence is subject to debate. Initially in cadherin literature it was assumed that the cadherin *trans* interaction consisted of EC1 between cadherins of adjacent cells. Recent data has arisen that supports the idea that cadherins are fully intercalated, with *trans* interactions between EC1 and EC5, EC2 and EC4, and EC3 and EC3 [Sivasankar et al., 1999] (Figure 6). The data presented in this thesis supports a crucial role to cadherin binding in the region of EC1, but it does not support the theory that the sole point of interaction between two cadherins is the EC1 domain (Figure 13). Also unlike previous reports, the orientation of HAV sequence of the first extracellular domain appears irrelevant to the binding interface, implying that these residues may not be important to adhesion.

Two mutations of the cadherin L-CAM first extracellular domain were constructed: a point mutation converting the putative *trans* binding site HAV (78, 79, and 80) to VAH and a deletion of the first extracellular cadherin domain ( $\Delta I$ ). Both plasmid sequences were transfected into S180 cells and the identities of the clones were verified with PCR, sequencing, and Western Blotting (Figures 7 and 8). Immunofluorescence revealed that both HAV/VAH and  $\Delta I$  mutants were expressed at the plasma membrane at the lateral region of the cell (Figure 9). The membranes of cells of these mutants are flattened at points between two cells in confluent and subconfluent cultures, indicating that the mutant cadherins are capable of forming cell-cell contacts. However, cells plated on a substrate are not subjected to shearing forces and stress on the contacts.

A more functional test of cadherin based adhesion is the aggregation assay. Results of the aggregation assay revealed that HAV/VAH transfected cells are as adhesive as the unmutated L-CAM transfectants (Figures 10 and 11). This data refutes the theory that HAV is an important point of adhesive contact (Blaschuk et al., 1990a; Blaschuk et al., 1990b). As mentioned previously, if HAV was the adhesive point of

contact, then it either directly interacted with the HAV of the cadherin of an adjacent cell or it adhered to a point of the ectodomain closer to the plasma membrane than HAV. If HAV interaction was direct, then HAV/VAH could be expected to aggregate with other HAV/VAH cells because the adhesive interface would still be complementary (i.e. His still interacts with Val, Ala with Ala, and Val with His). If HAV interacts with a different interface, then likely the mutation to VAH would have compromised adhesion. HAV/VAH aggregated homotypically (Figure 10), implying that HAV interacts directly with HAV of another cadherin. If HAV was the result of a direct interaction, then HAV/VAH would not be able to associate with unmutated L-CAM and would not be expected to coaggregate with it. However, HAV/VAH mutants did coaggregate with wild type L-CAM, contradicting the model of a direct interaction as well (Figures 12, 13, 14, and 18). It appears that neither HAV interaction model supports its behavior, endorsing an alternative explanation that the orientation of HAV is not important to the adhesive interface. Because the order of amino acids can be manipulated without an apparent effect on the protein's function, it is likely that HAV is not an essential part of the adhesive interface.

Most research investigating the adhesive interface of classical cadherins focuses on the first cadherin extracellular domain. Also, most function blocking antibodies have been found to react to sequences of EC1. Mutation deleting the first extracellular domain was expected to severely debilitate adhesion. As anticipated, the  $\Delta I$  mutants were unable to homotypically associate (Figure 11). However, in coaggregation assays,  $\Delta I$  was able to coaggregate with unmutated L-CAM and HAV/VAH clones (Figures 12, 13, 14, 15, 16, and 18).  $\Delta I$  lacks essential binding sequences from the first domain but its binding partners HAV/VAH and unmutated L-CAM have regions that are capable of adhering to the remaining sequence of  $\Delta I$  (Figure 6).  $\Delta I$  cannot fully reciprocate with this binding interaction, so the adhesion is not as strong (Figure 6). This data supports the theory that the *trans* interaction is not EC1 to EC1, but EC1 to EC5, with weak adhesive interactions between domains EC2-EC4, EC3-EC3, and EC4-EC2 (Sivasankar et al., 1999). These weaker interactions are consistent with the immunofluorescence of  $\Delta I$  (Figure 9). The cells appear to be undergoing cadherin mediated cell-cell adhesion with membranes flattened between cells and cadherins are concentrated to the membranes of contact points.  $\Delta I$  seems to be adhesive in the absence of stress, but is nonadhesive in an assay situation, implying that the inter-domain interactions of EC2-EC4 and EC3-EC3 are not as strong as the EC1-EC5 interaction.

S180 cells are predisposed to form gap junctions and this tendency increases significantly in cells transfected with cadherin (Matsuzaki et al., 1990; Musil et al.,

1990). There is a positive correlation between phosphorylation of connexin 43 and gap junction formation. Connexin 43 was only abundantly phosphorylated in cells transfected with L-CAM or another cadherin (Musil et al., 1990; Musil and Goodenough, 1991). The role of the cadherins in gap junction formation appears to involve a signaling event, although it is possible that the cadherins merely convey the membranes of adjacent cells to a proximity that permits the connexons to join. Mutational analysis of the cadherins would test the involvement of cadherins in this role. Possibly the HAV tripeptide is involved in cell surface signaling, and its mutation may have a negative effect on gap junction formation. The next step of this study will be testing the effect of cadherin mutation on gap junction formation. It should be noted that the connexons may contribute to the cadherin mediated cell-cell adhesion in  $\Delta I$  monolayers. Gap junction channels are adhesive cell-cell interactions. Even if they are weak, they may coordinate with a weak  $\Delta I$  cadherin interaction to form somewhat stable contacts. Possibly the inability of  $\Delta I$  to adhere in a short term aggregation assay is due to the lack of gap junction support to the adhesion process, since gap junction kinetics may be slower than cadherin based adhesion.

L-CAM transfection into the S180 cell line produced a phenotypic change of fibroblastoid towards a more epitheloid phenotype (Mege et al., 1988). Recent work has revealed that L-CAM transfected S180 cells express MAPK phosphatase-1 at a five fold level compared to untransfected S180 cells, implicating L-CAM in a signaling pathway that upregulates transcription of this phosphatase (Paul Lampe, unpublished data). MAPK causes the activation of several proteins that participate in the mitogenic pathway, and downregulates many proteins involved in maintaining the cell in a nonproliferating state (e.g. the GEF Tiam1 (Kuroda et al., 1999)). The mutant L-CAMs may provide some insight into this novel signaling event.

This investigation tested two questions regarding cadherin based adhesion: the importance of HAV to the adhesive interface and the necessity and nature of EC1 to the adhesive interaction. However, there are several more questions that can be investigated using these mutant constructs. They may influence signaling events related to formation of gap junctions, and suppression of mitogenic pathways. There are also many avenues of investigating how these mutants may influence cytoskeletal components. For instance  $\Delta I$  mutants have a very rounded cell shape that is not well spread on the substrate. They may be deficient in focal adhesions compared to wild type L-CAM and HAV/VAH mutants. Lastly deletion mutations for each cadherin extracellular domain have been constructed by the Gallin lab and transfected into S180 cells. Assaying their

adhesive and signaling abilities will lead to a clearer understanding of the dynamics of the *cis* and trans interaction.

## **Bibliography**

- Acheson, A., and W.J. Gallin. 1992. Generation and characterization of function-blocking anti-cell adhesion molecule antibodies. *In Cell-cell interactions: a practical approach*. B.R. Stevenson, W.J. Gallin, and D.L. Paul, editors. IRL Press, New York.
- Aono, S., S. Nakagawa, A.B. Reynolds, and M. Takeichi. 1999. p120(ctn) acts as an inhibitory regulator of cadherin function in colon carcinoma cells. *J Cell Biol.* 145:551-62.
- Birchmeier, W., and J. Behrens. 1994. Cadherin expression in carcinomas: role in the formation of cell junctions and the prevention of invasiveness. *Biochim Biophys Acta.* 1198:11-26.
- Blaschuk, O.W., Y. Pouliot, and P.C. Holland. 1990a. Identification of a conserved region common to cadherins and influenza strain A hemagglutinins. *J Mol Biol.* 211:679-82.
- Blaschuk, O.W., R. Sullivan, S. David, and Y. Pouliot. 1990b. Identification of a cadherin cell adhesion recognition sequence. *Dev Biol.* 139:227-9.
- Brady-Kalnay, S.M., T. Mourton, J.P. Nixon, G.E. Pietz, M. Kinch, H. Chen, R. Brackenbury, D.L. Rimm, R.L. Del Vecchio, and N.K. Tonks. 1998. Dynamic interaction of PTPmu with multiple cadherins in vivo. *J Cell Biol.* 141:287-96.
- Brieher, W.M., A.S. Yap, and B.M. Gumbiner. 1996. Lateral dimerization is required for the homophilic binding activity of C-cadherin. *Journal of Cell Biology.* 135:487-496.
- Bronner-Fraser, M., J.J. Wolf, and B.A. Murray. 1992. Effects of antibodies against N-cadherin and N-CAM on the cranial neural crest and neural tube. *Dev Biol.* 153:291-301.
- Buxton, R.S., P. Cowin, W.W. Franke, D.R. Garrod, K.J. Green, I.A. King, P.J. Koch, A.I. Magee, D.A. Rees, J.R. Stanley, and et al. 1993. Nomenclature of the desmosomal cadherins. *J Cell Biol.* 121:481-3.
- Chen, W.C., and B. Obrink. 1991. Cell-cell contacts mediated by E-cadherin (uvomorulin) restrict invasive behavior of L-cells. *J Cell Biol.* 114:319-27.
- Chothia, C., and E.Y. Jones. 1997. The molecular structure of cell adhesion molecules. *Annu Rev Biochem.* 66:823-62.
- Collins, J.E., P.K. Legan, T.P. Kenny, J. MacGarvie, J.L. Holton, and D.R. Garrod. 1991. Cloning and sequence analysis of desmosomal glycoproteins 2 and 3 (desmocollins): cadherin-like desmosomal adhesion molecules with heterogeneous cytoplasmic domains. *J Cell Biol.* 113:381-91.

- Cowin, P., D. Matthey, and D. Garrod. 1984. Identification of desmosomal surface components (desmocollins) and inhibition of desmosome formation by specific Fab'. *J Cell Sci.* 70:41-60.
- Cunningham, B.A., Y. Leutzinger, W.J. Gallin, B.C. Sorkin, and G.M. Edelman. 1984. Linear organization of the liver cell adhesion molecule L-CAM. *Proc Natl Acad Sci U S A.* 81:5787-91.
- Dunham, L.J., and S. H.L. 1952. A survey of transplantable and transmissible animal tumors. *Journal of the National Cancer Institute.* 22:1299-1375.
- Edelman, G.M., W.J. Gallin, A. Delouee, B.A. Cunningham, and J.P. Thiery. 1983. Early epochal maps of two different cell adhesion molecules. *Proc Natl Acad Sci U S A.* 80:4384-8.
- Farquhar, M.G., and G.E. Palade. 1965. Cell junctions in amphibian skin. *J Cell Biol.* 26:263-91.
- Friedlander, D.R., R.M. Mege, B.A. Cunningham, and G.M. Edelman. 1989. Cell sorting-out is modulated by both the specificity and amount of different cell adhesion molecules (CAMs) expressed on cell surfaces. *Proc Natl Acad Sci U S A.* 86:7043-7.
- Fukata, M., S. Kuroda, M. Nakagawa, A. Kawajiri, N. Itoh, I. Shoji, Y. Matsuura, S. Yonehara, H. Fujisawa, A. Kikuchi, and K. Kaibuchi. 1999. Cdc42 and Rac1 regulate the interaction of IQGAP1 with beta-catenin. *J Biol Chem.* 274:26044-50.
- Gallin, W.J. 1998. Evolution of the "classical" cadherin family of cell adhesion molecules in vertebrates. *Mol Biol Evol.* 15:1099-107.
- Gallin, W.J., G.M. Edelman, and B.A. Cunningham. 1983. Characterization of L-CAM, a major cell adhesion molecule from embryonic liver cells. *Proc Natl Acad Sci U S A.* 80:1038-42.
- Gallin, W.J., B.C. Sorkin, G.M. Edelman, and B.A. Cunningham. 1987. Sequence analysis of a cDNA clone encoding the liver cell adhesion molecule, L-CAM. *Proc Natl Acad Sci U S A.* 84:2808-12.
- Goldberg, M., C. Peshkovsky, A. Shifteh, and Q. Al-Awqati. 2000. mu-Protocadherin, a novel developmentally regulated protocadherin with mucin-like domains. *J Biol Chem.* 275:24622-9.
- Haber, A., and R.P. Runyon. 1973. An introduction to the analysis of variance. *In* General Statistics. A. Haber and R.P. Runyon, editors. Addison Wesley Publishing Inc., New York.

- Hatta, K., and M. Takeichi. 1986. Expression of N-cadherin adhesion molecules associated with early morphogenetic events in chick development. *Nature*. 320:447-9.
- Hermiston, M.L., and J.I. Gordon. 1995. In vivo analysis of cadherin function in the mouse intestinal epithelium: essential roles in adhesion, maintenance of differentiation, and regulation of programmed cell death. *J Cell Biol.* 129:489-506.
- Hermiston, M.L., M.H. Wong, and J.I. Gordon. 1996. Forced expression of E-cadherin in the mouse intestinal epithelium slows cell migration and provides evidence for nonautonomous regulation of cell fate in a self-renewing system. *Genes Dev.* 10:985-96.
- Hoffman, S. 1992. Assays of cell adhesion. *In Cell-cell interactions: a practical approach*. B.R. Stevenson, W.J. Gallin, and D.L. Paul, editors. IRL Press, New York.
- Hoschuetzky, H., H. Aberle, and R. Kemler. 1994. Beta-catenin mediates the interaction of the cadherin-catenin complex with epidermal growth factor receptor. *J Cell Biol.* 127:1375-80.
- Huber, O., R. Kemler, and D. Langosch. 1999. Mutations affecting transmembrane segment interactions impair adhesiveness of E-cadherin. *J Cell Sci.* 112:4415-23.
- Hyafil, F., C. Babinet, and F. Jacob. 1981. Cell-cell interactions in early embryogenesis: a molecular approach to the role of calcium. *Cell.* 26:447-54.
- Hynes, R.O. 1992. Integrins: versatility, modulation, and signaling in cell adhesion. *Cell.* 69:11-25.
- Kaibuchi, K., S. Kuroda, M. Fukata, and M. Nakagawa. 1999. Regulation of cadherin-mediated cell-cell adhesion by the Rho family GTPases. *Curr Opin Cell Biol.* 11:591-6.
- Klymkowsky, M.W., and B. Parr. 1995. The body language of cells: the intimate connection between cell adhesion and behavior. *Cell.* 83:5-8.
- Koch, P.J., M.J. Walsh, M. Schmelz, M.D. Goldschmidt, R. Zimbelmann, and W.W. Franke. 1990. Identification of desmoglein, a constitutive desmosomal glycoprotein, as a member of the cadherin family of cell adhesion molecules. *Eur J Cell Biol.* 53:1-12.
- Kowalczyk, A.P., E.A. Bornslaeger, J.E. Borgwardt, H.L. Palka, A.S. Dhaliwal, C.M. Corcoran, M.F. Denning, and K.J. Green. 1997. The amino-terminal domain of



- desmoplakin binds to plakoglobin and clusters desmosomal cadherin-plakoglobin complexes. *J Cell Biol.* 139:773-84.
- Kuroda, S., M. Fukata, M. Nakagawa, and K. Kaibuchi. 1999. Cdc42, Rac1, and their effector IQGAP1 as molecular switches for cadherin-mediated cell-cell adhesion. *Biochem Biophys Res Commun.* 262:1-6.
- Laemmli, U.K. 1970. Cleavage of structural proteins during the assembly of the head of bacteriophage T4. *Nature.* 227:680-5.
- Leckband, D., and S. Sivasankar. 2000. Mechanism of homophilic cadherin adhesion [In Process Citation]. *Curr Opin Cell Biol.* 12:587-92.
- Legan, P.K., J.E. Collins, and D.R. Garrod. 1992. The molecular biology of desmosomes and hemidesmosomes: "what's in a name"? *Bioessays.* 14:385-93.
- Li, Z., W.J. Gallin, G. Lauzon, and M. Pasdar. 1998. L-CAM expression induces fibroblast-epidermoid transition in squamous carcinoma cells and down-regulates the endogenous N-cadherin. *J Cell Sci.* 111:1005-19.
- Lickert, H., A. Bauer, R. Kemler, and J. Stappert. 2000. Casein kinase II phosphorylation of E-cadherin increases E-cadherin/beta-catenin interaction and strengthens cell-cell adhesion. *J Biol Chem.* 275:5090-5.
- Marrs, J.A., and W.J. Nelson. 1996. Cadherin cell adhesion molecules in differentiation and embryogenesis. *Int Rev Cytol.* 165:159-205.
- Matsuzaki, F., R.M. Mege, S.H. Jaffe, D.R. Friedlander, W.J. Gallin, J.I. Goldberg, B.A. Cunningham, and G.M. Edelman. 1990. cDNAs of cell adhesion molecules of different specificity induce changes in cell shape and border formation in cultured S180 cells. *J Cell Biol.* 110:1239-52.
- McNeill, H., T.A. Ryan, S.J. Smith, and W.J. Nelson. 1993. Spatial and temporal dissection of immediate and early events following cadherin-mediated epithelial cell adhesion. *J Cell Biol.* 120:1217-26.
- Mege, R.M., F. Matsuzaki, W.J. Gallin, J.I. Goldberg, B.A. Cunningham, and G.M. Edelman. 1988. Construction of epithelioid sheets by transfection of mouse sarcoma cells with cDNAs for chicken cell adhesion molecules. *Proc Natl Acad Sci U S A.* 85:7274-8.
- Monier-Gavelle, F., and J.L. Duband. 1997. Cross talk between adhesion molecules: control of N-cadherin activity by intracellular signals elicited by beta1 and beta3 integrins in migrating neural crest cells. *J Cell Biol.* 137:1663-81.
- Moore, D. 1998. Purification and concentration of DNA from aqueous solutions. *In Current Protocols in Molecular Biology.* F.M. Ausubel, R. Brent, K. R.E., D. Moore, S. J.G., S. J.A., and S. K., editors. John Wiley & Sons Inc., New York.

- Murphy-Erdosh, C., C.K. Yoshida, N. Paradies, and L.F. Reichardt. 1995. The cadherin-binding specificities of B-cadherin and LCAM. *J Cell Biol.* 129:1379-90.
- Musil, L.S., B.A. Cunningham, G.M. Edelman, and D.A. Goodenough. 1990. Differential phosphorylation of the gap junction protein connexin43 in junctional communication-competent and -deficient cell lines. *J Cell Biol.* 111:2077-88.
- Musil, L.S., and D.A. Goodenough. 1991. Biochemical analysis of connexin43 intracellular transport, phosphorylation, and assembly into gap junctional plaques. *J Cell Biol.* 115:1357-74.
- Nagafuchi, A., and M. Takeichi. 1988. Cell binding function of E-cadherin is regulated by the cytoplasmic domain. *Embo J.* 7:3679-84.
- Nagar, B., M. Overduin, M. Ikura, and J.M. Rini. 1996. Structural basis of calcium-induced E-cadherin rigidification and dimerization. *Nature.* 380:360-4.
- Napolitano, E.W., K. Venstrom, E.F. Wheeler, and L.F. Reichardt. 1991. Molecular cloning and characterization of B-cadherin, a novel chick cadherin. *J Cell Biol.* 113:893-905.
- Navarro, P., M. Gomez, A. Pizarro, C. Gamallo, M. Quintanilla, and A. Cano. 1991. A role for the E-cadherin cell-cell adhesion molecule during tumor progression of mouse epidermal carcinogenesis. *J Cell Biol.* 115:517-33.
- Noe, V., J. Willems, J. Vandekerckhove, F.V. Roy, E. Bruyneel, and M. Mareel. 1999. Inhibition of adhesion and induction of epithelial cell invasion by HAV-containing E-cadherin-specific peptides. *J Cell Sci.* 112:127-35.
- Nose, A., and M. Takeichi. 1986. A novel cadherin cell adhesion molecule: its expression patterns associated with implantation and organogenesis of mouse embryos. *J Cell Biol.* 103:2649-58.
- Nose, A., K. Tsuji, and M. Takeichi. 1990. Localization of specificity determining sites in cadherin cell adhesion molecules. *Cell.* 61:147-55.
- Oda, H., T. Uemura, Y. Harada, Y. Iwai, and M. Takeichi. 1994. A Drosophila homolog of cadherin associated with armadillo and essential for embryonic cell-cell adhesion. *Dev Biol.* 165:716-26.
- Overduin, M., T.S. Harvey, S. Bagby, K.I. Tong, P. Yau, M. Takeichi, and M. Ikura. 1995. Solution structure of the epithelial cadherin domain responsible for selective cell adhesion [see comments]. *Science.* 267:386-9.
- Ozawa, M., J. Engel, and R. Kemler. 1990. Single amino acid substitutions in one Ca<sup>2+</sup> binding site of uvomorulin abolish the adhesive function. *Cell.* 63:1033-8.

- Ozawa, M., and R. Kemler. 1998a. Altered cell adhesion activity by pervanadate due to the dissociation of alpha-catenin from the E-cadherin.catenin complex. *J Biol Chem.* 273:6166-70.
- Ozawa, M., and R. Kemler. 1998b. The membrane-proximal region of the E-cadherin cytoplasmic domain prevents dimerization and negatively regulates adhesion activity. *J Cell Biol.* 142:1605-13.
- Pertz, O., D. Bozic, A.W. Koch, C. Fauser, A. Brancaccio, and J. Engel. 1999. A new crystal structure, Ca<sup>2+</sup> dependence and mutational analysis reveal molecular details of E-cadherin homoassociation. *Embo J.* 18:1738-47.
- Pouliot, Y. 1992. Phylogenetic analysis of the cadherin superfamily. *Bioessays.* 14:743-8.
- Prieto, A.L., and K.L. Crossin. 1995. Cell-cell adhesion molecules in epithelial-mesenchymal transformations. *Acta Anat.* 154:21-33.
- Ranscht, B. 1994. Cadherins and catenins: interactions and functions in embryonic development. *Curr Opin Cell Biol.* 6:740-6.
- Reynolds, A.B., J.M. Daniel, Y.Y. Mo, J. Wu, and Z. Zhang. 1996. The novel catenin p120cas binds classical cadherins and induces an unusual morphological phenotype in NIH3T3 fibroblasts. *Exp Cell Res.* 225:328-37.
- Rimm, D.L., and J.S. Morrow. 1994. Molecular cloning of human E-cadherin suggests a novel subdivision of the cadherin superfamily. *Biochem Biophys Res Commun.* 200:1754-61.
- Roura, S., S. Miravet, J. Piedra, A. Garcia de Herreros, and M. Dunach. 1999. Regulation of E-cadherin/Catenin association by tyrosine phosphorylation. *J Biol Chem.* 274:36734-40.
- Sander, E.E., J.P. ten Klooster, S. van Delft, R.A. van der Kammen, and J.G. Collard. 1999. Rac downregulates Rho activity: reciprocal balance between both GTPases determines cellular morphology and migratory behavior. *J Cell Biol.* 147:1009-22.
- Sander, E.E., S. van Delft, J.P. ten Klooster, T. Reid, R.A. van der Kammen, F. Michiels, and J.G. Collard. 1998. Matrix-dependent Tiam1/Rac signaling in epithelial cells promotes either cell-cell adhesion or cell migration and is regulated by phosphatidylinositol 3-kinase. *J Cell Biol.* 143:1385-98.
- Sano, K., H. Tanihara, R.L. Heimark, S. Obata, M. Davidson, T. St John, S. Taketani, and S. Suzuki. 1993. Protocadherins: a large family of cadherin-related molecules in central nervous system. *Embo J.* 12:2249-56.

- Shapiro, L., and D.R. Colman. 1999. The diversity of cadherins and implications for a synaptic adhesive code in the CNS. *Neuron*. 23:427-30.
- Shapiro, L., A.M. Fannon, P.D. Kwong, A. Thompson, M.S. Lehmann, G. Grubel, J.F. Legrand, J. Als-Nielsen, D.R. Colman, and W.A. Hendrickson. 1995a. Structural basis of cell-cell adhesion by cadherins [see comments]. *Nature*. 374:327-37.
- Shapiro, L., P.D. Kwong, A.M. Fannon, D.R. Colman, and W.A. Hendrickson. 1995b. Considerations on the folding topology and evolutionary origin of cadherin domains. *Proc Natl Acad Sci U S A*. 92:6793-7.
- Shimoyama, Y., T. Yoshida, M. Terada, Y. Shimosato, O. Abe, and S. Hirohashi. 1989. Molecular cloning of a human Ca<sup>2+</sup>-dependent cell-cell adhesion molecule homologous to mouse placental cadherin: its low expression in human placental tissues. *J Cell Biol*. 109:1787-94.
- Sivasankar, S., W. Brieher, N. Lavrik, B. Gumbiner, and D. Leckband. 1999. Direct molecular force measurements of multiple adhesive interactions between cadherin ectodomains [In Process Citation]. *Proc Natl Acad Sci U S A*. 96:11820-4.
- Stappert, J., and R. Kemler. 1992. Functional analysis of uvomorulin by site-directed mutagenesis and gene transfer into eukaryotic cells. In *Cell-cell interactions: a practical approach*. B.R. Stevenson, W.J. Gallin, and D.L. Paul, editors. IRL Press, New York.
- Suzuki, S.T. 1996. Protocadherins and diversity of the cadherin superfamily. *J Cell Sci*. 109:2609-11.
- Takai, Y., T. Sasaki, and T. Matozaki. 2001. Small GTP-Binding Proteins. *Physiol Rev*. 81:153-208.
- Tamura, K., W.S. Shan, W.A. Hendrickson, D.R. Colman, and L. Shapiro. 1998. Structure-function analysis of cell adhesion by neural (N-) cadherin. *Neuron*. 20:1153-63.
- Tanihara, H., K. Sano, R.L. Heimark, T. St John, and S. Suzuki. 1994. Cloning of five human cadherins clarifies characteristic features of cadherin extracellular domain and provides further evidence for two structurally different types of cadherin. *Cell Adhes Commun*. 2:15-26.
- Thiery, J.P., A. Delouvee, W.J. Gallin, B.A. Cunningham, and G.M. Edelman. 1984. Ontogenetic expression of cell adhesion molecules: L-CAM is found in epithelia derived from the three primary germ layers. *Dev Biol*. 102:61-78.

- Thoreson, M.A., P.Z. Anastasiadis, J.M. Daniel, R.C. Ireton, M.J. Wheelock, K.R. Johnson, D.K. Hummingbird, and A.B. Reynolds. 2000. Selective uncoupling of p120(ctn) from E-cadherin disrupts strong adhesion. *J Cell Biol.* 148:189-202.
- Tomschy, A., C. Fauser, R. Landwehr, and J. Engel. 1996. Homophilic adhesion of E-cadherin occurs by a co-operative two-step interaction of N-terminal domains. *Embo J.* 15:3507-14.
- Townes, P.S., and J. Holtfreter. 1955. Directed movements and selective adhesion of embryonic amphibian cells. *Journal of Experimental Zoology.* 128:53-120.
- Van Aelst, L., M. Barr, S. Marcus, A. Polverino, and M. Wigler. 1993. Complex formation between RAS and RAF and other protein kinases. *Proc Natl Acad Sci U S A.* 90:6213-7.
- Williams, A.F., and A.N. Barclay. 1988. The immunoglobulin superfamily--domains for cell surface recognition. *Annu Rev Immunol.* 6:381-405.
- Wu, C., S.Y. Keightley, C. Leung-Hagesteijn, G. Radeva, M. Coppolino, S. Goicoechea, J.A. McDonald, and S. Dedhar. 1998. Integrin-linked protein kinase regulates fibronectin matrix assembly, E-cadherin expression, and tumorigenicity. *J Biol Chem.* 273:528-36.
- Wu, Q., and T. Maniatis. 1999. A striking organization of a large family of human neural cadherin-like cell adhesion genes. *Cell.* 97:779-90.
- Wu, Q., and T. Maniatis. 2000. Large exons encoding multiple ectodomains are a characteristic feature of protocadherin genes. *Proc Natl Acad Sci U S A.* 97:3124-9.
- Xia, Z., H. Dudek, C.K. Miranti, and M.E. Greenberg. 1996. Calcium influx via the NMDA receptor induces immediate early gene transcription by a MAP kinase/ERK-dependent mechanism. *J Neurosci.* 16:5425-36.
- Xu, Y., and G. Carpenter. 1999. Identification of cadherin tyrosine residues that are phosphorylated and mediate Shc association. *J Cell Biochem.* 75:264-71.
- Yap, A.S., W.M. Briher, and B.M. Gumbiner. 1997. Molecular and functional analysis of cadherin-based adherens junctions. *Annu Rev Cell Dev Biol.* 13:119-46.
- Yap, A.S., C.M. Niessen, and B.M. Gumbiner. 1998. The juxtamembrane region of the cadherin cytoplasmic tail supports lateral clustering, adhesive strengthening, and interaction with p120ctn. *J Cell Biol.* 141:779-89.
- Yoshida-Noro, C., N. Suzuki, and M. Takeichi. 1984. Molecular nature of the calcium-dependent cell-cell adhesion system in mouse teratocarcinoma and embryonic cells studied with a monoclonal antibody. *Dev Biol.* 101:19-27.

Zondag, G.C., E.E. Evers, J.P. ten Klooster, L. Janssen, R.A. van der Kammen, and J.G. Collard. 2000. Oncogenic Ras downregulates Rac activity, which leads to increased Rho activity and epithelial-mesenchymal transition. *J Cell Biol.* 149:775-82.